National Library
of Canada

Bibliothèque nationale
du Canada

Canadian Theses Service

Services des thèses canadiennes

Ottawa, Canada
K1A 0N4

CANADIAN THESES

NOTICE

The quality of this microfiche is heavily dependent upon the quality of the original thesis submitted for microfilming. Every effort has been made to ensure the highest quality of reproduction possible.

If pages are missing, contact the university which granted the degree.

Some pages may have indistinct print especially if the original pages were typed with a poor typewriter ribbon or if the university sent us an inferior photocopy.

Previously copyrighted materials (journal articles, published tests, etc.) are not filmed.

Reproduction in full or in part of this film is governed by the Canadian Copyright Act, R.S.C. 1970, c. C-30.

THIS DISSERTATION
HAS BEEN MICROFILMED
EXACTLY AS RECEIVED

THÈSES CANADIENNES

AVIS

La qualité de cette microfiche dépend grandement de la qualité de la thèse soumise au microfilmage. Nous avons tout fait pour assurer une qualité supérieure de reproduction.

S'il manque des pages, veuillez communiquer avec l'université qui a conféré le grade.

La qualité d'impression de certaines pages peut laisser à désirer, surtout si les pages originales ont été dactylographiées à l'aide d'un ruban usé ou si l'université nous a fait parvenir une photocopie de qualité inférieure.

Les documents qui font déjà l'objet d'un droit d'auteur (articles de revue, examens publiés, etc.) ne sont pas microfilmés.

La reproduction, même partielle, de ce microfilm est soumise à la Loi canadienne sur le droit d'auteur, SRC 1970, c. C-30.

LA THÈSE A ÉTÉ
MICROFILMÉE TELLE QUE
NOUS L'AVONS REÇUE

NL-339 (r.86/06)

Canada

THE UNIVERSITY OF ALBERTA

GEOMETRY OF THE STEADY STATES OF REACTION NETWORKS

by

Baltazar Dacuycuy Aguda

A THESIS

SUBMITTED TO THE FACULTY OF GRADUATE STUDIES AND RESEARCH
IN PARTIAL FULFILMENT OF THE REQUIREMENTS FOR THE DEGREE
OF DOCTOR OF PHILOSOPHY

CHEMISTRY

EDMONTON, ALBERTA

Spring 1986

Permission has been granted to the National Library of Canada to microfilm this thesis and to lend or sell copies of the film.

The author (copyright owner) has reserved other publication rights, and neither the thesis nor extensive extracts from it may be printed or otherwise reproduced without his/her written permission.

L'autorisation a été accordée à la Bibliothèque nationale du Canada de microfilmer cette thèse et de prêter ou de vendre des exemplaires du film.

L'auteur (titulaire du droit d'auteur) se réserve les autres droits de publication; ni la thèse ni de longs extraits de celle-ci ne doivent être imprimés ou autrement reproduits sans son autorisation écrite.

ISBN 0-315-30187-2

THE UNIVERSITY OF ALBERTA

RELEASE FORM

NAME OF AUTHOR : *Baltazar Dacuycuy Aguda*

TITLE OF THESIS : **GEOMETRY OF THE STEADY STATES OF REACTION NETWORKS**

DEGREE FOR WHICH THESIS WAS PRESENTED : DOCTOR OF PHILOSOPHY

YEAR THIS DEGREE GRANTED : Spring 1986

Permission is hereby granted to THE UNIVERSITY OF ALBERTA LIBRARY to reproduce single copies of this thesis and to lend or sell such copies for private, scholarly or scientific research purposes only.

The author reserves other publication rights, and neither the thesis nor extensive extracts from it may be printed or otherwise reproduced without the author's written permission.

(SIGNED) Baltazar D. Aguda

PERMANENT ADDRESS:

Barrio 3 -
Pasuquin, Ilocos Norte
Philippines

DATED 21 April 1986

THE UNIVERSITY OF ALBERTA

FACULTY OF GRADUATE STUDIES AND RESEARCH

The undersigned certify that they have read, and recommend to the Faculty of Graduate Studies and Research, for acceptance, a thesis entitled **GEOMETRY OF THE STEADY STATES OF REACTION NETWORKS** submitted by *Baltazar Dacuycuy Aguda* in partial fulfilment of the requirements for the degree of DOCTOR OF PHILOSOPHY.

Bruce L Clarke
....
Supervisor

M. J. Bulle
....
H B Dunford
....
P. Kebarle
....
Loren G. Hepler
....
V. Balakotaiah
....
External Examiner

Date....April 21, 1986..........

To Mom,
for her sacrifices.

Abstract

A study of the geometry of the steady states of reaction networks was undertaken (i) to derive conditions on the parameters that lead to the existence, uniqueness or multiplicity of steady states, (ii) to determine the patterns of steady state concentrations as functions of a given parameter (bifurcation diagrams), and (iii) to apply the results to a complex mechanism, namely, that of the peroxidase-oxidase (PO) reaction.

Two steady state parametrizations were considered, each characterized by a different geometry. Using rate constants and conservation constraints as parameters, the surface of positive steady states embedded in concentration-parameter space is a simply-connected manifold *M* possibly with singularities that ultimately determine the number of steady states and the kinds of bifurcation diagrams. Alternatively, in reaction velocity space, all steady state velocities are found in a convex cone. Every steady state of the network is a linear superposition of elementary steady state pathways called 'extreme currents', and it is shown that the structure of this cone helps identify which pathways are dominant under certain conditions. Based on this convex geometry, a systematic approach towards the modeling of bistability in chemical reaction systems is found. It is then applied successfully to the PO reaction. This enzyme reaction, with NADH and O_2 as substrates, exhibits bistability in an open

system.

In Chapter III, an algebro-geometric analysis on the steady state manifold *M* is carried out for reduced steady state problems. The system of steady state equations can usually be reduced to a one-dimensional problem when there are only a few extreme currents. After reduction, *M* is interpreted as a catastrophe manifold. Elucidation of its singularity structure followed by projection onto the parameter space provides an exact description of the regions (called 'state sets') in parameter space where there are 0, 1, 2, 3,... steady states. The fold, cusp and swallowtail catastrophes are analyzed and convenient formulas derived for the various state sets and bifurcation sets. An application to the analysis of the characteristic polynomial in linear stability analysis, including Hopf bifurcation sets, is also illustrated.

Chapter IV deals with the problem of enumerating all possible kinds of bifurcation diagrams for a given network. 'Imperfect Bifurcation Theory' developed by Golubitsky and co-workers is the mathematical method to use. The calculations of bifurcation varieties are illustrated and applied to some reaction networks. Formulas for the bifurcation varieties of reduced steady state problems are derived.

In the last chapter, a model for the bistability in the PO reaction is extracted from a list of possible elementary processes, known or postulated, in the mechanism. First, a

simple reversible substrate-inhibition enzyme mechanism is analyzed and the essential extreme currents responsible for the bistability are identified. Similar extreme currents are found in the PO reaction and are shown to be sufficient in producing bistability. Using all the 11 steady state parameters of this model, a complete determination of the conditions on the parameters to give 3, 2, 1 or 0 steady states is accomplished, owing to the results of the previous chapters. The model reproduces many of the qualitative features of the kinetics observed experimentally like bistability and damped oscillations in an open system. Computer simulations of open and closed systems are presented.

Acknowledgements

I am grateful to my research supervisor, Dr. Bruce L. Clarke, for all his help and the freedom he allowed to pursue my interests. To interact with an original thinker is an experience.

I would also like to thank the Chemistry Department, University of Alberta, for the financial support in the form of a research assistantship from 1981 to 1985, and the University of Alberta for the dissertation fellowship in my last year.

I have learned much, and my life as a graduate student made a lot more exciting, because of good friends. My friendship and discussions with Karo ('Boy') Michaelian on scientific, political and even personal affairs will always be cherished. Maria Villa, in so many ways, helped me keep my humanity. G. Bandarage and V. Epa, fellow graduate students in the theoretical division, had been very accomodating with my crazy ideas and stories.

To the bunch of Filipinas - Linda, Leah, Josie, Cecille, Nenette, my sister Madelyn - who always gave me solace (voluntarily or otherwise) when needed, my heartfelt thanks.

Table of Contents

Chapter Page

I. INTRODUCTION 1

- A. Formulation of the Problem 1
- B. Stoichiometric Network and its Kinetics 13

II. GEOMETRIC ASPECTS OF STOICHIOMETRIC DYNAMICAL SYSTEMS 22

- A. Introduction 22
- B. The Nonlinear Dynamical Equations 24
- C. Constraints on Phase Space due to Stoichiometry 27
- D. Dynamics and Steady States of a CSTR 30
- E. Linearization of the Dynamical Equations 35
- F. Convex Geometry of the Steady State Velocities .38
- G. The Current Polytope and a Topology on the Network Steady States 44
- H. Some Classification of Steady States and Corresponding Regions in Π_V 48
- I. Boundary Steady States, Stoichiometric Explosions and Extinction 59
- J. Sufficient Conditions for $\alpha_d \equiv 0$ 72
- K. Networks Without Explosion or Extinction Dynamics 75

III. STATE SETS AND BIFURCATION SETS 81

- A. Reduction of the Steady State Problem 81
- B. An Algebro-Geometric Analysis on M : The Cusp Catastrophe 84
- C. Steady States of the Edelstein Network 96
- D. Bounded Steady States 98
- E. Steady States of an Oscillatory Model for the Peroxidase-Oxidase Reaction 102
- F. The Fold Catastrophe 105

G. Complete Linear Stability Regions and Hopf Bifurcation Sets of Dynamical Systems with $d \leq 3$ 110

H. The Swallowtail Catastrophe 121

IV. BIFURCATION VARIETIES AND DIAGRAMS 135

A. Cross-sections of *M* 135

B. Equivalence and Stability of Bifurcation Diagrams 137

C. Calculating Bifurcation Varieties 139

D. A Hysteresis Variety of the Edelstein Network .149

E. Enumeration of Bifurcation Diagrams 154

F. A Flowchart for Determining Bifurcation Diagrams 160

G. Bifurcation Varieties of Reduced Steady State Problems 163

Isolas 164

Quadratic Steady State Equations 166

Cubic Steady State Equations 168

Quartic Steady State Equations 172

V. SYSTEMATIC MODELING OF BISTABILITY IN CHEMICAL REACTION SYSTEMS 178

A. Introduction 178

B. A Modeling Approach to Bistability 180

C. Elements in the Substrate-Inhibition Mechanism Essential for Bistability 186

D. Mechanism and Models of the Peroxidase-Oxidase Reaction 195

E. A Bistable Model for the PO Reaction 199

Bistability and Damped Oscillations 205

Dominant Extreme Currents in the 3 Steady States 215

Simulation of Closed System Kinetics 219

Network Steady States vs. Experimental Bistability 223

F. Conclusions 224

Bibliography 227

APPENDIX A 231

APPENDIX B 233

APPENDIX C 235

APPENDIX D 237

APPENDIX E 240

APPENDIX F 241

APPENDIX G 242

List of Tables

Table page

III.1 State Sets of Cubic Steady State Equations 89

III.2 Bifurcation Sets of Cubic Steady State Equations 90

III.3 State Sets of Quadratic Steady State Equations 108

III.4 Bifurcation Sets of Quadratic Steady State Equations 108

IV.1 A Hysteresis Variety of the Edelstein Network 153

IV.2 Bifurcation Varieties and Rank of a Bifurcation Problem 162

IV.3 Singularity Types for the Isola and Hysteresis Varieties 162

V.1 Two-faces of the Π_V of Network N_{17} 190

V.2 Elementary Processes in the Peroxidase-Oxidase (PO) Reaction Mechanism 198

V.3 $\alpha_d(h,j)$ for the PO Bistable Model (d=7) 206

V.4 Computed Steady State Concentrations of all Species in the PO Bistable Model 212

V.5 Computed Eigenvalues of the Jacobian Matrix for the Linearized Dynamics of the PO Bistable Model 214

V.6 Computed Steady State Concentrations of all Species in the PO Bistable Model 217

List of Figures

Figure — Page
1.1 The Cusp Catastrophe Manifold 10
2.1 The Current Cone C_v for a Simple Network 40
2.2 Extreme Subnetworks of the Edelstein Network 45
2.3 The Current Polytope Π_v of the Edelstein Network 47
2.4 Π_v of Network N_4 51
2.5 Trajectories on the Phase Plane for Network N_5 61
Steady State Manifold *M* of Network N_5 62
2.6 Steady State Manifold *M* of Network N_6 64
2.7 Phase Portrait and *M* of Network N_7 66
2.8 Phase Portraits of Network N_8 69
2.9 Graph of Steady State X° as a function of k_1 for Network N_8 71
2.10 Steady State S° and α_d as functions of E_t for Network N_{10} 80
3.1 Portion of the Cusp Catastrophe Manifold Corresponding to the Positive Roots of the Cubic 86
3.2 Regions on the ρ_1-ρ_0 plane where there are 0,1,2,3 Positive Roots of the Cubic 88
3.3 Flowchart for Determining the State Sets and Bifurcation Sets for the Cubic 92-94
3.4 State Sets of the Edelstein Network for the case $k_1=k_{-1}=k_2=k_{-2}=k_3=k_{-3}=1$ 99
3.5 State Sets for the Cubic when the Steady States

are Bounded 101

3.6 The Fold Catastrophe and Positive Roots of the Quadratic 107

3.7 Roots of the Cubic Characteristic Polynomial on the ρ_1-ρ_0 plane 112

3.8 Roots of the Quadratic Characteristic Polynomial on the α_1-α_2 plane 116

3.9 Limit Cycle of the Brusselator and its collapse to a stable focus when the Hopf Bifurcation Set is crossed 120

3.10 Presence or absence of a Limit Cycle for the Oregonator on either side of the Hopf Bifurcation Set 122

3.11 The Swallowtail Catastrophe 124

3.12 Bifurcation Sets and Diagrams for the Quartic 126

3.13 State Sets of Quartic Steady State Equations 128-130

4.1 Three Unstable Bifurcation Diagrams and their Perturbations 141

4.2 Bifurcation Varieties for the Finite Element Analogue of the Euler Beam Problem 157

4.3 Flowchart for Determining the Singularity Types of a Bifurcation Problem 161

4.4 Four Types of Isola Points 167

4.5 Paths-Through-the-Cusp and Corresponding Bifurcation Diagrams (Hysteresis Variety) 170

4.6 Paths-through-the-Cusp (Isola Variety) 171

4.7 Bifurcation Diagrams Corresponding to Figure 4.6 173

4.8 How Multilocal Singularities Arise 174

4.9 Sequence of Bifurcation Diagrams for the IO_3^--H_3AsO_3 Model 177

5.1 Extreme Subnetworks of the Reversible Substrate-Inhibition Enzyme Mechanism 189

5.2 Π_v of the Reduced Substrate-Inhibition Mechanism 192

5.3 Minimal Bistable Model for the Substrate-Inhibition Mechanism and Graph of v(S) vs. S 196

5.4 Four Important Extreme Currents in the PO Mechanism 202

5.5 Network Diagram of the PO Bistable Model 204

5.6 Π_v and $\alpha_6=0$ curve for the PO Bistable Model 207

5.7 Damped and Synchronous Oscillations in the PO Model 213

5.8 Steady State of NAD$\cdot$ vs. E_t 216

5.9 Simulation of Closed System Kinetics using the PO Model 220

5.10 Steady Rate of Oxygen Consumption vs. Initial Oxygen Concentration from the PO Model 222

I. INTRODUCTION

A. Formulation of the Problem

This work is concerned with the steady states of chemical reaction systems. A chemical species is at steady state if its concentration is constant in time, and we say that a reaction system is at steady state if all the pertinent species involved are at steady state simultaneously. For example, chemical equilibrium is the only steady state for a system that is not interacting with its environment; this system eventually evolves towards this equilibrium point no matter what the initial conditions are. Non-equilibrium steady states may also occur in systems that are open to mass or energy flux and may result to far more interesting behavior. For example, when the right set of reactions occur in a continuous flow stirred tank reactor (CSTR), one may be able to observe exotic dynamical features like sustained oscillations(42), the existence of more than one stable steady state (multistability)(12,31,42,61) and even chaotic oscillations (42,48,49). These 'far-from-equilibrium' phenomena are usually caused by certain features in the coupled reactions, an example of which is the presence of appropriate nonlinear feedback in the mechanism.(4)

The problems that are considered in this work can quickly be understood using an example of a realistic mechanism. We therefore look at the following mechanism of the peroxidase-oxidase(43,47) reaction which will be analyzed in detail in Chapter V:

$$
\begin{array}{lrcl}
R_1 & Per^{3+} + H_2O_2 & \rightarrow & CoI \\
R_2 & CoI + NADH & \rightarrow & CoII + NAD\cdot \\
R_3 & CoII + NADH & \rightarrow & Per^{3+} + NAD\cdot \\
R_4 & CoIII + NAD\cdot & \rightarrow & CoI + NAD^{+} \\
R_5 & Per^{3+} + O_2^{\cdot -} & \rightarrow & CoIII \\
R_6 & NAD\cdot + O_2 & \rightarrow & NAD^{+} + O_2^{\cdot -} \\
R_7 & H^{+} + O_2^{\cdot -} + NADH & \rightarrow & H_2O_2 + NAD\cdot \\
R_8 & 2NAD\cdot + H^{+} & \rightarrow & NADH + NAD^{+} \\
R_9, R_{10} & & \rightleftarrows & O_2
\end{array}
$$

where Per^{3+} = ferriperoxidase, CoI = compound I, CoII = compound II, CoIII = compound III, NADH = nicotinamide adenine dinucleotide and $O_2^{\cdot -}$ = superoxide anion radical. The reactions will be referred to using their labels given on the leftmost column. The pseudo-reactions R_9 and R_{10} represent a continuous supply of oxygen from the environment. To describe the dynamics of the reaction system, one first decides which of the species are to be taken as 'dynamical species'. This decision depends much on the relevant experimental conditions. In the present case, the concentration of NADH is usually taken in excess in related experiments(42) and can therefore be assumed constant. The product NAD^+ is terminal and does not participate further in the feedback loops present in the mechanism; therefore, it will not be necessary to include it in the equations describing the evolution of the system. Finally, the system is buffered at a fixed pH so that the concentration of H^+ is constant. Assuming a mass-action rate expression for each reaction, the kinetic equations under isothermal and homogeneous conditions are written as follows (the symbol [ ] means 'concentration of'):

$$
\begin{aligned}
d[H_2O_2]/dt &= k_7[O_2^{\cdot -}] - k_1[H_2O_2][Per^{3+}] \\
d[NAD\cdot]/dt &= -k_6[O_2][NAD\cdot] + k_7[O_2^{\cdot -}] + k_2[CoI] \\
&\quad +k_3[CoII] - k_4[NAD\cdot][CoIII] - 2k_8[NAD\cdot]^2 \\
d[O_2^{\cdot -}]/dt &= k_6[O_2][NAD\cdot] - k_7[O_2^{\cdot -}] - k_5[Per^{3+}][O_2^{\cdot -}] \\
d[O_2]/dt &= k_9 - k_{10}[O_2] - k_6[O_2][NAD\cdot] \qquad (1.1) \\
d[Per^{3+}]/dt &= -k_1[H_2O_2][Per^{3+}] + k_3[CoII] - k_5[Per^{3+}][O_2^{\cdot -}] \\
d[CoI]/dt &= k_1[H_2O_2][Per^{3+}] - k_2[CoI] + k_4[NAD\cdot][CoIII] \\
d[CoII]/dt &= k_2[CoI] - k_3[CoII] \\
d[CoIII]/dt &= k_5[Per^{3+}][O_2^{\cdot -}] - k_4[NAD\cdot][CoIII] .
\end{aligned}
$$

Note that the constant concentrations of the non-dynamical species are incorporated in the rate constants of the corresponding reactions where they are found as reactants.

To solve the set of equations (1.1), the values of the 10 rate constants as well as the initial concentrations for the 8 species must be specified. The behavior of the solutions (that is, the changes in the individual species concentrations as functions of time) may vary wildly depending on the values of the parameters (rate constants and initial conditions) used. Are there sets of parameters that will lead to sustained or damped oscillations? Of primary interest in the present work are the following questions: Is there always a steady state, and if there is, is it always unique? What are the conditions on the rate constants that will lead to multiple steady states? The results that will be shown in Chapter V claim that for the mechanism given above, there are rate constants that will give three steady states - two of these are stable and each can be reached with the right set of initial conditions. Other sets of rate constants may give 2, 1 or 0 steady states.

The number and values of the steady states of a chemical reaction system are determined by the rate constants and an additional set of parameters called 'conservation constraints'. Observe in (1.1) that the sum (d[Per^{3+}]/dt + d[CoI]/dt + d[CoII]/dt + d[CoIII]/dt) vanishes identically implying that the total concentration of the enzymic species Per^{3+}, CoI, CoII and CoIII is always conserved. Thus, for system (1.1), a total of 11 *steady state parameters* are needed to determine the number and values of the steady states. (We reserve the symbol **p** for the vector of steady state parameters throughout this work). It is a totally different question to ask which steady state will be reached (assuming no oscillations) when there are more than one steady state. In this case, specifying the rate constants and initial conditions are sufficient to answer the question.

Let us now formulate the problem precisely. For compactness of notation, we define the 'species concentration vector' **X** whose components are the concentrations of the *n* individual dynamical species, and the 'rate constant vector' **k** whose components are the *r* rate constants. The expressions on the right sides of the '=' signs above are functions of $(\mathbf{X},\mathbf{k})$ and are symbolized as $f_1(\mathbf{X},\mathbf{k})$, $f_2(\mathbf{X},\mathbf{k})$, ..., $f_n(\mathbf{X},\mathbf{k})$, respectively. Next, we gather these functions to form the components of the vector **F**, that is, $\mathbf{F}(\mathbf{X},\mathbf{k}) = (f_1, f_2, ..., f_n)$. Thus, the set of differential equations given above can be written succinctly as

$$d\mathbf{X}/dt = \mathbf{F}(\mathbf{X},\mathbf{k}) \ . \qquad (1.2)$$

Unless certain physical bounds are specified, it will be convenient to take the domain of **X** as the whole positive orthant of n-dimensional Euclidean space, R^n_+, and the domain of **k** to be R^r_+.

In general, chemical reaction systems give rise to a special class of nonlinear ordinary differential equations as a result of 'stoichiometry', that is, the property of each chemical reaction indicating a definite proportion between the reactants and products. For this reason, we shall also refer to these systems as stoichiometric dynamical systems. In the remainder of this introductory chapter, we will show that the vector function **F** can be expressed as a product of two factors, one associated with stoichiometry while the other contains the rate expressions for each individual reaction. This serves as a motivation for the discussion presented in Chapter II where the stage is set by analyzing geometrically the full system of nonlinear dynamical equations bringing out clearly the influence of stoichiometry on the structure of the space where all the solutions of the differential equations reside. The analysis of the geometry of steady states starts in this chapter by discussing Clarke's(4) result that the set of steady state velocities (which he called 'currents') are all found in a convex cone called the 'current cone', C_v. The cross-section of C_v called the 'current polytope' Π_v has a structure that provides a systematic way of sorting any complicated mechanism. A consequence of this is a modeling approach to bistability (or, in general, multistability) in reaction systems. This is the subject of Chapter V where we also show that the mechanism just given above (which was extracted from a more comprehensive list) can model the experimentally observed bistability in the peroxidase-oxidase reaction system.(42,61) The results of Chapters III and IV were necessary for a detailed analysis of this model.

The set of all steady states in the positive orthant $R_+^n x R_+^r$ is represented by the steady state manifold M defined by the set

$$M = \{ (X^\circ, k) \in R_+^n x R_+^r \mid dX/dt = F(X^\circ, k) = 0 \} . \qquad (1.3)$$

M can be imagined as a 'hypersurface' of positive steady states embedded in (n+r)-dimensional space. (In general, the complete set of steady states include 'boundary steady states' which are discussed in the later part of Chapter II). Identifying a point on M requires a minimum number of parameters. This number is called geometrically as the dimension of M, or dim M. It includes the r rate constants and the $(n-d)$ conservation constraints (d is the number of independent species; we will also reserve the symbol C for the 'conservation constraint' vector whose components are the n-d conservation constraints). dim M is usually an inconveniently large number for realistic networks. However, we shall find that the steady state concentrations of the species are usually related to each other. In Chapter III, we will see that the problem of solving the steady states in terms of the steady state parameters **p** = (C,**k**) can sometimes be transformed into a tractable 1-dimensional problem. When this can be done, a drastic reduction on the essential parameters arises. Only a few lumped parameters are then required in determining the essential geometry of M, in particular the features that determine the number of steady states. For example, the bistable model for the peroxidase-oxidase reaction given above has an 11-dimensional *M*. It turns out that the values of only 2 lumped parameters are actually sufficient to determine its essential geometry! What we mean by the essential geometry of *M* in the context of the present problem will be discussed next.

Certain global features of *M* are known. For example, *M* cannot possess disconnected pieces and is therefore described as 'simply-connected'. A proof of this property has been given by Clarke(9). It relies on the fact mentioned above that the steady state velocities are found in a cone C_v. Mainly because of this, the set of positive steady states is shown to be diffeomorphic to a simply-connected cone. Since a diffeomorphism does not change the topological properties of a set, the conclusion that *M* is simply-connected follows. However, disconnected pieces appear when cross-sections of *M* are taken (that is, certain parameters fixed). A further consequence of the diffeomorphism between *M* and a cone is that *M* must end at the boundary of the orthant $R^n_+ x R^r_+$ and just cannot terminate or 'hang' inside this orthant.

There are important local features of *M* that affect its global appearance considerably. When *M* folds back inside the positive orthant $R^n_+ x R^r_+$, then there exists at least two isolated positive steady states for some ranges of parameter values. Figure 1.1 shows the famous cusp catastrophe manifold. When the fold points are projected down to the parameter space (the μ-p^- plane in this case), we find a curve B_{31} in parameter space separating sets of parameters that give one steady state (outside the cusp) from the set of parameters giving three steady states (inside the cusp). The parameters found on this curve form what is called the steady state bifurcation set. Thus, we say that the projection of the fold points of M onto parameter space are steady state bifurcation points. As we will see in Chapter III, these are not the only steady state bifurcation points. In general, we will call a parameter value as a bifurcation point if on either side of that value there corresponds a different number of steady states. The fold points of M are called singular points in mathematics and are characterized by the vanishing of the Jacobian associated with the set of independent kinetic equations.

Furthermore, there are singular points that are degenerate, an example of which is the cusp point itself. Figure 1.1(b) is a cut through the cusp point on the manifold. Our interest on such points lies in the fact that cuts through M on either side will give qualitatively different diagrams as exemplified by diagrams 1.1(a) and 1.1(c).

Imagine the whole of M to be projected onto parameter space. Different regions of parameter space will be 'covered' a different number of times, i.e. some will be singly-covered, doubly-covered, triply-covered, etc. The task of Chapter III will be to enumerate and identify

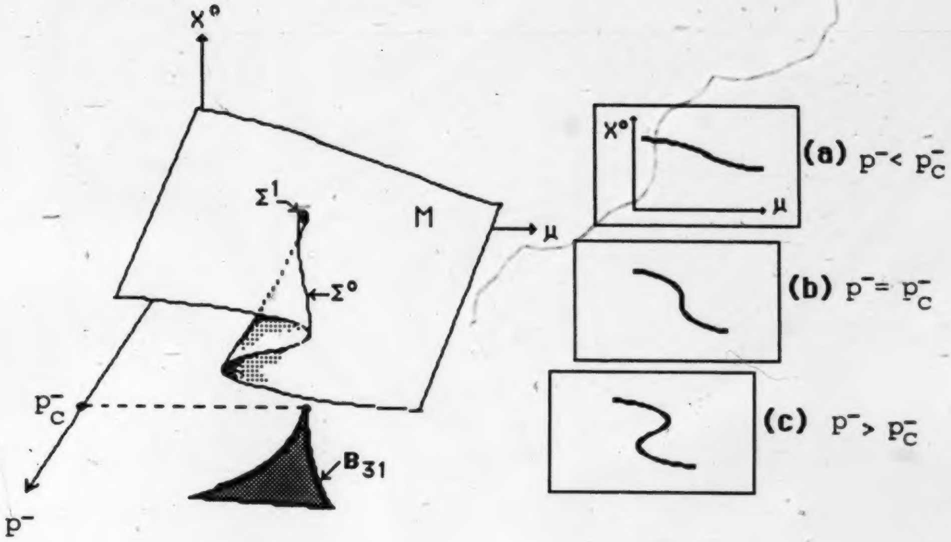

Figure 1.1

Some chemical reaction networks have steady state manifolds whose cross-sections are of the type represented by the cusp catastrophe manifold M shown above. X° is the steady state concentration of species X and μ, p^- are steady state parameters. The μ-p^- parameter plane is either singly-covered or triply-covered by M. The projection of the points where the surface folds (Σ°) onto the μ-p^- plane correspond to bifurcation points where there is a transition from 3 to 1 steady states (B_{31}). When μ is taken as the bifurcation parameter, two kinds of bifurcation diagrams (a) and (c) are possible. The cut through the cusp point (Σ^1) gives the diagram (b) which is the transition between (a) and (c).

exactly all the regions in parameter space that have different coverings. These regions in parameter space which correspond to different number of positive steady states are called collectively as state sets. The boundary between two different state sets are steady state bifurcation sets.

We must not lose sight of the fact that physical reality actually corresponds to certain cross-sections of M because we are dealing with a particular reaction system at a time. For a given experimental reaction system, there are usually very few parameters that can be externally controlled or parameters that can vary within a certain range. Most of the rate constants are intrinsic to the system being considered (at a given temperature). Parameters like flow rates and concentrations of external species can be varied and the system can be subjected to steady state analysis. Mathematically, this investigation is equivalent to making a cut through M along some direction specified by a parameter which will be called the bifurcation parameter. A cross-section of M plotted against the bifurcation parameter is called a steady state bifurcation diagram. For a given bifurcation parameter, one may be able to generate various qualitatively different bifurcation diagrams depending on the values taken for the other parameters. This idea is clearly illustrated again by figure 1.1 where the bifurcation parameter is μ. The value of the parameter p^- that corresponds to the cusp point is very important because it separates the values of p^- that will give a 'straight' (no folds) bifurcation diagram from the values of $\mathbf{p}^-$ that give Z-shaped bifurcation diagrams. In general, let the parameter vector be $\mathbf{p}=(\mu,\mathbf{p}^-)$ where μ is distinguished as the bifurcation parameter. The sets of $\mathbf{p}^-$ that delineate ? qualitatively different bifurcation diagrams are called bifurcation varieties.[1] Chapter IV is devoted to finding general expressions for these bifurcation varieties. The determination of these varieties leads the way to an exhaustive enumeration of all possible bifurcation diagrams that a reaction system can exhibit for a given bifurcation parameter.

The algebro-geometric approach I have employed in the analysis of *M* in Chapter III involves the study of the singularity structures of the cuspoid catastrophes(10). In Chapter IV, the results in particular of Golubitsky and Schaeffer(18) on the application of singularity theory to imperfect bifurcations were studied and applied. The wealth of mathematical results already available must be adapted and applied to the solution of chemical problems. Work has to be done in deriving convenient formulas that chemists can use. The applicability of these mathematical methods to chemical reaction networks will be shown explicitly by the various examples provided at each important stage of the discussions. In Chapter V, a realistic mechanism of the peroxidase-oxidase reaction with NADH (nicotinamide adenine dinucleotide) as the hydrogen-donor was analyzed. A minimal model for the bistability observed in an open system is arrived at systematically using a proposed modeling approach to complex systems with multiple steady states. The analysis of the steady states of the model is exact and comprehensive owing to the results of the preceding chapters.

---

[1] Readers familiar with the work of Golubitsky and Schaeffer(8) are forewarned that the name 'bifurcation variety' as used in this work is a collective name that includes the Hysteresis variety, Double Limit variety and the Isola Variety to be discussed in Chapter IV. This last variety is called specifically the 'bifurcation variety' by Golubitsky and Schaeffer, a practice that we will not follow.

B. Stoichiometric Network and its Kinetics

We now define precisely what we mean by a reaction network. A given network is composed of reactions whose individual rate expressions (the kinetics) can have several forms subject to certain conditions. A reaction system is a network endowed with a kinetics and the parameter values are specified.

The Meaning of a Reaction Network

Let there be *r* one-way chemical reactions R_1, R_2, ..., R_r involving *n* species X_1, X_2,..., X_n. We will consider a reversible reaction to be composed of two one-way reactions. The set of reactions can be written as

$$\sum_{i=1}^{n} \nu^{R}_{ij} X_i \rightarrow \sum_{i=1}^{n} \nu^{P}_{ij} X_i \qquad j=1,..,r \tag{1.4}$$

where ν^{R}_{ij} and ν^{P}_{ij} are the molecularities or stoichiometric coefficients of species X_i on the reactant and product side, respectively, of reaction R_j.

The species considered are only those whose concentrations have significant variation in the time scale used and are therefore dynamical species. These species will be referred to as 'internal' species as opposed to the 'external' species whose concentrations may be assumed constant throughout the reaction. Because these external species will not be written explicitly in the chemical equations, we will be seeing some 'funny'-looking reactions like $( ) \rightarrow X$, $X \rightarrow ( )$, or $X \rightarrow 2X$. The first two are pseudo-reactions which may represent diffusive exchange with the surroundings. The third reaction which per se is impossible because it does not conserve mass may actually represent a valid chemical reaction like $(A)+X \rightarrow 2X+(P)$ where (A) and (P) are external species whose 'constant' concentrations are incorporated as constants in the reaction rate expression. Thus, the formalism now being presented subsumes open systems like a continuous flow stirred-tank reactor (CSTR) and heterogeneous systems where some or all species are diffusing. In fact, a heterogeneous system can be modeled by breaking it up into interconnected cells (see for example reference 1) and species are diffusing in and out of the cells due to concentration gradients. In further discussions, unless otherwise noted, we will understand the set of species S to be the set of internal species:

$$S = \{ X_1, X_2, \ldots, X_n \} . \qquad (1.5)$$

A precise language associated with the description of the set of reactions R is available$^{(1,2)}$. The entity on either side of the reaction arrow is called a complex. For example, in the reaction A+2B → 3C, the two complexes are (A+2B) and (3C). Thus, we can say that R is a 'reacts to' binary relation among the complexes$^{(1)}$. To each complex, there is an associated complex vector which has n components. These components are the stoichiometric coefficients of the n species (of the network) in the complex. For the 3 species reaction in the present example, the complex (A+2B) corresponds to the complex vector (1,2,0) while (3C) corresponds to the complex vector (0,0,3). In general, let the set of complexes (assuming there are s distinct complexes) corresponding to the set of reactions (1.2) be

$$C = \{ C_1, C_2, \ldots, C_s \} . \qquad (1.6)$$

A reaction network can now be defined formally:

Definition 1.1.

A reaction network is the set $N = \{ S, C, R \}$. (1.7)

Strictly speaking, the above definition will consider two networks to be different if their set of chemical species are not identical although the reaction set may be the same. Mathematically, however, the problems represented by these networks will be identical.

Kinetics Assigned to a Reaction Network

Let v_j be the rate of reaction R_j. Due to this single reaction, the rate in the change of the concentration of species X_i is

$$(dX_i/dt)_j = (\nu^P_{ij}-\nu^R_{ij})v_j$$

and the total rate due to all reactions is

$$dX_i/dt = \sum_{j=1}^{r} (\nu^P_{ij}-\nu^R_{ij})v_j \ . \tag{1.8}$$

This equation can be written in a vector notation which permits a clear geometric interpretation of the solutions later on. Let $\mathbf{X} \in R^n_+$ be a vector in the non-negative orthant of n-dimensional Euclidean space. This is called the (species) concentration vector whose components are the concentrations of all internal species at some time t. Define the reaction vector ν_j associated with reaction R_j as the difference between the product complex vector and the reactant complex vector:

$$\begin{aligned} \nu_j &= \mathbf{V}^P_j - \mathbf{V}^R_j \\ &= (\nu^P_{1j},\ldots,\nu^P_{nj})' - (\nu^R_{1j},\ldots,\nu^R_{nj})' \ . \end{aligned} \tag{1.9}$$

Equation (1.8) now acquires the form

$$dX/dt = \sum_{j=1}^{r} v_j \nu_j \ .$$

Alternatively, in the formal treatment of Gavalas(3) and Clarke(4), for example, the r reaction vectors are treated as the columns of the stoichiometric matrix ν. If we now consider the rates v_j as components of the velocity vector in the non-negative orthant of r-dimensional Euclidean space, R^r_+, the set of kinetic equations has the compact form

$$dX/dt = \nu v(X,k) \ . \qquad (1.10)$$

Notice that the velocity vector v is in general a function of **X** and some rate parameters given by the vector **k**. The form that v takes is casually referred to as the kinetics of the reaction network. A given network can be endowed various different kinetics leading to different dynamical behaviors. Various authors(1,3,5,6) have discussed the requirements on the acceptable forms of v. The most essential of these requirements is that if $\nu_{ij}<0$ then as X_i approaches zero, the velocity v_j must approach zero and $dX_i/dt \geq 0$. This ensures that all concentrations are non-negative. We therefore adopt the following postulate stated by other authors(3,5) previously.

Postulate I.

The velocity functions $v_j \epsilon R_+$ $(j = 1,\dots,r)$ are defined and continuous in R_+^n. For any $X_i = 0$, we must have $\nu_{ij} v_j \geq 0$, $(j = 1,\dots,r)$.

When the kinetics is power law (in particular, mass action), v has the form

$$v = (\text{diag } k) X^{\kappa} \tag{1.11}$$

where (diag k) is a rxr diagonal matrix whose diagonal is $k \epsilon R_+^r$, a vector whose components are the rate constants of the network reactions; X^{κ} is a r-component vector whose j-th component is given by

$$(X^{\kappa})_j = \prod_{i=1}^{n} X_i^{\kappa_{ij}} \ . \tag{1.12}$$

Usually a small integer, κ_{ij} is the order of the reaction R_j with respect to species X_i. This defines the components of the nxr kinetic matrix κ.

Example I.1

Several of the networks that we will be considering are 'mathematical models' whose component 'reactions' do not actually correspond to the elementary reaction steps in the mechanism but are representations of the experimentally determined rate laws of reaction processes, as this example will illustrate.

The following network is a 2-species mathematical model for the iodate oxidation of arsenous acid in a continuous flow stirred tank reactor. This model gave a near quantitative description of the experimental reaction system (with arsenous acid in stoichiometric excess), including the appearance of hysteresis, mushroom and isola, as demonstrated by the work of Ganapathisubramanian and Showalter(7).

Network N_1

R_1, R_{-1} $\rightleftarrows X$

R_2, R_{-2} $\rightleftarrows B$

R_3 $B + X \rightarrow 2X$

R_4 $B + 2X \rightarrow 3X$

B corresponds to IO_3^- while X corresponds to I^-. The network as given above was assigned kinetics of the mass action form although obviously the reaction steps are not the elementary steps in the actual mechanism which is, in fact, much more complex. Let us now see how this mathematical model was arrived at using some experimental information. There are two known processes that dominate the iodate-arsenous acid reaction, namely, the Dushman reaction (A) and the Roebuck reaction (B).

$$IO_3^- + 5I^- + 6H^+ \rightarrow 3I_2 + 3H_2O \tag{A}$$

$$I_2 + H_3AsO_3 + H_2O \rightarrow 2I^- + H_3AsO_4 + 2H^+ \tag{B}$$

When arsenous acid is in stoichiometric excess, the net reaction is given by (A) + 3(B) = (N):

$$IO_3^- + 3H_3AsO_3 \rightarrow I^- + 3H_3AsO_4 \ . \tag{N}$$

The kinetics of process A has been determined experimentally(8) as having the form

$$v_n = (k + k'[I^-])[I^-][IO_3^-][H^+]^2$$

where k and k' are some rate constants. It is also known that process A is rate determining for the overall reaction. From the stoichiometric relation between IO_3^- and I^- in the net reaction (N), the dynamical equations of the system in the continuous flow reactor are

$$d[I^-]/dt = v_n + k_1'[I^-]_0 - k_{-1}'[I^-]$$
$$d[IO_3^-]/dt = -v_n + k_2'[IO_3^-]_0 - k_{-2}'[IO_3^-]$$

where k_1', k_{-1}', k_2' and k_{-2}' are flow rate constants not necessarily equal. With pH constant, these dynamical equations are fully modeled by network N_1 given above. ■

II. GEOMETRIC ASPECTS OF STOICHIOMETRIC DYNAMICAL SYSTEMS

A. Introduction

In this chapter we look at the whole dynamical setting of reaction kinetics of which the steady states are just a part, but a part that exerts a significant influence on the overall portrait of the kinetics. Under homogeneous and isothermal conditions, the instantaneous state of a given reaction system is specified by the set of concentrations of the chemical species present. All the possible chemical interactions among these species that modify the composition of the system form a network of reactions which the chemical kineticist would like to elucidate as completely as possible. With some observed or postulated kinetics assigned to each of these reactions the kineticist comes up with a system of autonomous ordinary differential equations that hopefully simulates the state evolution of the system. A criterion for a rigorous description of this evolution or dynamics of the system will now be described.

If we establish a Euclidean coordinate system wherein a point in the non-negative orthant corresponds to the instantaneous concentrations of the system, then the evolution of the state of the system will correspond to the motion (or trajectory) of this point as time goes on. We will sometimes refer to this space as as 'concentration space', 'state space' or in a more restricted sense, 'phase space'. The initial point of this trajectory (i.e. initial concentrations of the reacting species) as well as the equations of motion (our kinetic equations) will completely specify the course of evolution of any given experiment (assumption: the deterministic equations of motion are followed by the system). If we imagine that all initial conditions are tried, then in state space one gets an infinite number of trajectories whose portrait is a consequence of the form of the equations of motion. The forms of these equations of course is a property of the system. Hence, a complete description of the system requires a picture of the set of all possible trajectories in n-dimensional state space, where n is the number of species. Such a system, i.e. a set of trajectories each specified by an initial condition and equations of motion, will be referred to as a dynamical system. I believe that the most comprehensive way of studying the kinetic equations of chemistry requires treating them as dynamical systems. The characterization of the trajectories in the different regions of state space and the study of the changes of the phase portraits under different experimental conditions should be the basis for the description of any physical system in general. In this chapter, I present the kinetic equations as much as possible in the language of dynamical systems. We have in hand a special class of ordinary differential equations whose phase spaces are strongly influenced by stoichiometry.

The studies being presented in this chapter can be grouped into three parts : (i) sections B-E present the nonlinear and linearized dynamical equations in forms that give the 'factorization' in terms of stoichiometry and kinetics, and then these equations are used to bring out the influence of stoichiometry on the geometry of the phase space where all the possible trajectories could lie; (ii) sections F-H then focus on the set of steady states and discuss the convex geometry of the set of steady state velocities, an important feature in Clarke's(4) formalism called stoichiometric network analysis; (iii) finally, sections I-K will illustrate the fact that the complete set of steady states may include not only the steady state manifold *M* (surface of positive steady states analyzed in chapters III and IV) but also, in certain cases, boundary steady states having some species extinct; furthermore, related cases where there are stoichiometric explosions or extinction, and the emergence of a continuum of steady states are discussed.

B. The Nonlinear Dynamical Equations

Because of the strong influence of stoichiometry on the solutions, we shall refer to the following set of autonomous ordinary differential equations induced by a given reaction network as a stoichiometric dynamical problem :

$$dX/dt = \nu v(X,k) \quad , \quad X(t=0) = X(0) \tag{2.1}$$

where $X \in R^n_+$ and $v : R^n_+ x R^r_+ \to R^r_+$. For a given form of v, when the rate parameter vector $k \in R^r_+$ is specified (along with the initial condition $X(0)$), then we have what is called a stoichiometric dynamical system. In addition, Postulate I given in the first chapter is assumed for any such system that is studied in the present work. To solve (2.1), there are $(n+r)$ parameters that must be specified - n initial conditions $X(0)$, and r rate parameters like rate constants k.

Equation (2.1) acquires an elegant form when we switch to scaled dynamical variables as was done by Clarke(4). This form assumes that the steady state $X°$ is strictly positive, i.e. $X_i>0$ for all $i = 1,..,n$. Define the scaled concentration x_i as

$$x_i = X_i/X_i^\circ \quad ; \; i = 1,...,n$$

or in matrix form

$$x = (\text{diag } 1/X°)X \tag{2.2}$$

where (diag $1/X°$) is a diagonal matrix with $1/X° \equiv (1/X_1^\circ, ..., 1/X_n^\circ)$ on the diagonal. Differentiating (2.2) with respect to time and substituting (2.1) results to

$$dx/dt = (\mathrm{diag}\ 1/\mathbf{X}^\circ)\nu \mathbf{v}(\mathbf{X},\mathbf{k}) \ . \qquad (2.3)$$

When the kinetics is power law (in particular, mass action), $\mathbf{v}$ can be expressed explicitly in terms of $\mathbf{x}$ as follows :

$$\begin{aligned} v_j &= k_j \prod_{i=1}^{n} X_i^{\kappa_{ij}} \\ &= (k_j \prod_{i=1}^{n} (X_i^\circ)^{\kappa_{ij}}) \prod_{i=1}^{n} x_i^{\kappa_{ij}} \\ &= v_j^\circ \prod_{i=1}^{n} x_i^{\kappa_{ij}} \end{aligned}$$

or in matrix form

$$\mathbf{v} = (\mathrm{diag}\ \mathbf{v}^\circ)\mathbf{x}^{\kappa} \qquad (2.4)$$

where the j-th component of the vector $\mathbf{x}^{\kappa}$ is $(\mathbf{x}^{\kappa})_j = \prod_{i=1}^{n} x_i^{\kappa_{ij}}$ and $\mathbf{v}^\circ$ is the steady state velocity vector corresponding to the steady state $\mathbf{X}^\circ$.

Thus, for power law kinetics (in particular, mass action kinetics), the stoichiometric dynamical equations have the form

$$dx/dt = (\mathrm{diag}\ 1/\mathbf{X}^\circ)\nu(\mathrm{diag}\ \mathbf{v}^\circ)\mathbf{x}^{\kappa} \ . \qquad (2.5)$$

Note that the factor $(1/X_i^\circ)$ $(i=1,\ldots,n)$ gives each equation a characteristic time scale for the motion.

C. Constraints on Phase Space due to Stoichiometry

The stoichiometry in a chemical reaction network is coded in the stoichiometric matrix ν. From the equation of motion (equation 2.1 or 2.5), one expects that ν must play a major role in the geometry of the phase space of the dynamical system. By 'phase space' we mean the space where all solutions (trajectories) $\mathbf{X}(t;\mathbf{X}(0))$ of the dynamical problem are found.

Due to the conservations of atoms and net charge in each reaction, and sometimes of certain species or other subunits in the course of all the reactions, some combinations of species concentrations are maintained. These conservation constraints can be considered as a consequence of stoichiometry as will now be shown. Let there be d $(\leq n)$ independent species so that there are $(n-d)$ conservation conditions:

$$\sum_{i=1}^{n} \gamma_{mi} X_i = C_m \qquad m = 1,\ldots,n-d$$

or in matrix form

$$\gamma\mathbf{X} = \mathbf{C} \tag{2.6}$$

where γ is an (n-d)xn conservation matrix and $\mathbf{C} \in R_{+}^{n-d}$ is a vector of conservation constraints. Note that $\mathbf{C}$ is specified implicitly by the initial conditions $\mathbf{X}(0)$. To prove that γ

is a consequence of ν and is independent of the kinetics, differentiate (2.6) with respect to time and substitute (2.1) to get $\gamma\nu v=0$ for any v. Thus,

$$\gamma\nu = 0 \ . \tag{2.7}$$

This equation means that γ can be derived from ν. The rows of γ are vectors in the left null space of ν.

Another way (but completely equivalent) of showing the effect of stoichiometry on the phase space is to use the reaction vectors, ν_j (j=1,...,r), defined in (1.9). We have seen that equation (2.1) can be written as

$$dX/dt = \sum_{j=1}^{r} v_j \nu_j \tag{2.8}$$

where ν_j is the j-th column of ν (or the j-th reaction vector) and v_j is the correponding component of the velocity vector v. Equation (2.8) says that the species formation vector (dX/dt) is always a non-negative linear combination of the reaction vectors ν_j (j = 1,...,r). In other words, (dX/dt) is found in a subspace (of R^n) spanned by the columns of ν. This subspace is called$^{(1,2)}$ the stoichiometric subspace, S_ν. The dimension of S_ν is equal to the number of independent columns of ν (≡ rank ν) which is also equal to the number of independent species, d.

The initial condition X(0), and S_ν (or indirectly, ν) are sufficient to determine completely the space where all solutions $\mathbf{X}(t;\mathbf{X}(0))$ of (2.1) lie (the phase space). Integrating (2.8) after an arbitrary time t,

$$\mathbf{X}(t)-\mathbf{X}(0) = \sum_{j=1}^{r} \{\textstyle\int_0^t v_j dt\}\nu_j = \sum_{j=1}^{r} d_j \nu_j \qquad (d_j \geq 0)$$

implying that

$$\mathbf{X}(t)-\mathbf{X}(0) \in S_\nu$$

or

$$\mathbf{X}(t) \in \{\mathbf{X}(0)+S_\nu\}$$

where

$$\{\mathbf{X}(0)+S_\nu\} = \{ \mathbf{X} \mid \mathbf{X}=\mathbf{X}(0)+\xi \ , \ \xi \in S_\nu \} . \tag{2.9}$$

This last set is called(1,2) the stoichiometric compatibility class represented by $\mathbf{X}(0)$. $\mathbf{X}(t_1)$ and $\mathbf{X}(t_2)$ are said to be stoichiometrically compatible if and only if both are members of $\{\mathbf{X}(0)+S_\nu\}$ for some $\mathbf{X}(0)$. Since $\mathbf{X} \geq 0$, we are only interested in the intersection of $\{\mathbf{X}(0)+S_\nu\}$ and R_+^n. This intersection is a polyhedron and is identical to Clarke's(4) concentration polyhedron $\Pi_x(C)$ which is defined by

$$\Pi_x(C) = \{ \mathbf{X} \in R_+^n \mid \gamma\mathbf{X}=C \ , \ C \in R_+^{n-d} \} . \tag{2.10}$$

The equivalence between $\Pi_x(C)$ and $\{\mathbf{X}(0)+S_\nu\}$ is easily understood in the following way: The initial condition $\mathbf{X}(0)$ determines the conservation constraint vector C. The definition of S_ν involves using the stoichiometric matrix ν which we have shown to determine the conservation matrix γ. We are assured that solutions of the stoichiometric dynamical problem starting inside $\Pi_x(C)$ will at any time remain inside it. This is a consequence of Postulate I.

D. Dynamics and Steady States of a CSTR

Let us now illustrate the ideas discussed in the preceding section by considering a constant-volume, isothermal continuous flow stirred tank reactor (CSTR). The CSTR is a popular open system among experimentalists who investigate exotic chemical kinetics like sustained oscillations, multiplicity of steady states and chaos. Below is a list of the quantities to be used in the analysis.

X : vector (ϵ R^n_+) of concentrations of all molecular or ionic species that are present at some time in the reactor

A : vector (ϵ R^m_+) of concentrations of the (m-1) atoms and net charge (the m-th component) present at some time in the reactor

γ° : (mxn) atom/charge conservation matrix v : vector ($\in R^r_+$) of 'true' chemical reactions, i.e. excluding the pseudo-reactions corresponding to the flux of species through the reactor

k_0 : flow rate constant

The net charge in the reactor is assumed to be zero. The m-th row of γ° contains the ionic charges (including algebraic signs) of the ionic/molecular species. At any time t,

$$\mathbf{A}(t) = \gamma^\circ \mathbf{X}(t) \tag{2.11}$$

with the m-th equation corresponding to the zero net charge:

$$\sum_{i=1}^{n} \gamma^\circ_{mi} X_i = 0 \ .$$

This equation determines a hyperplane passing through the origin and entering the positive orthant of R^n.

Assume a constant species concentration $\mathbf{X}_f$ in the feed stream. Due to the chemical reactions occurring inside the reactor and the flux through it, the rate of species formation is

$$d\mathbf{X}/dt = \nu v + k_0(\mathbf{X}_f - \mathbf{X}) \ . \tag{2.12}$$

Differentiating equation (2.11) with respect to time and substituting (2.12) gives the rate of change in the atom/charge concentration vector:

$$dA/dt = \gamma^{\circ}\nu v + k_0\gamma^{\circ}(X_f - X) \ . \tag{2.13}$$

But chemical reactions do not create nor produce atoms so

$$\gamma^{\circ}\nu = 0 \ . \tag{2.14}$$

This equation is always followed by the set of r true chemical reactions both for closed and open systems. Using equation (2.11) into (2.13), we get

$$dA/dt = k_0(A_f - A(t)) \tag{2.15}$$

which integrates to

$$A(t) = [A(0) - A_f]e^{-k_0 t} + A_f \tag{2.16}$$

where $A(0)$ is the atom concentration inside the reactor at t=0 while A_f is the constant feed stream concentration corresponding to X_f. What equation (2.16) says is that the effect of the initial condition $A(0)$ quickly disappears and the state of the system is eventually determined by the influx A_f. In other words, the state trajectories rapidly approach the manifold defined by $dA/dt = 0$ or $A(t) = A_f$, or in terms of the molecular/ionic species concentrations,

$$\gamma^{\circ}(X-X_f) = 0 \ . \tag{2.17}$$

It is now important to realize that although dA/dt = 0, dX/dt may not vanish. We will define as the steady state of the CSTR the set of X° satisfying $dX/dt = dA/dt = 0$ corresponding to the following system of equations:

$$\begin{aligned} \gamma^{\circ}(X_f-X^{\circ}) &= 0 \\ \nu v(X^{\circ},k)+k_0(X_f-X^{\circ}) &= 0 \ . \end{aligned} \tag{2.18}$$

Example II.1

The following seven-step (reversible) mechanism for the autocatalytic reaction between ferrous ion and nitric acid was used by Orban and Epstein⁽¹²⁾ to simulate the observed bistability in a CSTR.

Fe^{2+}-HNO_3 System

$R_{1,-1}$ $Fe^{2+} + NO_3^- + 2H^+ \rightleftarrows Fe^{3+} + NO_2 + H_2O$

$R_{2,-2}$ $Fe^{2+} + NO_2 + H^+ \rightleftarrows Fe^{3+} + HNO_2$

$R_{3,-3}$ $Fe^{2+} + HNO_2 + H^+ \rightleftarrows Fe^{3+} + NO + H_2O$

$R_{4,-4}$ $Fe^{2+} + NO \rightleftarrows FeNO^{2+}$

$R_{5,-5}$ $2NO_2 + H_2O \rightleftarrows HNO_2 + NO_3^- + H^+$

$R_{6,-6}$ $2HNO_2 \rightleftarrows NO + NO_2 + H_2O$

$R_{7,-7}$ $NO + NO_3^- + H^+ \rightleftarrows NO_2 + HNO_2$

There are 9 species and 14 reactions. Let $\mathbf{X}$ = ($[Fe^{2+}]$, $[Fe^{3+}]$, $[FeNO^{2+}]$, $[H^+]$, $[H_2O]$, $[NO_3^-]$, $[NO_2]$, $[HNO_2]$, $[NO]$)'. In the stoichiometric matrix ν given below, we give only the first seven columns corresponding to the forward reactions numbered as listed in the above table. The columns corresponding to the reverse reactions are just the negative of the columns of corresponding forward reactions.

$$\nu = \begin{bmatrix} -1 & -1 & -1 & -1 & 0 & 0 & 0 \\ 1 & 1 & 1 & 0 & 0 & 0 & 0 \\ 0 & 0 & 0 & 1 & 0 & 0 & 0 \\ -2 & -1 & -1 & 0 & 1 & 0 & -1 \\ 1 & 0 & 1 & 0 & -1 & 1 & 0 \\ -1 & 0 & 0 & 0 & 1 & 0 & -1 \\ 1 & -1 & 0 & 0 & -2 & 1 & 1 \\ 0 & 1 & -1 & 0 & 1 & -2 & 1 \\ 0 & 0 & 1 & -1 & 0 & 1 & -1 \end{bmatrix}$$

Let the atom/charge concentration vector be $\mathbf{A}$ = ([Fe], [N], [O], [H], [charge])'. The atom/charge conservation matrix γ° is

$$\gamma^{\circ} = \begin{bmatrix} 1 & 1 & 1 & 0 & 0 & 0 & 0 & 0 & 0 \\ 0 & 0 & 1 & 0 & 0 & 1 & 1 & 1 & 1 \\ 0 & 0 & 1 & 0 & 1 & 3 & 2 & 2 & 1 \\ 0 & 0 & 0 & 1 & 2 & 0 & 0 & 1 & 0 \\ +2 & +3 & +2 & +1 & 0 & -1 & 0 & 0 & 0 \end{bmatrix}$$

One can check that

$$\gamma^{\circ}\nu = \mathbf{0} \, . \qquad (2.19)$$

The rank of ν is 4 and therefore the rank of γ° must be 5 which, in fact, is the case. This justifies the inclusion of the row of γ° corresponding to the conservation of the net charge in the reactor. Thus, there are only 4 independent species out of the 9 species. For example, we can choose Fe^{2+}, $FeNO^{2+}$, H^+ and NO as the independent ones. The concentrations of the dependent species in terms of the independent ones are given by equation (2.17).■

E. Linearization of the Dynamical Equations

It is rarely possible to obtain closed-form solutions for nonlinear differential equations. In contrast, the theory of linear differential equations is well established, and the qualitative picture of the trajectories around the steady states can be determined using certain tests. In this section, we present the forms taken by the linearized equations of motion for reaction networks.

Observe from the nonlinear equations (2.5) that $\mathbf{x}^\circ = \mathbf{e}_n \equiv (1,1,\ldots,1)^t$ is a particular steady state solution corresponding to $\mathbf{X}^\circ$ (see equation 2.2). Let us express the right hand side of the dynamical equations (equation 2.5) in terms of factors of $(\mathbf{x}-\mathbf{e}_n)$. For example,

$$dx_i/dt = \Sigma_j\, m_{ij}(x_j-1) + \Sigma_{j,k}\, d_{ijk}(x_j-1)(x_k-1) + \ldots \qquad (2.20)$$

Let us assume that each reaction in the network has mass action kinetics which is utmost bimolecular. Then equation (2.20) has the following matrix-vector form ($\zeta = \mathbf{x} - \mathbf{e}_n$) :

$$d\zeta/dt = \mathbf{M}\zeta + (1/2)\zeta'\mathbf{D}\zeta \ . \tag{2.21}$$

Notice that (2.21) is actually the Taylor expansion of the dynamical equations around the steady state $\mathbf{e}_n$ up to quadratic terms.

We find that the Jacobian matrix, $\partial(d\zeta/dt)/\partial\zeta$ ($\equiv\mathbf{M}$) has the following expression:

$$\mathbf{M} = (\mathrm{diag}\ 1/\mathbf{X}^\circ)\nu(\mathrm{diag}\ \mathbf{v}^\circ)\kappa' \tag{2.22}$$

and the quadratic terms are given by

$$\zeta'\mathbf{D}\zeta = (\mathrm{diag}\ 1/\mathbf{X}^\circ)\nu(\mathrm{diag}\ \mathbf{v}^\circ)\{(\mathrm{diag}\ \kappa'\zeta)\kappa' - \kappa'(\mathrm{diag}\ \zeta)\}\zeta. \tag{2.23}$$

The details in the derivation of (2.23) are given in appendix A. The explicit expressions for the components of **D** are also given in that appendix.

Since, in general, there are conservation constraints, not all the equations above are independent. Below, we shall derive explicitly the set of independent equations. Let us arrange our objects in the following way:

$$\zeta = (\zeta_I{}', \zeta_D{}')' \;, \quad \mathbf{X} = (\mathbf{X}_I{}', \mathbf{X}_D{}')'$$
$$\gamma = (\gamma_I, \gamma_D) \;, \quad \nu = (\nu_I{}', \nu_D{}')'$$
$$\kappa = (\kappa_I{}', \kappa_D{}')' \;.$$

The above notation mean, for example, that the first d components of **X** correspond to the Independent species, and the rest of the components to the Dependent species. One can solve the dependent species from the independent ones as follows:

$$\zeta_D = -(\mathrm{diag}\ 1/\mathbf{X}_D^{\circ})\gamma_D^{-1}\gamma_I(\mathrm{diag}\ 1/\mathbf{X}_I^{\circ})^{-1}\zeta_I$$
$$\partial\zeta_D/\partial\zeta_I = -(\mathrm{diag}\ 1/\mathbf{X}_D^{\circ})\gamma_D^{-1}\gamma_I(\mathrm{diag}\ 1/\mathbf{X}_I^{\circ})^{-1} \;. \qquad (2.24)$$

The set of independent dynamical equations is then given by

$$d\zeta_I/dt = (\mathrm{diag}\ 1/\mathbf{X}_I^{\circ})\nu_I(\mathrm{diag}\ v^{\circ})\{\kappa' - (1/2)\kappa'(\mathrm{diag}\ \zeta) + (1/2)(\mathrm{diag}\ \kappa'\zeta)\kappa'\}\zeta \;. \qquad (2.25)$$

The linearized equations of motion in terms of the independent species are

$$d\zeta_I/dt = \mathbf{M}_I\zeta_I \qquad (2.26)$$

where

$$\mathbf{M}_I = (\mathrm{diag}\ 1/\mathbf{X}_I^{\circ})\nu_I(\mathrm{diag}\ v^{\circ})\kappa_g' \qquad (2.27)$$
$$\kappa_g' = \kappa_I' + \kappa_D'(\partial\zeta_D/\partial\zeta_I) \;. \qquad (2.28)$$

We shall refer to κ_g as the generalized kinetic matrix.

In linear stability analysis, one solves for the eigenvalues which are the roots of the characteristic polynomial associated with the matrix M_I:

$$P(\lambda) = \det(\lambda I - M_I) = \sum_{i=0}^{d} \alpha_i \lambda^{d-i} \ . \tag{2.29}$$

The reader is referred to the book of Hirsch and Smale[15] for a good introduction to elementary stability analysis of dynamical systems, a basic knowledge of which is assumed in this work. Clarke[4] also gives a stability classification of reaction networks.

F. Convex Geometry of the Steady State Velocities

In the nonlinear equations of motion using the scaled concentrations as dynamical variables (equation 2.5), the steady state velocity v° appears as a parameter. However, due to stoichiometric constraints, v° cannot be an arbitrary parameter. There are some relationships among the components of v° as given by the steady state equation

$$\nu v^\circ = 0 \ . \tag{2.30}$$

The geometric interpretation of this equation is the essential step in Clarke's discovery of extreme currents. He found that any steady state velocity v° (which can also be called a 'current' in analogy to electrical networks) can be expressed as a linear combination of these extreme currents.

Equation (2.30) means that any solution v° must be orthogonal to all of the rows of ν (the rows of ν are vectors in R^r). Let there be d linearly independent row vectors of ν. Then v° must lie in a $(r-d)$-dimensional subspace S_v which is orthogonal to the d-dimensional subspace spanned by the row vectors of ν. Since all the components of v° are non-negative, v° must lie in the intersection of S_v and R^r_+. This intersection is a convex polyhedral cone which Clarke(4) called the current cone, C_v.

Example II.2

Consider the network

Network N_2

$R_1 \qquad \rightarrow X$

$R_2 \qquad X \rightarrow$

$R_3 \qquad X \rightarrow$

In reaction velocity space, the set of steady state velocities is given by the intersection of the plane defined by $v_1=v_2+v_3$ and the non-negative orthant R^3_+ as illustrated in figure 2.1. Note that the intersection is a cone with 2 edge vectors $\mathbf{E}^1$ and $\mathbf{E}^2$. ■

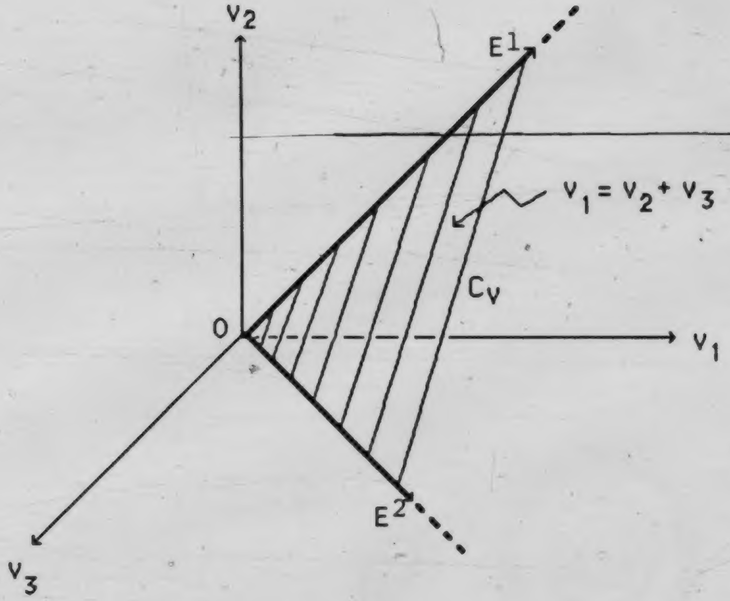

Figure 2.1

The plane defined by $v_1 = v_2 + v_3$ in velocity space. The intersection of this plane and the non-negative orthant ($\bar{R}^3_+$) is the current cone, C_V. Note that there are two extreme edges of C_V, namely, E^1 and E^2. All vectors in C_V are expressible as non-negative linear combination of these extreme edge vectors.

Let there be f edge vectors $\{E^1, E^2, \ldots, E^f\}$ constituting the frame of the cone C_v. Then every $v^\circ \epsilon\ C_v$ can be expressed as a non-negative linear combination of these edge vectors:

$$v^\circ = \sum_{i=1}^{f} j_i E^i \quad , \quad j_i \geq 0$$

or in matrix form,

$$v^\circ = Ej \ . \tag{2.31}$$

The rxf-matrix E is called the current matrix(4) and $j \ \epsilon\ R_+^f$ is the current parameter. The explicit definition of the current cone can now be given :

$$C_v = \{ \ v^\circ \epsilon R_+^r \mid v^\circ = Ej \ , \ j \epsilon R_+^f \ \} \ . \tag{2.32}$$

In the formalism of stoichiometric network analysis due to Clarke(4), j is one of the steady state parameter vectors; the other parameter has components which are the reciprocals of the steady state concentrations:

$$h = 1/X^\circ \equiv (1/X_1{}^\circ, 1/X_2{}^\circ, \ldots, 1/X_n{}^\circ) \ . \tag{2.33}$$

Thus, the full domain for the steady state parameters (h,j) (also referred to as convex parameters) for the general stoichiometric dynamical problem (2.1) is given by the convex set

$$C_M = R_+^n \times C_v \tag{2.34}$$

whose dimension is $n+r-d$.

The current matrix **E** is determined by stoichiometry (ν) as indicated by the relationship

$$\nu \mathbf{E} = 0 \; . \tag{2.35}$$

This equation is a direct consequence of equations (2.30) and (2.31). An APL algorithm called CURRENTS, already published(9), will determine **E** for a given ν. As example II.2 illustrated, the columns of **E** correspond to the extreme currents comprising the network at steady state. In general, every positive steady state of a network is a non-negative linear superposition of its extreme currents. To a given extreme current corresponds an extreme subnetwork whose component reactions are indicated by the non-zero elements in the corresponding column of **E**. The following example hopes to illustrate the interpretation of **E** more clearly.

Example II.3 The Edelstein Network

Edelstein(10) first proposed the following simple biochemical model that generates bistability (that is, 3 steady states - 2 stable, 1 unstable). The substrate S catalyzes its own production (autocatalysis) and then gets degraded by the enzyme E.

Network N_3

R_1, R_{-1} $A + S \rightleftarrows 2S$

R_2, R_{-2} $S + E \rightleftarrows ES$

R_3, R_{-3} $ES \rightleftarrows E + B$

ES is an enzyme-substrate complex. The overall reaction is $A \rightleftarrows B$. The species A and B will be considered as external species in the analysis below. Let $X = (S, E, ES)'$ and $k = (k_1A,\ k_{-1},\ k_2,\ k_{-2},\ k_3,\ k_{-3}B)'$. The stoichiometric matrix ν and the current matrix **E** generated from ν are given below.

$$\nu = \begin{bmatrix} 1 & -1 & -1 & 1 & 0 & 0 \\ 0 & 0 & -1 & 1 & 1 & -1 \\ 0 & 0 & 1 & -1 & -1 & 1 \end{bmatrix}$$

$$\mathbf{E} = \begin{bmatrix} 1 & 0 & 1 & 0 & 0 \\ 1 & 0 & 0 & 0 & 1 \\ 0 & 1 & 1 & 0 & 0 \\ 0 & 1 & 0 & 0 & 1 \\ 0 & 0 & 1 & 1 & 0 \\ 0 & 0 & 0 & 1 & 1 \end{bmatrix}$$

The total enzyme concentration is conserved as represented by the 1x3 conservation matrix

$$\gamma = (0\ 1\ 1)\ .$$

The extreme subnetworks corresponding to the columns of **E** are shown in figure 2.2. Any steady state velocity v° of the network can be expressed as a non-negative linear combination of the velocities of the above extreme currents as given explicitly by equation (2.31). ■

G. The Current Polytope and a Topology on the Network Steady States

Consider a change in the (h,j) parameters where h is fixed and j is multiplied by $\lambda>0$. (This corresponds to a motion along a ray j in C_v). The corresponding change in the rate constants is λk, that is, all the rate constants are multiplied by the same amount. This operation does not affect the value of the steady state X° (= 1/h). This means that h and j can be assigned values independently. It is also clear that any cross-section of C_v contains all the information available from this cone. This $(r-d-1)$-dimensional cross-section of C_v is called the current polytope, Π_v, defined as follows

$$\Pi_v = \{ v^\circ \mid v^\circ=Ej \ , \ e'v^\circ=1 \} \ . \qquad (2.36)$$

The vertices of Π_v correspond to the extreme currents. The structure of Π_v, that is, the adjacency relation among the vertices, the edges, 2-faces up to (r-d-2)-faces can be determined using already existing APL programs due to von Hohenbalken$^{(11)}$.

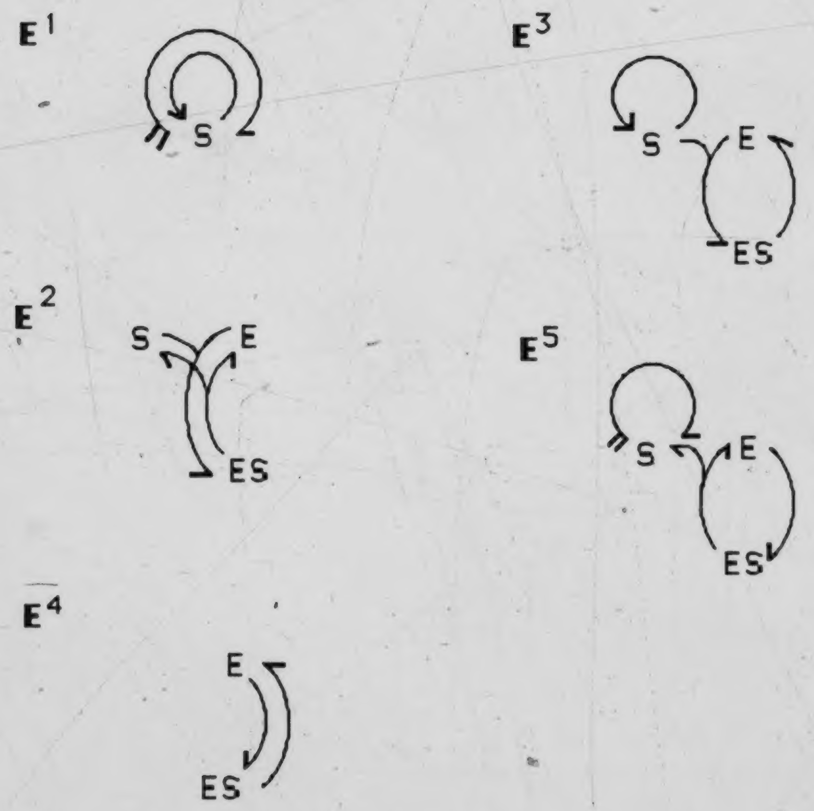
E^1
S
E^3
S
E
ES
E^2
S
E
ES
E^5
S
E
ES
E^4
E
ES

Figure 2.2

The 5 extreme subnetworks corresponding to the 5 columns of the current matrix **E** (given in the text) for the Edelstein network.

Example II.4 Π_v of the Edelstein Network

After normalizing the columns of **E** ($\sum_{i=1}^{r} E_{im} = 1$ for all m) for the Edelstein network in the preceding example, we come up with the structure of the current polytope, Π_v, as shown in figure 2.3. Π_v is 3-dimensional and is not a simplex. Any point inside the polytope can be expressed as a linear combination of any 4 vertices. ▪

In sorting complex mechanisms, the structure of Π_v is useful in the following way. When one reaction listed in the reaction mechanism is known experimentally to be very slow, then the extreme currents involving this reaction must have a small contribution to the steady state. The point inside Π_v corresponding to the steady state parameter j must be far from the vertices corresponding to those extreme currents. The dominant extreme currents are those represented by the remaining vertices. These extreme currents consist entirely of reactions that are relatively fast at steady state. Two distant extreme currents or vertices of Π_v cannot be both important under the same conditions. Thus, Π_v contains topological information that forces us to make either-or decision about the importance of subsets of the reactions in the network.

Stoichiometric relationships among major reactants and products are often known experimentally. Sometimes several

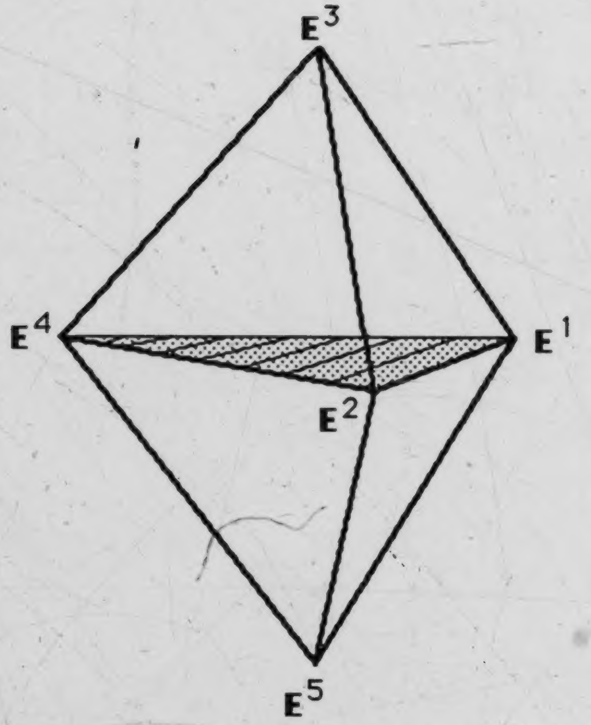

Figure 2.3

The current polytope Π_V of the Edelstein network is a bipyramid as shown above. The vertices correspond to the extreme currents and the shaded triangle represents all detailed-balanced steady states ($j_3 = j_5$).

different possible stoichiometries for the overall reaction are consistent with the mechanism. These stoichiometries are associated directly with different parts of Π_v. Thus, experimental information about the overall stoichiometry can also help locate the dominant extreme currents, or equivalently, the dominant vertices of Π_v. These ideas will be applied in Chapter V where the dominant extreme currents in the peroxidase-oxidase reaction mechanism are determined under bistable conditions.

H. Some Classification of Steady States and Corresponding Regions in Π_v

A complete steady state analysis of a given reaction network would entail a description of all regions in the steady state cone C_M defined by (2.34). The current polytope Π_v serves as a basis for the analysis. When there are no conservation constraints, equations (2.5) and (2.31) say that the steady states can be fully described by the current parameters **j**. When some conservation conditions exist, then the values of **h** matter as shown by the dependence of the Jacobian matrix $\mathbf{M}_I$ on both **h** and **j** (see equation 2.27); in this case, regions of Π_v should be analyzed for each fixed value of **h**. In this section, we give the regions in Π_v occupied by certain steady states called 'detailed-balanced steady states' and 'complex-balanced steady states', and then outline an approach for further characterizing other regions in Π_v.

Detailed Balanced Steady States

Isolated reaction systems always evolve towards a unique steady state called the 'chemical equilibrium' state which is already well characterized by classical thermodynamics. For example, one could define various potentials (e.g. chemical potential, μ), or state functions, each having a unique extremum corresponding to the equilibrium point. The approach to this equilibrium point is usually monotonic but can also be a damped oscillatory one in some cases. The global stability of this unique equilibrium point for isolated mass action systems has also been proven analytically. Shear(16), for example, showed that for isolated systems governed by mass-action rate laws of arbitrary order, the equilibrium point is unique and asymptotically stable. This conclusion follows from the existence of a Lyapunov function defined globally in phase space and having a unique extremum at the equilibrium point. Another important characteristic of thermodynamic chemical equilibrium is the detailed-balancing (DB) of every elementary reaction. This means that for every reaction (which, in general, is reversible), the rate of the forward reaction is equal to the rate of the reverse reaction.

Definition 2.1

The steady state X° is a DB-steady state if every reaction R_j has a reverse R_k $(j \neq k)$ and $v_j^{\circ} = v_k^{\circ}$.

For a reversible network with a total of r reactions (reverse reactions included), the set of detailed balanced currents is a subcone C_E of dimension $r/2$. The corresponding polytope Π_E is a $((r/2)-1)$-dimensional simplex because the vertices (or the corresponding columns of **E**) are independent.

Example II.5

Consider the following reversible triangular network:

Network N_4

R_1, R_{-1} $\quad A \rightleftarrows B$

R_2, R_{-2} $\quad B \rightleftarrows C$

R_3, R_{-3} $\quad C \rightleftarrows A$

The extreme currents are shown in figure 2.4 beside the corresponding vertices of Π_V. The subcone of DB steady states, Π_E, is 2-dimensional as indicated by the shaded triangle. In terms of the rate constants, detailed balancing requires that $k_1 k_2 k_3 = k_{-1} k_{-2} k_{-3}$. Note that any set of $k \in R_+^6$ will give a unique positive steady state for the network most of which is non-detailed balanced. For example, the network

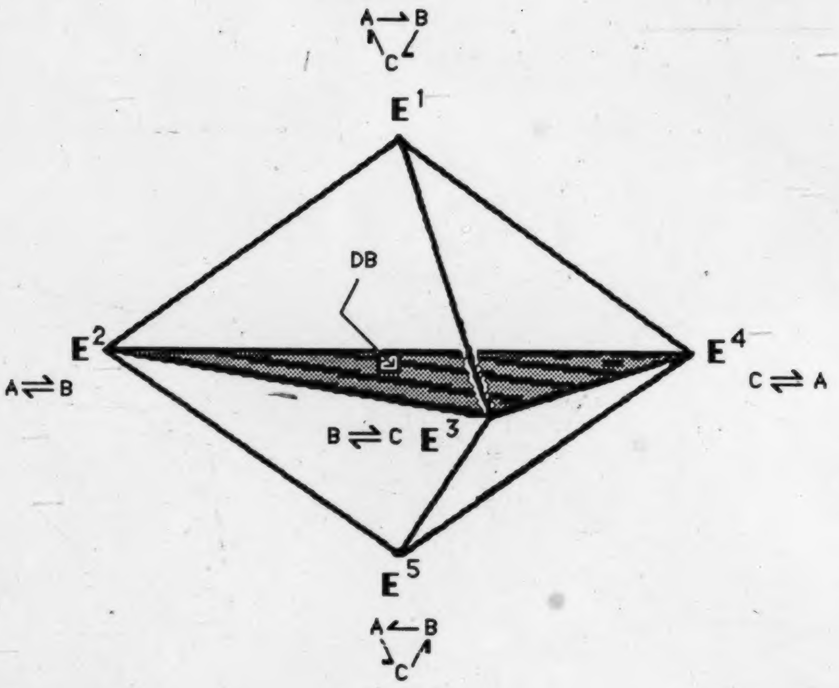
A → B
C
E^1
DB
E^2
A ⇌ B
E^4
C ⇌ A
B ⇌ C
E^3
E^5
A ← B
C

Figure 2.4

The current polytope (Π_V) of network N_4 is a bipyramid. The shaded triangle represents the detailed-balanced (DB) steady states (vertices E^2, E^3 and E^4). The corresponding extreme subnetworks are shown at each vertex.

is at a non-equilibrium steady state when $v_1=v_2=v_3 \neq v_{-1}=v_{-2}=v_{-3}$ correponding to the following constraints on the rate constants: $k_1k_{-1} = k_2k_{-3}$ and $k_3k_{-3} = k_1k_{-2}$. ■

Complex-Balanced Steady States

Model networks, or networks that are valid approximations to complex mechanisms under certain specified conditions, are often irreversible. These networks have no DB-steady states. However, we can extend the meaning of 'reversibility' and thereby characterize some steady states that have properties similar to the DB-steady states of reversible networks. Observe that each reversible reaction is a 2-complex cycle, that is, a closed path of reaction arrows (of the same direction) that originates from a complex and terminates at that same complex. In some irreversible networks, n-complex cycles ($n \geq 2$) can be found. A special class of networks (which is a generalization of, and including, reversible networks) have been investigated by Feinberg, Horn and Jackson(1,2,13,20-25) who described them as weakly reversible for having the property that each and every complex belongs to at least one n-complex cycle ($n \geq 2$).

One can view any given reaction network as a 'unimolecular' network with the complexes $C_1,\ldots,C_n$ considered as 'species'. To do this, it is necessary to associate a 'concentration' for every complex C_i which we can define as

$$[C_i] = \prod_{i=1}^{n} (X_i^\circ)^{\kappa_{ij}}$$

when the j-th reaction involving C_i as the reactant complex has mass-action kinetics. In the equation above, X_i° is the steady state concentration of species X_i. To this 'unimolecular' network is associated a stoichiometric matrix $\underline{W}$ having only 0, 1 and -1 as elements. When the network is complex-balanced, the complexes have steady state 'concentrations'. This occurs when the steady states X° are complex-balanced (CB) steady states.

Definition 2.2

X° is a CB-steady state when

$$\underline{W}v(X^\circ,k) = 0 \ . \tag{2.37}$$

For reversible networks, DB-steady states are also CB-steady states but not vice-versa. In the preceding example (Example II.5), the steady states defined by $v_1 = v_2 = v_3 \neq v_{-1} = v_{-2} = v_{-3}$ are CB-steady states but are not DB. All the steady states of this network are CB. In fact, all steady states of unimolecular networks are CB because $\nu \equiv \underline{W}$.

The stoichiometric matrix ν is of course directly related to the complex stoichiometric matrix $\underline{W}$. The relationship is given by

$$\nu = \underline{YW} \ . \tag{2.38}$$

The nxs matrix $\underline{Y}$ is called the complex matrix whose columns are the s complex vectors (or the stoichiometric coefficients of the species in the complexes).

The factorization of ν (which comes about as a result of the introduction of the concept of a 'complex') also allows us a way of subdividing the current cone C_v. CB - steady states, if they exist, are found in a sub-cone of C_v defined by the set

$$C_{cb} = \{ v^\circ \mid \underline{W}v^\circ = 0 \} . \tag{2.39}$$

Clarke (ref. 4, p.78) has shown that the difference between the dimensions of C_v and C_{cb} is actually the number called the deficiency (δ) of a network which was introduced by Feinberg, Horn and Jackson(1,2,13,20-25) and was used to put networks into broad classes believed to have common dynamical or static features. If the rank of $\underline{W}$ is $(s-\ell)$ then the dimension of C_{cb} is equal to $r-(s-\ell)$ where s is the number of complexes and ℓ is the number of 'linkage classes' or disconnected pieces in a reaction diagram where each complex appears no more than once. (The following example will illustrate this). Thus, the deficiency of a network is

$$\begin{aligned} \delta &= \dim C_v - \dim C_{cb} \\ &= s-\ell-d . \end{aligned} \tag{2.40}$$

where d is the number of independent species (= rank ν).

Example II.6

A standard reaction diagram⁽²⁾ for the Edelstein network introduced in example II.3 is given below.

$$A + S \rightleftarrows 2S$$

$$S + E \rightleftarrows ES \rightleftarrows E + B$$

There are two disconnected pieces and therefore $\ell=2$. Note that the reactions on the first line involve the complexes (A+S) and (2S), while the reaction on the second line involved the complexes (S+E), (ES) and (E+B). The network is disconnected because no complex is common to the two sets of complexes. The dimension of C_v is 4 and that of C_{cb} is 3 giving a deficiency of $\delta=1$. From equation (2.37), when $j_3 = j_5$, the steady states are CB. In the current polytope shown in figure 2.3, the CB steady states are located on the median plane of the bipyramid. ■

Deficiency zero networks are therefore networks whose steady states are all CB. Horn, Jackson and Feinberg[3]// proved a theorem describing this kind of networks. A statement of this theorem is included here because of its importance.

---

[3]// Reference 1 gives a proof of the zero deficiency theorem.

The Zero Deficiency Theorem.(1,2)

Let N be a reaction network with $\delta = 0$.

(a) If N is not weakly reversible then, for arbitrary form of the kinetics, no positive steady state exists for the network for any $(C,k) \in R_+^{n+r-d}$ and no cyclic trajectory in concentration space is possible.

(b) If N is weakly reversible and the kinetics is mass action, then there always exists a unique positive steady state for any $(C,k) \in R_+^{n+r-d}$ which is also asymptotically stable ; furthermore, no nontrivial cyclic trajectory in concentration space is possible.

In general, CB steady states are always globally asymptotically stable and are the only steady state possible for the given set of parameters (see Theorem 6A of reference 13). For other parameter values, the same network might have non-CB steady states. These steady states are points of C_v that are not in C_{cb}.

For networks with several linkage classes (ℓ>1) but each linkage class having a deficiency not exceeding 1, Feinberg (1) has offered the following theorem:

The Deficiency One Theorem.(Feinberg(1))

Let N be a reaction network with a deficiency δ and ℓ linkage classes. Let δ_i denote the deficiency of the i-th linkage class; and suppose that both the following conditions are satisfied :

(i) $\delta_i \leq 1$, $i = 1,..,\ell$

(ii) $\delta = \Sigma_i \delta_i$.

If N is weakly reversible and the kinetics is mass action, then a unique positive steady state exists for every $(C,k) \in R_+^{n+r-d}$.

Example II.7

The following example was provided by Feinberg(1). Assume that the kinetics is mass action for the following reversible network:

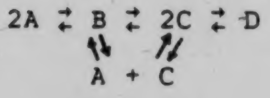

$$\begin{tikzcd} 2A \arrow[r, shift left] & B \arrow[l, shift left] \arrow[r, shift left] \arrow[dr, shift left] & 2C \arrow[l, shift left] \arrow[r, shift left] & D \arrow[l, shift left] \\ & & A + C \arrow[ul, shift left] \arrow[u, shift left] & \end{tikzcd}$$

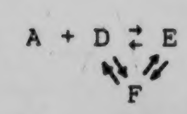

$$\begin{tikzcd} A + D \arrow[rr, shift left] \arrow[dr, shift left] & & E \arrow[ll, shift left] \arrow[dl, shift left] \\ & F \arrow[ul, shift left] \arrow[ur, shift left] & \end{tikzcd}$$

$C + E \rightleftarrows 2G$.

The deficiency δ of the network is 1. The three linkage classes shown above have deficiencies 1, 0 and 0, respectively (from top to bottom). Thus, the requirements of the Deficiency One Theorem are satisfied and we conclude that there exists precisely one positive steady state for every set of parameters (C,k). ■

Stable and Unstable Regions in Π_v

Stable and unstable steady states, in principle, can be determined using expressions involving the coefficients $\alpha_i(h,j)$ (i=1,...,d) of the characteristic polynomial P(λ) as in the Routh-Hurwitz(14) criteria for the number of eigenvalues with positive real parts. For example, a necessary and sufficient condition for linear asymptotic stability of a steady state is that all the Hurwitz determinants must be positive. The last three sections of this chapter will investigate the role of the d-th coefficient of P(λ) in the existence, uniqueness or multiplicity of steady states including the condition for the presence of a continuum of steady states. For example, it can be seen right away that if at the steady state (h,j) we have $\alpha_d(h,j)<0$, then there must be at least one positive real eigenvalue therefore making this steady state exponentially unstable. It will also be seen that α_d is relevant to the singularities of the steady state manifold. The hypersurface defined by $\alpha_d(h,j) = 0$ can be plotted inside Π_v for a given h and thus enabling us to see the regions where $\alpha_d>0$ and $\alpha_d<0$. Chapter V will give an example of such a calculation using a realistic complex network.

I. Boundary Steady States, Stoichiometric Explosions and Extinction

We say that a chemical species X_i explodes if its concentration increases without limit as time goes to infinity. It becomes extinct if the limit of the concentration is zero. The occurrence of boundary steady states is closely associated with explosion-extinction dynamics. In concentration space, a steady state X^o is in the boundary if at least one of its components, say X_i^o is zero. This vanishing of X_i^o must not be solely a consequence of the vanishing of some rate constants. (Recall that we have required all the rate constants to be positive). To understand the several possibilities that may lead to explosion or extinction, we study some simple examples below. Networks N_5 and N_6 exemplify networks that can only have positive steady states if a strict relationship among the rate constants is satisfied, otherwise explosion or extinction occur. These networks possess an infinite number (a continuum) of positive steady states for a specified set of rate constants following the required relationship. Network N_6 exhibits boundary steady states. Explosion or extinction of certain species in a network may also depend on the initial conditions as network N_7 will demonstrate. Finally, network N_8 is one simple network that embodies almost all of the above features under different conditions on the parameters.

Network N_5

$$\begin{array}{ll} R_1 & X + Y \rightarrow \\ R_2 & \quad\quad\ \rightarrow X \\ R_3 & \quad\quad\ \rightarrow Y \end{array}$$

$$dX/dt = k_2 - k_1XY$$

$$dY/dt = k_3 - k_1XY$$

This network has positive steady states only if $k_2 = k_3$. When this is satisfied, $dX/dt = dY/dt$ and $X(t) = Y(t) + \text{constant}$. Notice that although rank $\nu = d = 2$, the trajectories on the X-Y plane are restricted to lie on a straight line (see figure 2.5(a)). On the phase plane, there is a continuum of steady states lying on the hyperbola defined by

$$X^\circ = k_2/k_1Y^\circ.$$

When $k_2 = k_3$, the eigenvalues associated with the linearized dynamics are $\lambda_1 = 0$ and $\lambda_2 = -k_1(X^\circ + Y^\circ) < 0$. Hence, the steady states are marginally stable. When $k_2 \neq k_3$, no steady state is possible and explosion and extinction occurs as shown in figure 2.5(b),(c). Note that $\alpha_d \equiv 0$ for the positive steady states. If we plot the steady states of any one species against k_2 and k_3 (k_1 does not affect the qualitative picture), we get the picture shown in figure 2.5(d). On one

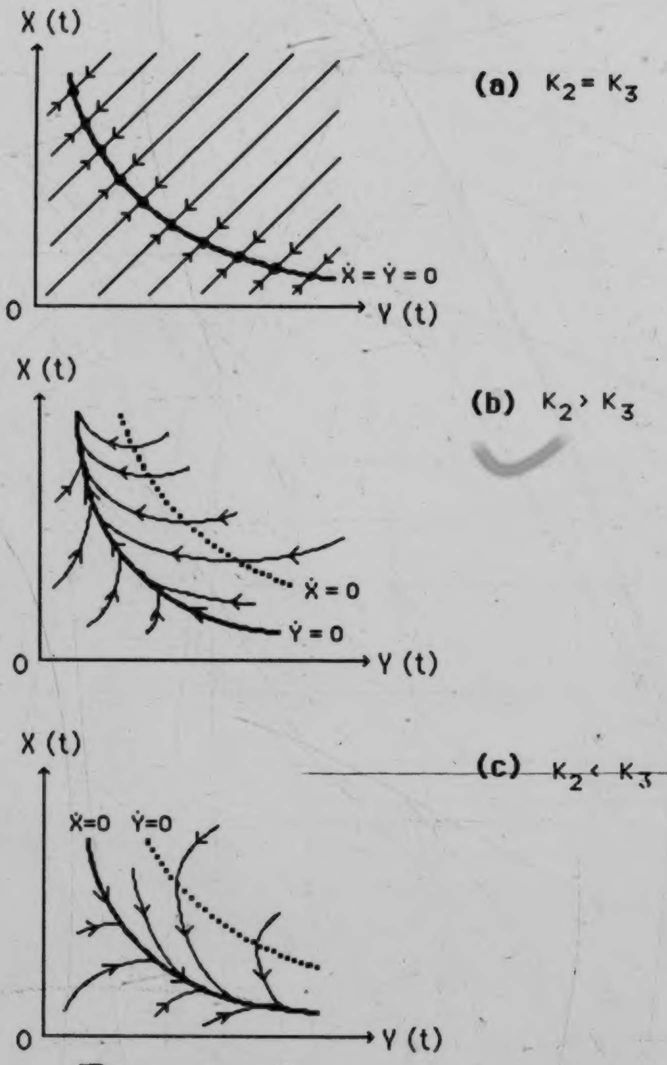
X (t)
(a) $K_2 = K_3$
$\dot{X} = \dot{Y} = 0$
0
Y (t)
X (t)
(b) $K_2 > K_3$
$\dot{X} = 0$
$\dot{Y} = 0$
0
Y (t)
X (t)
(c) $K_2 < K_3$
$\dot{X}=0$
$\dot{Y}=0$
0
Y (t)

Figure 2.5

(a): For Network N_5, a continuum of steady states occurs on the phase plane when $k_2 = k_3$. For a given initial condition, the trajectory is a straight line.
(b)-(c) : When $k_2 \neq k_3$, explosion and extinction occurs and no positive steady state is possible.

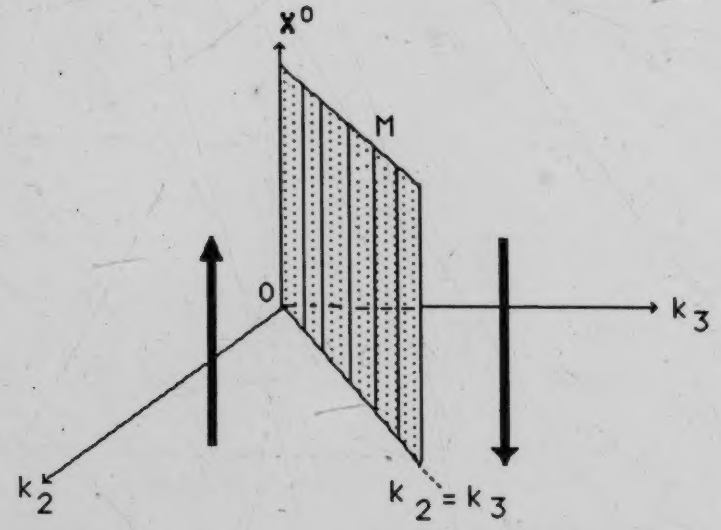

Figure 2.5 (d)

The steady state manifold M of network N_5 is orthogonal to the $k_2 - k_3$ parameter plane. A continuum of positive steady states exists when $k_2 = k_3$, otherwise one of the species becomes extinct while the other explodes.

side of *M*, there is explosion while on the other side extinction occurs.

Network N_6

R_1 $X \rightarrow 2X$

R_2 $X \rightarrow$

$$dX/dt = (k_1-k_2)X$$

This network has an infinite number of positive steady states $X^o>0$ when $k_1=k_2$. If $k_1 \neq k_2$, there is only one possible steady state, i.e. $X^o=0$ which is a boundary steady state. If $k_1>k_2$, explosion occurs for any positive perturbation of this boundary steady state. If $k_1<k_2$, the boundary steady state is stable, or in other words, extinction occurs. We reproduce the figure given by Clarke(8) in ~~f~~figure 2.6. Again, note that $\alpha_d \equiv 0$ (d=1) and $\lambda_1=0$ for the marginally stable positive steady states.

Network N_7

R_1 $X + Y \rightarrow$

R_2 $X \rightarrow 2X$

R_3 $\rightarrow Y$

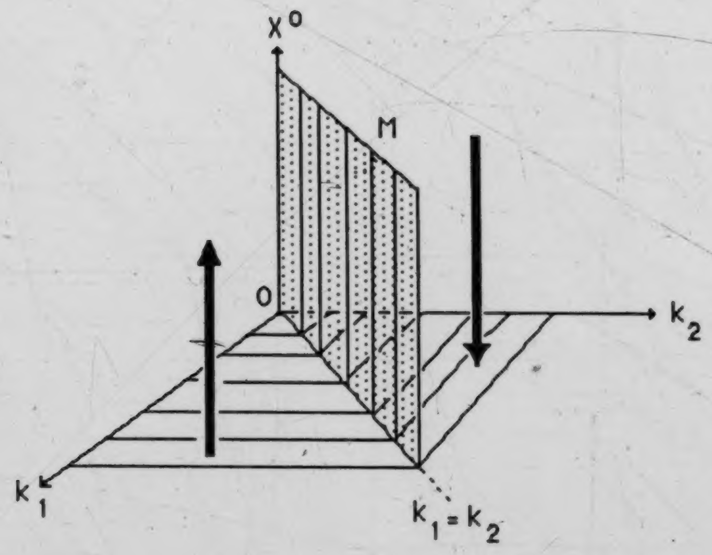

Figure 2.6

A continuum of steady states exists when $k_1 = k_2$ for network N_6. As for network N_5 in figure 2.5, M is orthogonal to the parameter plane. On one side of M explosion occurs while on the other side extinction is the case. Mathematically, boundary steady states exist when $k_1 \neq k_2$.

$$dX/dt = k_2X - k_1XY$$

$$dY/dt = k_3 - k_1XY \ .$$

There is a unique positive steady state $(X^\circ, Y^\circ) = (k_3/k_2, k_2/k_1)$. The Jacobian matrix associated with the linearized dynamics is

$$M = \begin{bmatrix} 0 & -k_1k_3/k_2 \\ -k_2 & -k_1k_3/k_2 \end{bmatrix}$$

and the eigenvalues are

$$\lambda\pm = (-k_1k_3 \pm [k_1^2k_3^2 + 4k_1k_3k_2^2]^{1/2})/2k_2$$

which are both real but of opposite signs. The steady state is thus a saddle point. The phase portrait looks like figure 2.7(a). Figure 2.7(b) gives a plot of the steady state Y° against k_2 and k_1.

For any given values of k_1 and k_2, there is a unique $Y^\circ > 0$. Note that the surface of steady states totally projects onto the k_1-k_2 parameter plane and does not divide the plane into regions where explosion and extinction occur as in the case of networks N_5 and N_6. In fact, for network N_7, for any (k_1, k_2, k_3), it is the initial condition $(X(0), Y(0))$ that will determine whether or not explosion or extinction occurs. There is an invariant curve γ, (figure 2.7(a)), called the 'stable manifold', that separates the initial conditions leading to explosion from those that lead to extinction. In this case, $\alpha_4 = \alpha_2 < 0$.

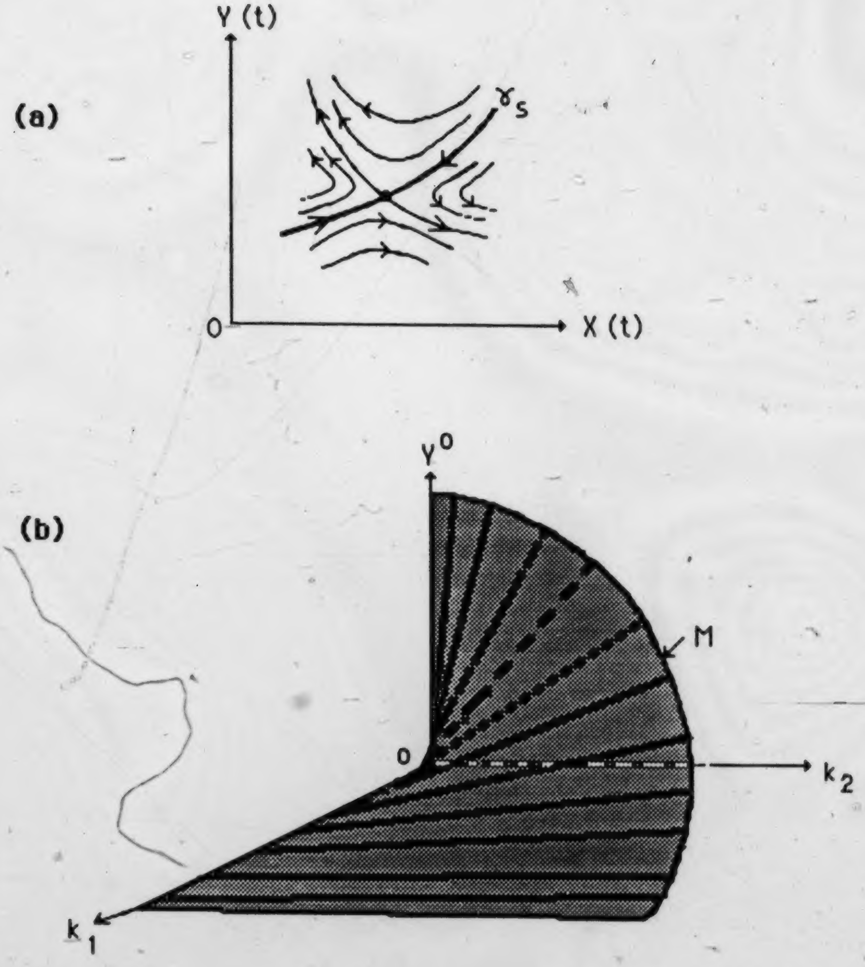
(a)
Y (t)
γ_s
0
X (t)
(b)
Y^0
M
0
k_2
k_1

Figure 2.7

(a). A representative phase portrait of network N_7 near the steady state which is a saddle-point.

(b). A cross-section of the steady state manifold showing the steady state Y^o against k_1 and k_2.

The next network is one of the extreme currents of the Oregonator(4) which is a model for the oscillations observed in the Belousov-Zhabotinsky reaction(26).

Network N_8

R_1 $\quad X \rightarrow 2X + 2Z$

R_2 $\quad 2Z \rightarrow Y$

R_3 $\quad X + Y \rightarrow$

The trajectories in concentration space are restricted to lie on the plane defined by

$$(-2\ 2\ 1)(X,Y,Z)' = C, \text{ constant.}$$

Let $v_1=k_1X$, $v_2=k_2Z$ and $v_3=k_3XY$. Note that reaction R_2 is assumed first order with respect to Z. Choosing X and Y as the independent species, the independent kinetic equations are

$$dX/dt = k_1X-k_3XY$$
$$dY/dt = k_2C+2k_2X-2k_2Y-k_3XY \ .$$

There are two steady states, one of them in the boundary:

$$S_1 = (X_1^{\circ},Y_1^{\circ},Z_1^{\circ}) = (0,C/2,0)$$

$$S_2 = (X_2^\circ, Y_2^\circ, Z_2^\circ) = (k_2(2k_1-k_3C)/k_3(2k_2-k_1),\ k_1/k_3,$$
$$k_1(2k_1-k_3C_1)/k_3(2k_2-k_1)\ ).$$

It is required that $2k_2 \neq k_1$ otherwise X_2° and Z_2° blow up. Note that S_1 and S_2 become identical when $k_1 = k_3C/2$ or when the initial concentrations of the species are such that $C = 2k_1/k_3$. Since the steady state concentrations are always non-negative, there are three cases to consider: (parameter sets outside these cases will correspond to the case where non-negative steady states are absent)

(i). $2k_1 > k_3C$ and $2k_2 > k_1$
(ii). $2k_1 < k_3C$ and $2k_2 < k_1$
(iii). $2k_1 = k_3C$ $(2k_2 \neq k_1)$

Linear stability analysis about S_1 and S_2 gives the phase portraits shown in figure 2.8. Observe that going from case (iiia) to case (i), as k_1 increases beyond $k_3C/2$ (maintaining $k_1 < 2k_2$), a stable node bifurcates from the boundary steady state which now has become an unstable saddle point. When k_1 decreases below $k_3C/2$ (maintaining $k_1 > 2k_2$) as represented by the process case (iiib) → case (ii), the boundary steady state becomes a stable node, and an unstable saddle point bifurcates from it. We may call this type of steady state bifurcation exhibited by network N_8 as a saddle-node bifurcation. Since we are presently interested in explosion-extinction dynamics, cases (ii) and (iii) are

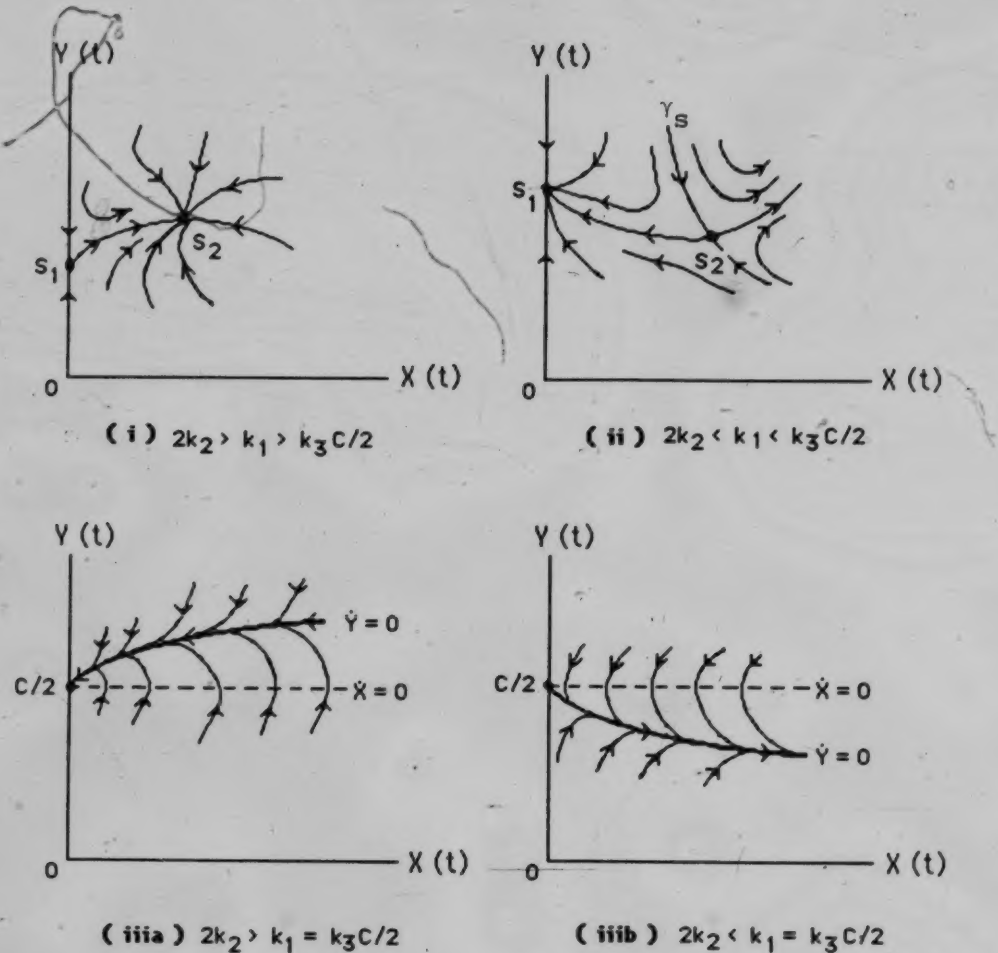
Y (t)
X (t)
0
S_1
S_2
Y (t)
X (t)
0
S_1
S_2
γ_S
Y (t)
X (t)
0
C/2
$\dot{Y} = 0$
$\dot{X} = 0$
Y (t)
X (t)
0
C/2
$\dot{X} = 0$
$\dot{Y} = 0$

(i) $2k_2 > k_1 > k_3C/2$

(ii) $2k_2 < k_1 < k_3C/2$

(iiia) $2k_2 > k_1 = k_3C/2$

(iiib) $2k_2 < k_1 = k_3C/2$

Figure 2.8

Phase portraits of network N_8 for the different cases as indicated. Two steady states S_1 and S_2 exist for cases (i) and (ii); only a boundary steady state exists for cases (iiia) and (iiib).

the ones to look at. For the intermediate case, case (iiia and iiib), we have $\alpha_d \equiv 0$. In case (ii), for a given initial condition X(0), when the initial Y(0) is below the invariant stable manifold γ_s (shown in figure 2.8), species X becomes extinct; explosion occurs otherwise. The signs of α_d for steady states S_1 and S_2 for the 3 cases are summarized in the table below.

sign of α_d

case	(i)	(ii)	(iii)
S_1	(-)	(+)	0
S_2	(+)	(-)	($S_1 \equiv S_2$)

It is interesting to look at the graph of X^e as k_1 varies. This is done in figure 2.9. When $2k_2 = k_3C/2$, the boundary steady state S_1 changes stability at $k_1 = 2k_2 = k_3C/2$ where there also exists a continuum of positive steady states orthogonal to parameter space (figure 2.9(b)). In figures 2.9(a) and (c), as k_1 approaches $2k_2$, the branch of positive steady states approaches a vertical position with respect to the k_1 axis, and α_d approaches 0. At $k_1 = k_3C/2$, this same branch is perpendicular to the k_1 axis and α_d is identically zero.

Let us now summarize the features of the above networks that are responsible for their explosion or extinction dynamics. When $\alpha_d \equiv 0$, as in networks N_5 and N_6, the steady

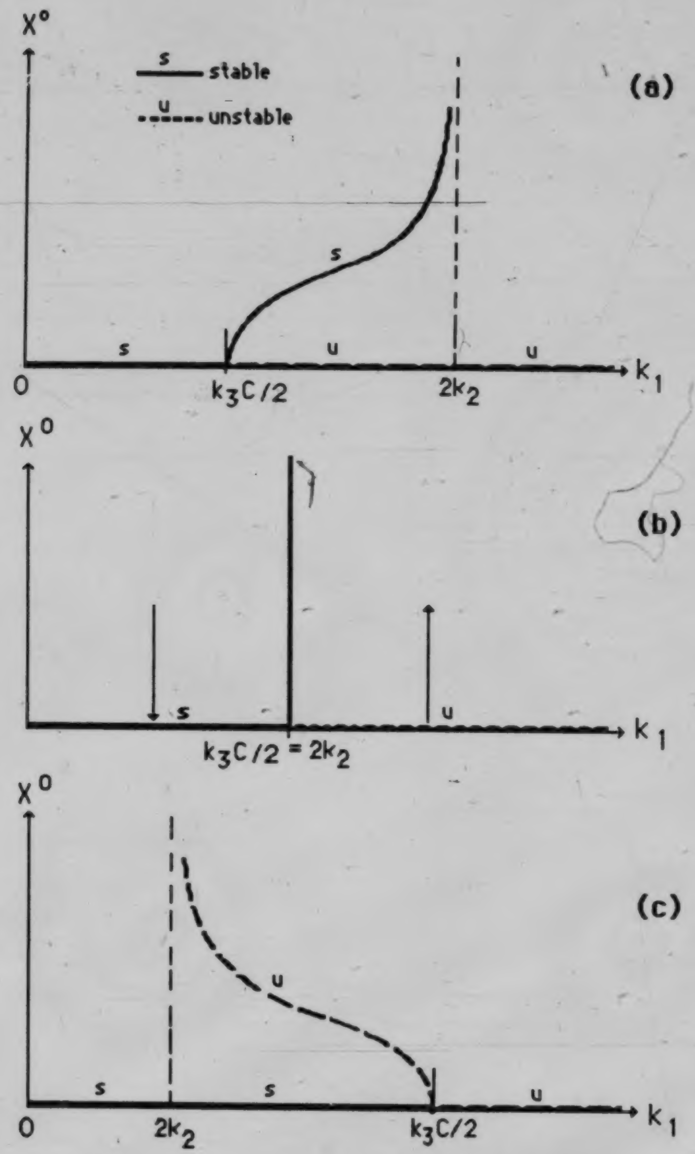

Figure 2.9

Graph of the steady state X^0 as a function of k_1 for the cases (a) $2k_2 > k_3C/2$, (b) $2k_2 = k_3C/2$ and (c) $2k_2 < k_3C/2$ for network N_8. Stable and unstable branches of steady states are indicated.

state manifold *M* in the positive orthant is orthogonal to the parameter space. In these networks, a relationship among the parameters (k,C) must be satisfied for positive steady states to exist; there is then a continuum of steady states. Furthermore, the relationship among the parameters divides parameter space into two regions, one corresponding to explosion dynamics and the other to extinction dynamics.

As demonstrated by networks N_7 and N_8, the vanishing (identically) of α_d is not a necessary requirement for explosion or extinction dynamics. When the positive steady state is unique but is an unstable saddle point, there is explosion or extinction of some species depending on the initial conditions. Note that depending on the orientation of the stable manifold γ_s (see figures 2.7 and 2.8), all species may explode, or all may go to extinction, or some may explode while others become extinct.

J. Sufficient Conditions for $\alpha_d \equiv 0$

In general, if α_d vanishes at the parameter **p**, the tangent plane on *M* at the point $(\mathbf{X}^\circ,\mathbf{p})$ is orthogonal to the parameter space. In particular, if α_d vanishes identically, then the whole of *M* is a hyperplane that is perpendicular to the parameter space, and therefore positive steady states exist only when a relationship among the parameters is satisfied. Furthermore, when this relationship is satisfied, there is a continuum of steady states.

The d-th coefficient of the characteristic equation (2.29), α_d, is related directly to the determinant of M_I whose explicit expression is given in equation (2.27). We have

$$\alpha_d = (-1)^d \det(M_I) . \tag{2.41}$$

Thus, using equation (2.27),

$$\begin{aligned} &\alpha_d=0 \text{ if and only if} \\ &\det[\nu_I(\text{diag } v^\circ)\kappa_g^t] = 0 \end{aligned} \tag{2.42}$$

where ν_I are the d independent rows of ν and κ_g is the generalized kinetic matrix defined by equation (2.28). Equation (2.42) means that there should be a non-zero vector $q \epsilon R^d$ such that

$$\nu_I(\text{diag } v^\circ)\kappa_g^t q = 0 . \tag{2.43}$$

Immediately we see that $\alpha_d \equiv 0$ if

$$\text{(i).} \quad \kappa_g^t q = 0 \quad \text{or} \tag{2.44}$$

$$\text{(ii).} \quad \kappa_g^t q = e_r \tag{2.45}$$

where e_r is a vector whose r components are all 1. Conditions (i) and (ii) are sufficient conditions for the vanishing of α_d identically. Condition (ii) was obtained from $\nu_I v^\circ = 0$ which is always satisfied for a steady state condition. Also, note that $(\mathrm{diag}\ v^\circ)\kappa_g' q=0$ implies condition (i) when v° has strictly positive components.

Network N_5 considered above falls under condition (i) with $q=(1,-1)'$. Network N_6 satisfies condition (ii) with $q=1$. If there are no conservation constraints, then condition (ii) is satisfied when all the reactions in a network have the same order, $O \geq 1$. Having the same order with no conservation conditions means

$$\kappa' e_n = O e_r \ .$$

Take $q = (1/O)e_n$ and get

$$\kappa' q = e_r \ . \tag{2.46}$$

If there are some conservation constraints, even in an 'iso-order' network, there does not necessarily exist a vector q such that (2.45) is satisfied. As an example, we consider network N_9 below.

Network N_9

R_1 $X \to Y$

R_2 $Y \to Z$

R_3 $Z \to X$

There is one conservation constraint:

$\gamma(X,Y,Z)' = C$, constant

with $\gamma = (1\ 1\ 1)$

and the kinetic matrix is

$$\kappa = \begin{bmatrix} 1 & 0 & 0 \\ 0 & 1 & 0 \\ 0 & 0 & 1 \end{bmatrix}$$

Choose X and Y as the independent species. Then

$$\gamma_I = (1\ 1)\ ,\ \gamma_D = (1)$$

$$\kappa_I = \begin{bmatrix} 1 & 0 & 0 \\ 0 & 1 & 0 \end{bmatrix}\ ,\ \kappa_D = (0\ 0\ 1)$$

and

$$\kappa_g' = \begin{bmatrix} 1 & 0 \\ 0 & 1 \\ -X^\circ/Z^\circ & -Y^\circ/Z^\circ \end{bmatrix}$$

No **q** exists such that $\kappa_g'\mathbf{q} = e_3$. In fact, $\alpha_2 \neq 0$ and there is always a unique steady state for any given set of positive parameters.

K. Networks Without Explosion or Extinction Dynamics

Denote by N_{nee} the set of networks having no species that explodes or becomes extinct in a sense strictly defined as follows: Let X_i $(i=1,..,n)$ be the concentration at any time of species i belonging to the network $N \epsilon \mathcal{N}_{nee}$. Then

(i). there exists a finite number $\epsilon_1 > 0$ such that if $X_i > \epsilon_1$ for any i, then $dX_i/dt < 0$, and

(ii). there exists a number ϵ_2, $0 < \epsilon_2 < \epsilon_1$, so that whenever $X_i < \epsilon_2$ for any i, then $dX_i/dt > 0$.

A topological theorem called the Poincare-Hopf Index Theorem[17] states some restrictions on the number and types of positive steady states for any $N \epsilon \mathcal{N}_{nee}$. This theorem is concerned directly with hyperbolic steady states. A steady state is described as hyperbolic if all of its associated eigenvalues have non-zero real parts. A consequence of the Poincare-Hopf Theorem describing the steady states of $N \epsilon \mathcal{N}_{nee}$ is the following :

$$\sum_{j=1}^{\rho} (-1)^{\pi_j} = 1 \ . \tag{2.47}$$

where ρ is the total number of isolated steady states and π_j is the number of eigenvalues with positive real parts for the j-th steady state. Equation (2.47) applies to any dimension. Appendix B gives some details on the derivation of this equation. An important consequence of (2.47) is the following :

For $N \epsilon \mathcal{N}_{nee}$ and having only hyperbolic steady states, the number of the steady states is always odd.

The simple proof for this statement is as follows. Let there be s stable steady states among the ρ steady states. Equation (2.47) implies

$$s + \Sigma_{j=s+1}^{\rho} (-1)^{\pi_j} = 1 \tag{2.48}$$

where the first term on the left-hand side comes from the s steady states with $\pi_i=0$ $(i=1,..,s)$; the summation is over all the unstable ones. Among the $(\rho-s)$ unstable steady states, let π_j be odd for $j = s+1,...,\theta$ and even for $j = \theta+1,...,\rho$. Equation (2.48) now gives

$$s + \{(\theta-s)(-1)+(\rho-\theta)(1)\} = 1$$
$$\therefore \rho = 1 + 2(\theta-s)$$

which proves that ρ is odd. The quantity $(\theta-s)$ is the number of steady states with odd π_j. An increase in the number of steady states is therefore associated with the emergence of an odd number of positive real eigenvalues. Because a complex conjugate pair of eigenvalues can only add 2 to the number of positive real parts, their emergence are irrelevant to the existence of multiple steady states.

Let the relevant characteristic polynomial be written as

$$P(\lambda) = \prod_{i=1}^{d} (\lambda+\lambda_i') = 0$$

where λ_i' is the negative of the i-th eigenvalue. In this form, we have

$$\alpha_d = \prod_{i=1}^{d} \lambda_i'$$

and $\alpha_d>0$ if and only if there is an even number (including 0) of negative λ_i', i.e. even positive eigenvalues. In this case $(\theta-s) = 0$ and $\rho = 1$. Thus,

> A network $N \in N_{nee}$ has a unique steady state for each $p=(C,k)$ if $\alpha_d(p)>0$ for all $p \in R_+^{n+r-d}$.

On the other hand, $\alpha_d<0$ if and only if there is an odd number of positive real eigenvalues or $(\theta-s)\geq1$. Thus,

> A network $N \in N_{nee}$ has at least 3 steady states for some k if there is found a steady state X° such that $\alpha_d(X^\circ,k)<0$.

Note that the assumption that the steady states are all hyperbolic was made in the above statements.

Example II.8

Consider the following network involving inhibition of the enzyme E by the substrate S. The species ES and SES are enzyme-substrate complexes.

Network N_{10}

$$\begin{array}{ll} R_1, R_2 & \rightleftarrows S \\ R_3 & S + E \rightarrow ES \\ R_4 & ES \rightarrow E \\ R_5, R_6 & S + ES \rightleftarrows SES \end{array}$$

Let us illustrate the preceding discussion using this network and the following values of the rate constants: $k_1 = 12$, $k_i = 1$ $(i=2,...,6)$. The total enzyme is conserved, that is, $E_t = E + ES + SES$. When the independent species are taken to be S, ES and SES, the expression for α_d is

$$\alpha_d = [S^\circ]^2+[S^\circ]+E_t+1-([S^\circ][ES^\circ]+[ES^\circ]+[SES^\circ]) \ .$$

Figure 2.10 shows a graph of the steady state $[S^\circ]$ versus the parameter E_t and the corresponding variation of α_d. ■

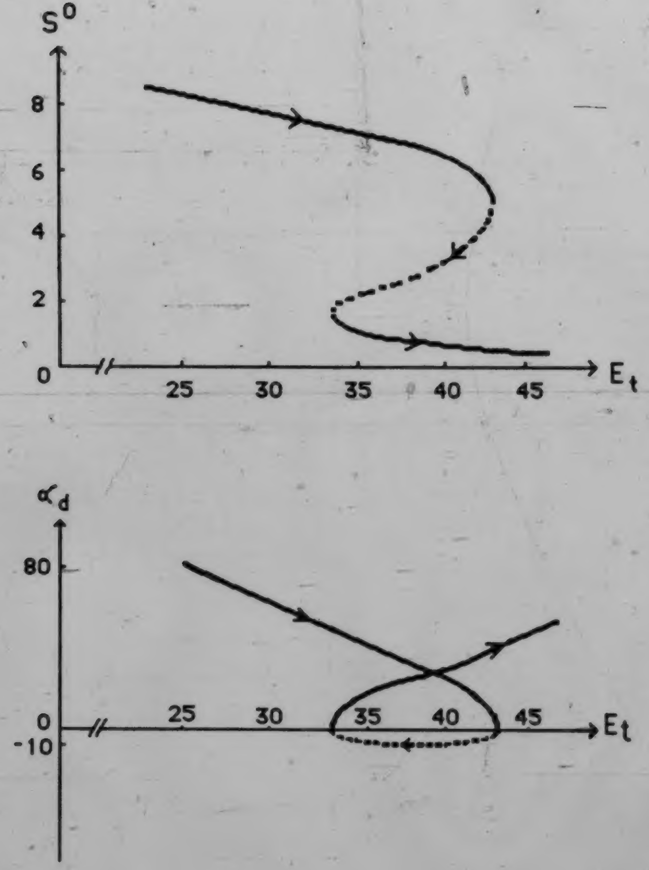

Figure 2.10

Steady state S° as a function of the total enzyme concentration (E_t) and the corresponding variation of α_d (d = 3) for Network N_{10} with $k_1 = 12$ and $k_i = 1$ for $i = 2,3,\ldots,6$.

III. STATE SETS AND BIFURCATION SETS

A. Reduction of the Steady State Problem

This chapter provides some solution to the problem of existence, uniqueness or multiplicity of steady states for a given set of steady state parameters p=(C,k). In particular, the solution is exact and complete for some cases where the system of steady state equations can be reduced to a problem in one dimension. When a network has only one extreme current, the individual reaction velocities are locked into fixed ratios at steady state, e.g. $v_m = r_{mj}v_j$ (r_{mj} is a rational positive number) for any two reactions R_m and R_j. Such expressions among the velocities also give the relationship among the concentrations of the species at steady state (unless, in the case of power law kinetics, $\prod_{i=1}^{n} X_i^{\kappa_{im}} = \prod_{i=1}^{n} X_i^{\kappa_{ij}}$, so that $k_m=k_j$ is required for the existence of positive steady states as exemplified by network N_6 in Chapter II). This leads us to suspect that when there are only a few extreme currents comprising the steady state, it must be possible to express the steady states of (n-1) of the n species in terms of the remaining one. Hence, knowing the steady state concentration of this single species is equivalent to solving the network steady state which, mathematically, is a system of nonlinear algebraic equations. Again, we realize that determining the component extreme currents of a network is essential to the solution of the steady state problem.

The form of the reduced steady state problem can be represented in general by the following m-th order polynomial and a set of functions $g_i(X)$:

$$f_m(X,\beta) = X^m+\beta_{m-1}X^{m-1}+\ldots+\beta_0 = 0 \qquad (3.1)$$

$$X_i=g_i(X) \;,\; X_i \neq X \qquad i=1,..,(n-1)$$

where $X \epsilon$ R. and $\beta = (\beta_{m-1},\beta_{m-2},..,\beta_0)$. The set of functions $g_i(X)$ is a direct consequence of the current structure and can be determined from equation (2.31). Without loss of generality, X in equation (3.1) corresponds to the n-th species X_n of the network. In certain cases that we will encounter, not all positive roots of (3.1) will qualify as physically feasible steady states because it may happen that a function g_i gives a negative value to the steady state concentration of the i-th species. This case will be fully considered in the method of analysis presented in this chapter.

The present method interprets $f_m(X,\beta)=0$ as a catastrophe manifold in RxR^m. Note that by some nonlinear transformation, equation (3.1) can be rewritten in the form

$$f_m(X',\rho) = (X')^m+\rho_{m-2}(X')^{m-2}+\rho_{m-3}(X')^{m-3}+\ldots+\rho_0 = 0 \qquad (3.2)$$

which reduces the number of parameters by one, i.e. ρ =

$(\rho_{m-2}, \rho_{m-3}, \ldots, \rho_0) \in R^{m-1}$. Equation (3.2) now defines the catastrophe manifold in RxR^{m-1}. The number (m-1) is called the dimension of ρ-parameter space. The dimension of the steady state manifold M is usually much larger than (m-1), hence the advantage of the reduction.

Since X is one-dimensional, the only singularities of the catastrophe manifold that can occur are the cuspoids. Woodcock and Poston(19) provide very illustrative computer graphics of these cuspoids up to m = 7. The common names of these cuspoids are as follows :

m	Name of catastrophe
2	fold
3	cusp
4	swallowtail
5	butterfly
6	wigwam
7	star .

It can be checked (reference 19, p.9) that each higher order catastrophe, when plotted on the appropriate plane, generates the lower order ones.

The essential problem here is to find the portions of the particular catastrophe manifold that correspond to the non-negative roots of (3.1) and from their projections onto the parameter space, one can conveniently derive the exact expressions (in terms of the parameters) that determine the number of steady states. The algebro-geometric analysis is best illustrated by showing in detail the analysis on the cusp manifold. The results on the fold and the swallowtail will then be summarized. When m≥5, the exact expressions are quite cumbersome to find and it is suggested that one resorts to numerical procedures in finding the roots of the polynomial $f_m(X,\beta)$. This is still a much simpler problem compared to that of finding the simultaneous roots of a system of nonlinear equations.

B. An Algebro-Geometric Analysis on *M* : The Cusp Catastrophe

The algebro-geometric analysis on the steady state manifold *M* is demonstrated in detail in this section using the cusp catastrophe manifold. Consider the cubic polynomial

$$f_3(X,\beta) = X^3+\beta_2X^2+\beta_1X+\beta_0 = 0 \ . \tag{3.3}$$

This can be reduced in the form

$$f_3(X',\rho) = (X')^3 + \rho_1X' + \rho_0 = 0 \tag{3.4}$$

using the following transformation:

$$\begin{aligned} X' &= X + (\beta_2/3) \\ \rho_1 &= \beta_1 - 3(\beta_2/3)^2 \\ \rho_0 &= \beta_0 - \beta_1(\beta_2/3) + 2(\beta_2/3)^3 \ . \end{aligned} \tag{3.5}$$

Equation (3.4) defines the cusp catastrophe manifold in $X'-\rho_1-\rho_0$ space (figure 3.1). The fold points (or singular points) of the manifold determined by $f_3(X')=\partial f_3(X')/\partial X'=0$ project onto the $\rho_1-\rho_0$ plane as the cusp catastrophe set Σ^0:

$$\Sigma^0 = \{(\rho_0,\rho_1)\epsilon R^2 \mid 4\rho_1^3 + 27\rho_0^2 = 0 \} \qquad (3.6)$$

Observe that Σ^0 is empty for all $\rho_1>0$. The cusp point, Σ', coincides with the origin.

The problem is to determine the regions on the $\rho_1-\rho_0$ plane where there are 3,2,1 or 0 positive real roots of the original polynomial (3.3). From (3.5), $X>0$ if and only if

$$X' > (\beta_2/3) \ . \qquad (3.7)$$

This means that the part of the surface $f_3(X')=0$ that is above the plane $P = \{ (X',\rho_0,\rho_1)\epsilon R^3 \mid X' = \beta_2/3 \}$ represents all the positive roots of $f_3(X,\beta)$ as illustrated in figure 3.1 The intersection of P and the cusp manifold is always a straight line L and corresponds to $\beta_0=0$. Figure 3.2 describes all the possible regions on the $\rho_1-\rho_0$ parameter plane where there are 3,2,1 or 0 positive roots X. Note that L_ρ , the projection of L onto the $\rho_1-\rho_0$ plane, is always tangent to Σ^0 on one side. The coordinates of the points labeled in figure 3.2 are:

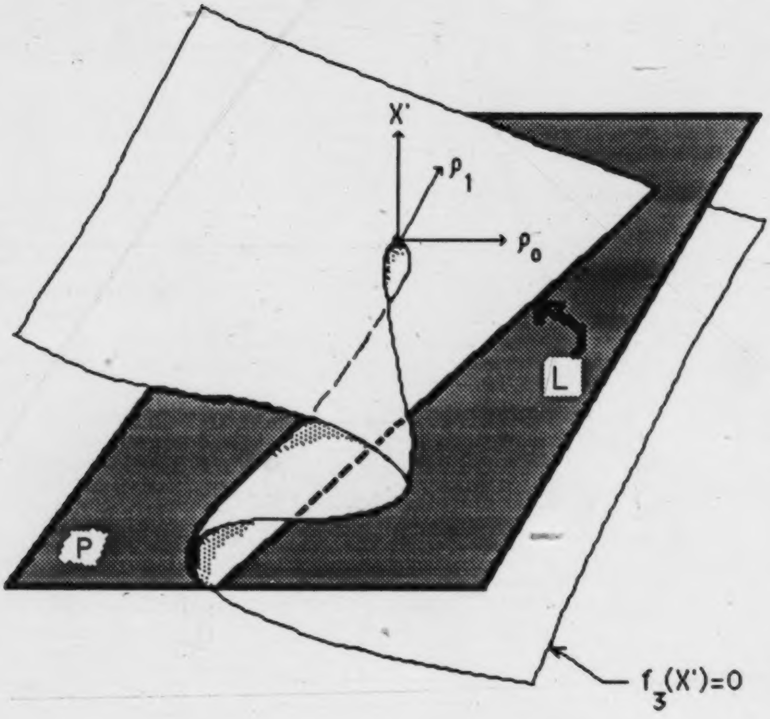

Figure 3.1

The cusp catastrophe manifold representing the roots of the cubic polynomial $f_3(X')=0$, equation 3.4. The portion of the manifold above the plane P corresponds to the positive roots of the polynomial $f_3(X)=0$, equation 3.3.

$$(\rho_0^1,\rho_1^1) = [2(\beta_2/3)^3\ ,-3(\beta_2/3)^2\ ]$$
$$(\rho_0^2,\rho_1^2) = [\ -(1/4)(\beta_2/3)^3\ ,-(3/4)(\beta_2/3)^2\ ]\ .$$

Figure 3.2 is all that is needed to solve the present problem. Define 2 groups of sets, namely, the 'state sets' and 'bifurcation sets'. A state set of order q is an open region in parameter space each point of which induces q distinct positive steady states of a reaction network. Call the state sets of orders 3,2,1,0 as Tristate (T), Bistate (D), Unistate (U) and Nilstate (N) sets, respectively.

Let the pq-bifurcation set, B_{pq}, be the set of parameters that separate the state sets of orders p and q ($p \neq q$). In the present case, these are B_{10}, B_{20}, B_{21}, B_{32}, B_{31} and B_{30}. Note that $B_{30} = (\rho_0^2,\rho_1^2)$. When $\beta_2 \geq 0$, $T = B_{31} = B_{32} = B_{30} = \emptyset$.

The pq-bifurcation sets are curves (1-dimensional) on the ρ_1-ρ_0 plane. Bifurcation sets with lower dimensions can also occur. On the ρ_1-ρ_0 plane, they will correspond to points where at least 3 state sets of different orders meet. Let $O_{pqr..}$ symbolize the pqr..-bifurcation set where state sets of orders p,q,r,.. meet. For the cubic, these are

$$O_{120} = \{(\rho_0^1,\rho_1^1) \text{ with } \beta_2 \geq 0\}$$
$$O_{123} = \{(\rho_0^1,\rho_1^1) \text{ with } \beta_2 < 0\}$$
$$O_{1320} = \{(\rho_0^2,\rho_1^2) \text{ with } \beta_2 < 0\}\ .$$

Note that $B_{30} = O_{1320}$. The state sets and bifurcation sets

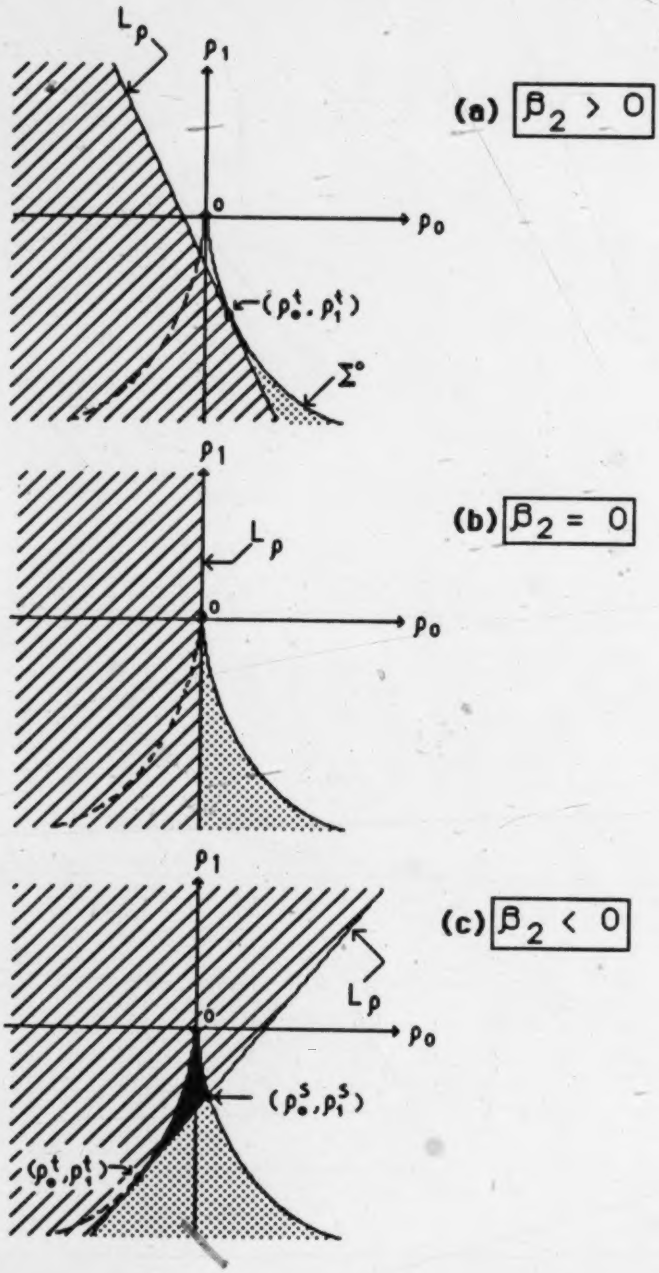
L_ρ
ρ_1
(a) $\beta_2 > 0$
0
ρ_0
(ρ_0^t, ρ_1^t)
Σ°
ρ_1
(b) $\beta_2 = 0$
L_ρ
0
ρ_0
ρ_1
(c) $\beta_2 < 0$
L_ρ
0
ρ_0
(ρ_0^s, ρ_1^s)
(ρ_0^t, ρ_1^t)

Figure 3.2

Projection of the portion of the cusp catastrophe manifold above the plane $X' = \beta_2/3$ onto the $\rho_1 - \rho_0$ plane for different signs of β_2. The number of positive roots of the cubic polynomial $f_3(X,\beta)=0$ correspond to the regions shaded as follows: ☐ 0, ▨ 1, ▒ 2 and ■ 3.

TABLE III.1

STATE SETS OF CUBIC STEADY STATE EQUATIONS

State Set	Defining Conditions
T	$\beta_2<0$, $\beta_1>0$, $\beta_0<0$, $K_3<0$
D₁	$\beta_2\leq 0$, $\beta_0>0$, $K_3<0$
D₂	$\beta_2>0$, $\beta_1<0$, $\beta_0>0$, $K_3<0$
U₁	$\beta_2\geq 0$, $\beta_0<0$
U₂	$\beta_2<0$, $\beta_0<0$, $K_3>0$
U₃	$\beta_2<0$, $\beta_0<0$, $\beta_1<0$, $K_3\leq 0$
N₁	$\beta_0>0$, $K_3>0$
N₂	$\beta_0>0$, $\beta_2>0$, $\beta_1>0$, $K_3\leq 0$

TABLE III.2

BIFURCATION SETS OF CUBIC STEADY STATE EQUATIONS

B^1_{10}	$\beta_0=0$	$\beta_2\geq 0$, $\beta_1>0$
B^2_{10}	$\beta_0=0$	$\beta_2<0$, $\beta_1>\beta_2{}^2/4$
B^1_{20}	$K_3=0$	$\beta_2\geq 0$, $\beta_1<0$
B^2_{20}	$K_3=0$	$\beta_2<0$, $\beta_0>0$
B_{21}	$\beta_0=0$	$\beta_1<0$
B_{31}	$K_3=0$	$\beta_2<0$, $\beta_0<0$, $\beta_1>0$
B_{32}	$\beta_0=0$	$\beta_2<0$, $0<\beta_1<\beta_2{}^2/4$
B_{30}	$\beta_0=0, \beta_1=\beta_2{}^2/4$	$\beta_2<0$
O_{120}	$\beta_1=\beta_0=0$	$\beta_2\geq 0$
O_{123}	$\beta_1=\beta_0=0$	$\beta_2<0$
O_{1320}	$\beta_0=0, \beta_1=\beta_2{}^2/4$	$\beta_2<0$

for the cubic are summarized in Tables III.1 and III.2. The definitions of these sets are expressed in terms of the β-coefficients of the original cubic polynomial, equation (3.3). The symbol K_3 stands for the expression

$$K_3 = 27\beta_0^2 + 4\beta_0\beta_2^3 - 18\beta_0\beta_1\beta_2 - \beta_1^2\beta_2^2 + 4\beta_1^3 \ . \qquad (3.8)$$

$K_3 = 0$ corresponds to the equation defining Σ^* (see equation (3.6)). Figure 3.3 gives a flow diagram for a convenient determination of the state set or bifurcation set corresponding to a given set of parameter values.

The following example illustrates how those defining conditions given in Tables III.1 and III.2 were arrived at starting from figure 3.2.

Example III.1.

The 3 unistate sets are derived as follows. For $\beta_2 \geq 0$, the unistate set corresponds to the left portion of the line L_ρ which has the equation $\beta_0 = 0$. This gives $\mathbf{U}_1$ immediately. For the case $\beta_2 < 0$, it is necessary to subdivide the unistate region into two, say for (i) $K_3 > 0$ and (ii) $K_3 \leq 0$. Region (i) is defined by $\mathbf{U}_2$. Region (ii) further requires that $\rho_1 < \rho_1'$. This gives the definition of $\mathbf{U}_3$. Note that a different way of partitioning the unistate set leads to different expressions but would cover exactly the same state set.

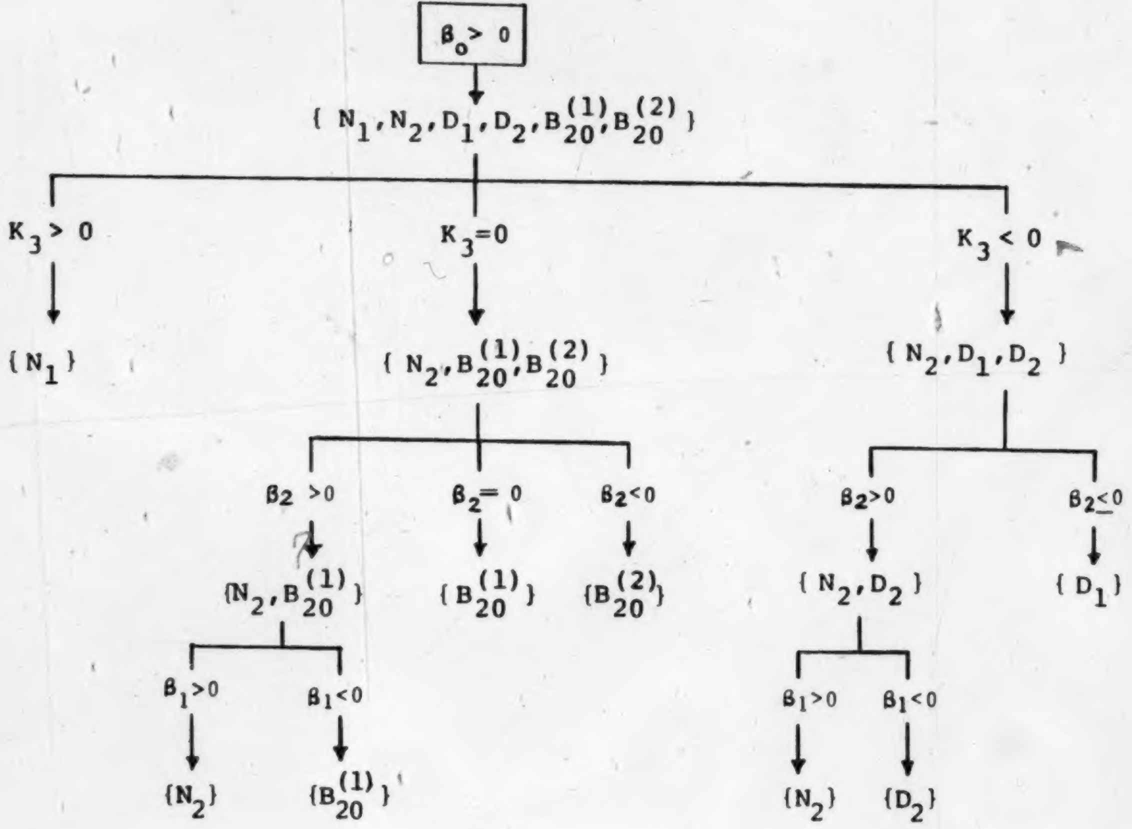
$\beta_o > 0$
$\{N_1, N_2, D_1, D_2, B_{20}^{(1)}, B_{20}^{(2)}\}$
$K_3 > 0$
$K_3 = 0$
$K_3 < 0$
$\{N_1\}$
$\{N_2, B_{20}^{(1)}, B_{20}^{(2)}\}$
$\{N_2, D_1, D_2\}$
$\beta_2 > 0$
$\beta_2 = 0$
$\beta_2 < 0$
$\beta_2 > 0$
$\beta_2 \leq 0$
$\{N_2, B_{20}^{(1)}\}$
$\{B_{20}^{(1)}\}$
$\{B_{20}^{(2)}\}$
$\{N_2, D_2\}$
$\{D_1\}$
$\beta_1 > 0$
$\beta_1 < 0$
$\beta_1 > 0$
$\beta_1 < 0$
$\{N_2\}$
$\{B_{20}^{(1)}\}$
$\{N_2\}$
$\{D_2\}$

FIGURE 3.3 Flowchart for determining the State Sets and Bifurcation Sets of cubic steady state equations, $f_3(X) = X^3+\beta_2X^2+\beta_1X+\beta_o = 0$.

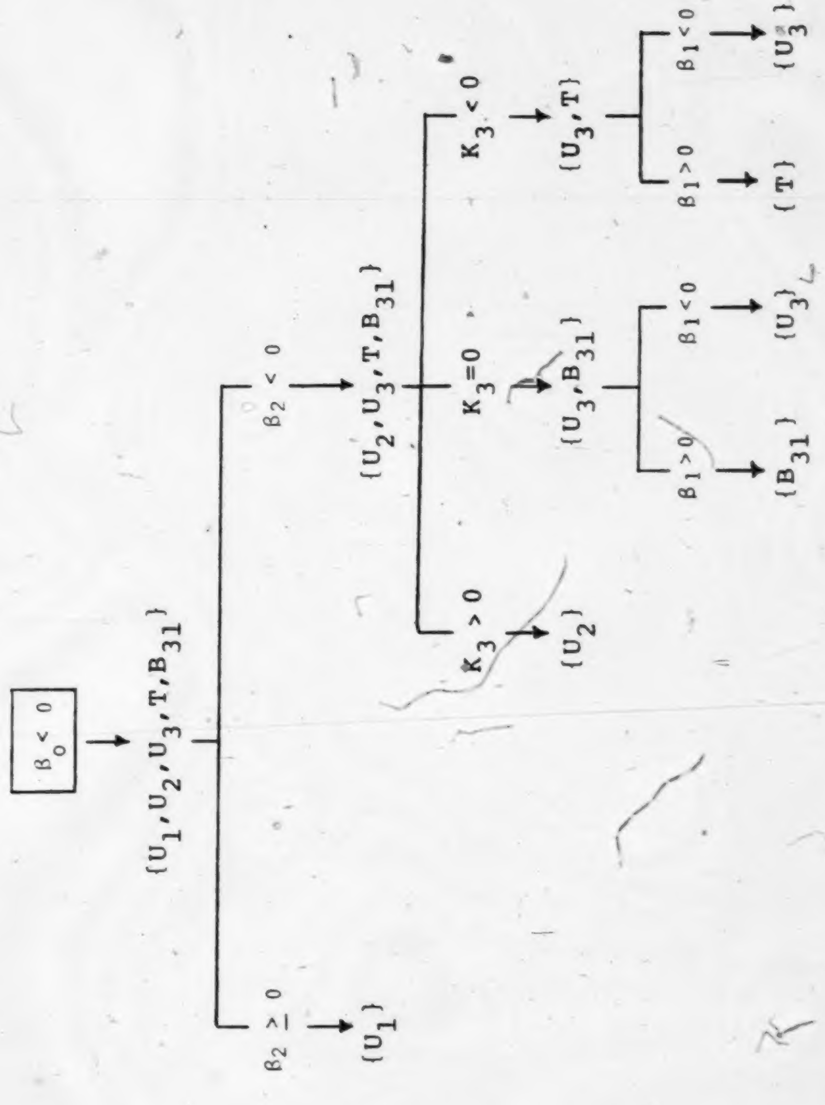
$\beta_o < 0$
$\{U_1, U_2, U_3, T, B_{31}\}$
$\beta_2 \geq 0$
$\{U_1\}$
$\beta_2 < 0$
$\{U_2, U_3, T, B_{31}\}$
$K_3 > 0$
$\{U_2\}$
$K_3 = 0$
$\{U_3, B_{31}\}$
$K_3 < 0$
$\{U_3, T\}$
$\beta_1 > 0$
$\{B_{31}\}$
$\beta_1 < 0$
$\{U_3\}$
$\beta_1 > 0$
$\{T\}$
$\beta_1 < 0$
$\{U_3\}$

FIGURE 3.3 (cont'd)

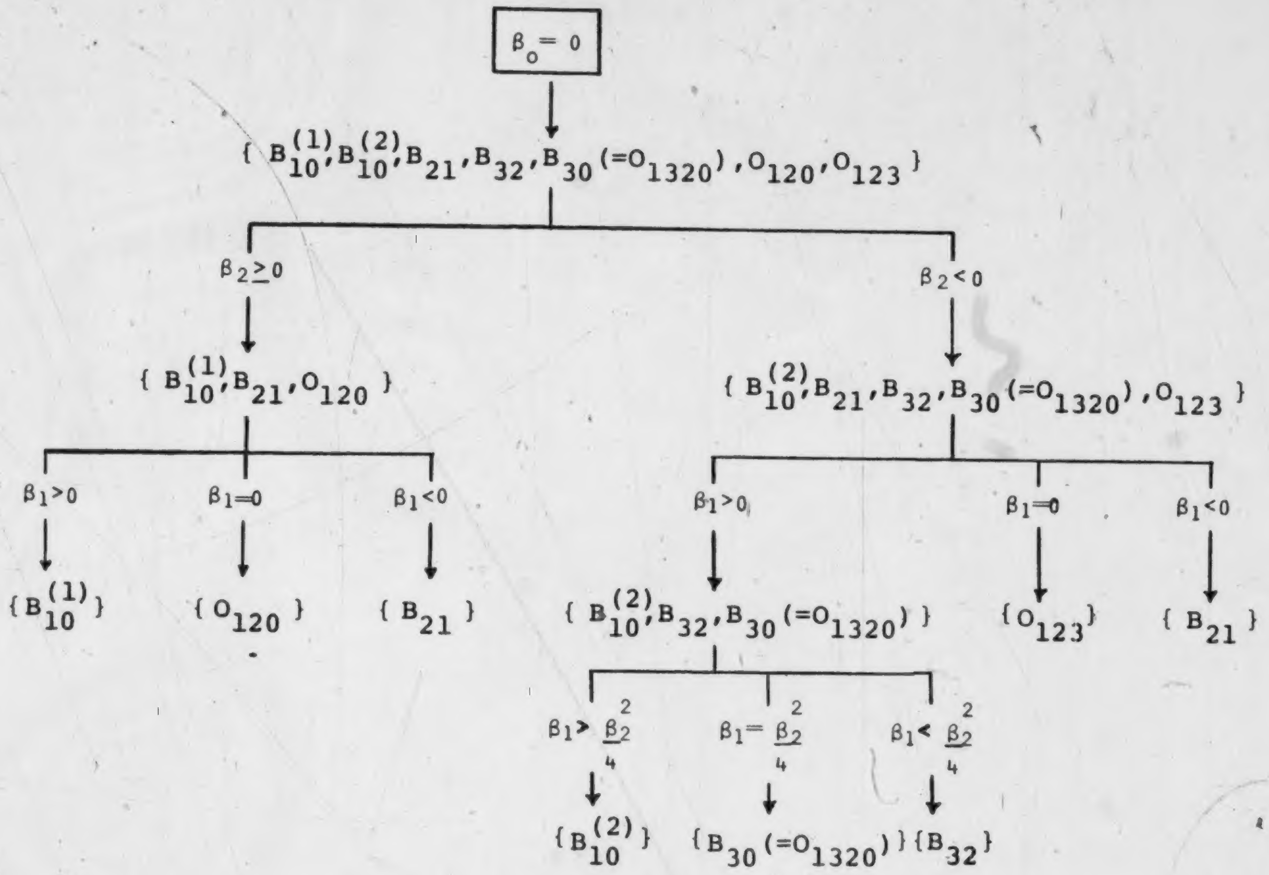
$\beta_o = 0$
$\{ B_{10}^{(1)}, B_{10}^{(2)}, B_{21}, B_{32}, B_{30}(=O_{1320}), O_{120}, O_{123} \}$
$\beta_2 \geq 0$
$\beta_2 < 0$
$\{ B_{10}^{(1)}, B_{21}, O_{120} \}$
$\{ B_{10}^{(2)}, B_{21}, B_{32}, B_{30}(=O_{1320}), O_{123} \}$
$\beta_1 > 0$
$\beta_1 = 0$
$\beta_1 < 0$
$\beta_1 > 0$
$\beta_1 = 0$
$\beta_1 < 0$
$\{ B_{10}^{(1)} \}$
$\{ O_{120} \}$
$\{ B_{21} \}$
$\{ B_{10}^{(2)}, B_{32}, B_{30}(=O_{1320}) \}$
$\{ O_{123} \}$
$\{ B_{21} \}$
$\beta_1 > \frac{\beta_2^2}{4}$
$\beta_1 = \frac{\beta_2^2}{4}$
$\beta_1 < \frac{\beta_2^2}{4}$
$\{ B_{10}^{(2)} \}$
$\{ B_{30}(=O_{1320}) \}$
$\{ B_{32} \}$

FIGURE 3.3 (cont'd)

The expression for B_{31} is seen readily from figure 3.2(c). This bifurcation set has the equation $K_3=0$ with the following important conditions: $\beta_2<0$, $\beta_0<0$ and $\rho_1>\rho_1'$. The last condition is equivalent to $\beta_1>0$. ■

It is known, in fact, that the roots of the cubic polynomial of the form (3.4) with $\rho_1\rho_0\neq 0$ can always be solved explicitly in terms of the coefficients[27]. This is done by some trigonometric transformation (see appendix C for details). The 3 roots of the original cubic polynomial (3.3) are :

$$X^{(1)}=2(-\rho_1/3)^{1/2}\cos\theta-(\beta_2/3)$$
$$X^{(2)}=2(-\rho_1/3)^{1/2}\cos(\theta+2\pi/3)-(\beta_2/3)$$
$$X^{(3)}=2(-\rho_1/3)^{1/2}\cos(\theta+4\pi/3)-(\beta_2/3)$$

where θ is determined from

$$\cos(3\theta)=3\rho_0/[2\rho_1(-\rho_1/3)^{1/2}] .$$

What has been accomplished up to this point deserves some emphasis. When the system of steady state equations is reducible to a cubic polynomial $f_3(X)$, one can actually express explicitly the steady states of the network in terms of the kinetic parameters (C,k). Regardless of the dimension of *M*, one can write exactly the conditions on the parameters satisfying the state sets and bifurcation sets that could possibly exist for a given network.

From figure 3.2, it is clear that the mathematical condition $\partial f_3(X')/\partial X' = 0$ (or $K_3=0$) is neither a sufficient nor a necessary criterion for the bifurcation of steady states. The reason for this is the constraint $X_i>0$ for all i. As the above analysis showed, there are other various bifurcation sets namely B_{10}, B_{21} and B_{32} that do not include $K_3=0$ as a condition.

The next section demonstrates how the results so far can be applied to a chemical reaction network.

C. Steady States of the Edelstein Network

The Edelstein(10) network was introduced in example II.3. It is a reversible enzyme network where a Michaelis-Menten reaction scheme is coupled with an autocatalytic reaction of the substrate. For homogeneous and isothermal conditions, with mass action kinetics, the steady states of the network are given by

$$f_3(S) = S^3+\beta_2 S^2+\beta_1 S+\beta_0 = 0$$

where

$$\beta_2 = (k_{-3}B+k_{-2}+k_3)/k_2 - k_1A/k_{-1}$$

$$\beta_1 = k_3E_0/k_{-1} - k_1A(k_{-3}B+k_{-2}+k_3)/k_{-1}k_2$$

$$\beta_0 = -k_{-2}k_{-3}BE_0/k_{-1}k_2$$

and

$$E = (k_{-2}+k_3)E_0/(k_{-3}B+k_{-2}+k_3+k_2S)$$

$$ES = E_0-E \ .$$

E_0 is the total enzyme concentration which is conserved. Notice that for every positive root of the cubic, there always correspond some positive steady state concentrations of the species E and ES. The expressions given in Table III.1 thus apply without any further constraints.

Since $\beta_0<0$, we see from figure 3.3 that there is always an odd number of steady states for every set of positive parameters. As a consequence of this, all the bifurcation sets are empty except $\mathbf{B}_{31}$. Observe that $\mathbf{T}=\emptyset$ when $\beta_2 \geq 0$. Thus, it is impossible for the network to exhibit multiple steady states if

$$k_1A/k_{-1} \leq (k_{-2}+k_{-3}B+k_3)/k_2 \ .$$

Such a set of parameters corresponds to some $(\beta_0,\beta_1,\beta_2) \in \mathbf{U}_1$.

When there are three steady states for a given set of parameters, it can be shown by standard linear stability analysis that the intermediate steady state is unstable and the other two are asymptotically stable. Thus, depending on the initial conditions, the system can be in either of the two stable steady states. This property is called bistability. The Edelstein network shows bistability when

$(C,k) \in T$. Later, it will be proven that this network cannot exhibit sustained oscillations no matter what the values of the parameters take.

Bistability occurs only under non-equilibrium conditions. It is interesting to see how far away from chemical equilibrium, and which direction, a reaction system should be 'pumped' to initiate bistability. This can be shown for the present network. Edelstein$^{(10)}$ presented computer calculations for the case $k_1 = k_{-1} = k_2 = k_{-2} = k_3 = k_{-3} = 1$ and therefore considered only the 3 parameters A, B and E_0. The expression for B_{31} from Table III.2 gives a volume which looks like a wedge in the A-B-E_0 parameter space (see Figure 3.4). Each interior point of this wedge induces 3 positive steady states. The rest of the positive orthant corresponds to parameters giving unique steady states. All the detailed-balanced steady states are given by the plane defined by A = B. The distance between the surface of the wedge and this plane gives an explicit measure of how far one has to pump the system away from equilibrium to be able to obtain multiplicity of steady states.

D. Bounded Steady States

In the Edelstein network, we saw that any positive root of the cubic determines a steady state of the network because there always correspond some positive steady state values of the other species. But this is not true in

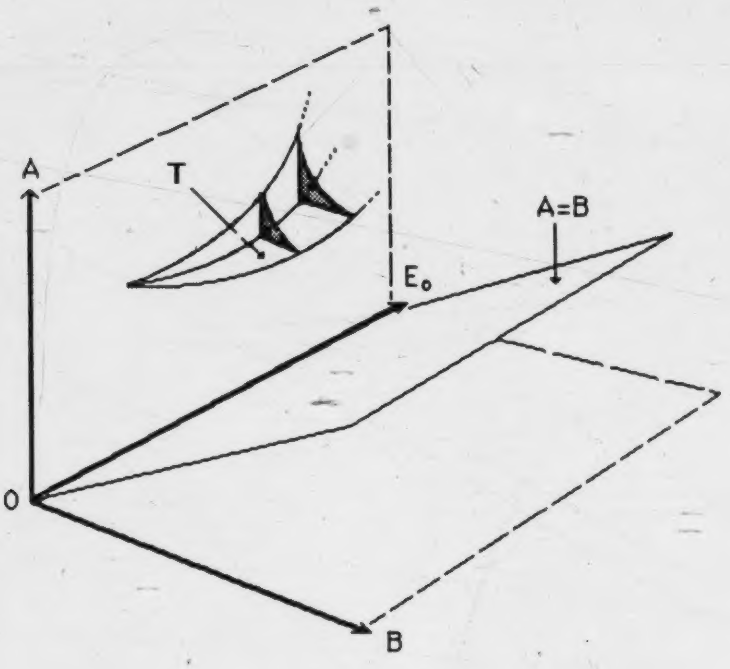

Figure 3.4

State sets for the Edelstein network for the case $k_1 = k_{-1} = k_2 = k_{-2} = k_3 = k_{-3} = 1$. **T** refers to the tristate set which is wedge-like volume shown.
The rest of the positive orthant is the unistate set **U**.
The plane defined by A=B represents the detailed-balanced steady states.

general. The expressions for the steady states of the other species may lead to further restrictions on the feasible positive roots of the reduced steady state equation. Let us consider restrictions of the form

$$X_L \le X \le X_H$$

where X_L is either 0 or a finite value and X_H may be $+\infty$ or a finite value greater than X_L. The case where $X_L = 0$ and $X_H = +\infty$ was already analyzed in detail for the cubic and the results given in figure 3.2. The case $0<X_L<X<X_H = +\infty$ has diagrams like figure 3.2 except that the line L_ρ will be rotated in the counterclockwise direction at some finite angle. Figure 3.5 gives the diagrams for the case $0=X_L<X<X_H<+\infty$. The case $0<X_L<X<X_H<+\infty$ will have diagrams similar to figure 3.5.

The state sets for the case depicted in figure 3.5 can likewise be defined explicitly in terms of the parameters. For example, the tristate set T requires two other constraints in addition to those given in Table III.1. First, looking at figure 3.5, the tristate region lies to the right of the line L_h, i.e. $\rho_0>\rho_0{}^h$. Secondly, the slope of L_h has to be negative. The equation of L_h is

$$L_h : \qquad \rho_1 = -\rho_0/[X_H+(\beta_2/3)] - [X_H+(\beta_2/3)]^2 \qquad (3.9)$$

Thus, the two further conditions for T are:

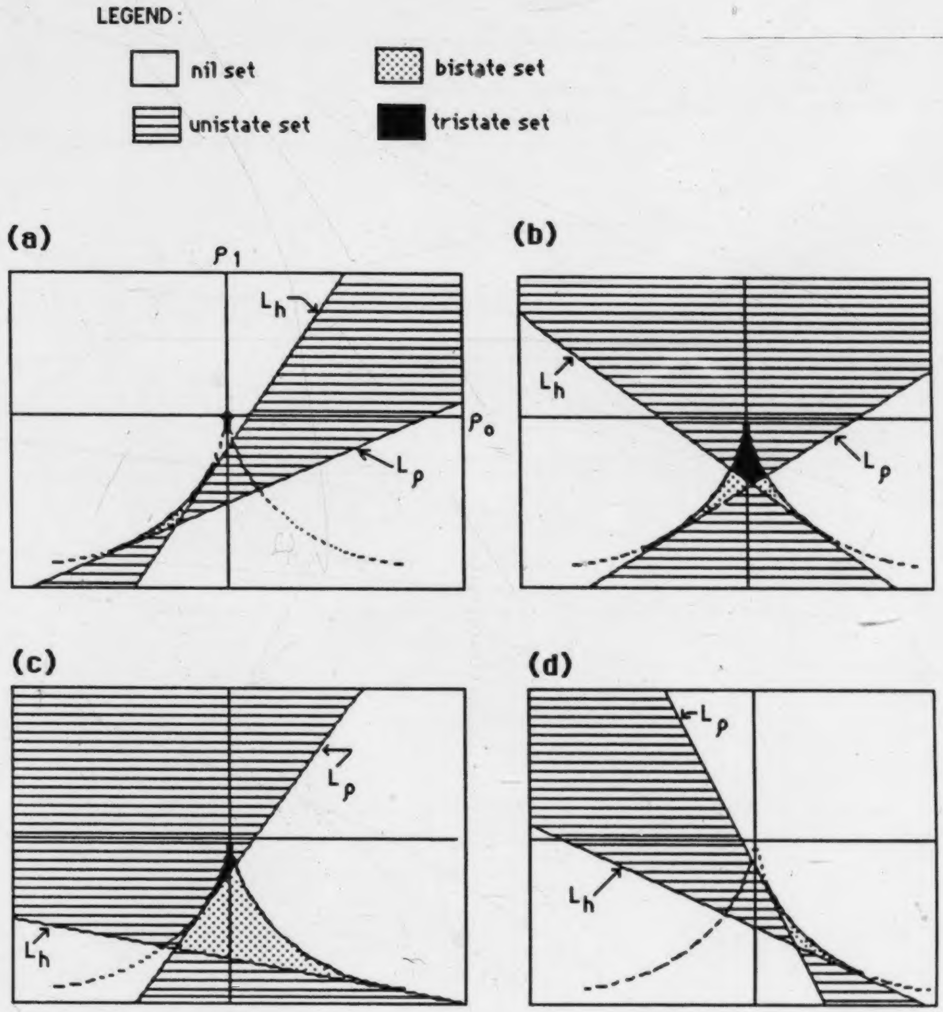
LEGEND:
nil set
bistate set
unistate set
tristate set
(a)
ρ_1
L_h
ρ_o
L_ρ
(b)
L_h
L_ρ
(c)
L_ρ
L_h
(d)
L_ρ
L_h

Figure 3.5

Possible state sets when $0=X_L < X < X_H < +\infty$. The line L_h corresponds to $X = X_H$ and the line L_ρ to $X = 0$. Cases (a)-(c) occur only if $\beta_2 < 0$, and case (d) for $\beta_2 \geq 0$.

$$f_3(X_H) > 0 \text{ and } 3X_H + \beta_2 > 0 \ . \tag{3.10}$$

Next, we analyze the steady states of a network that exemplifies the diagrams in figure 3.5.

E. Steady States of an Oscillatory Model for the Peroxidase-Oxidase Reaction

Degn, Olsen and Perram(27) came up with the following model that successfully simulates the qualitative form of the sustained oscillations observed in the peroxidase-oxidase reaction:

Network N_{11}

$$
\begin{array}{llcl}
R_1 & A + B + X & \rightarrow & 2X \\
R_2 & 2X & \rightarrow & 2Y \\
R_3 & A + B + Y & \rightarrow & 2X \\
R_4 & X & \rightarrow & \\
R_5 & Y & \rightarrow & \\
R_6 & & \rightarrow & X \\
R_7, R_{-7} & & \rightleftarrows & A \\
R_8 & & \rightarrow & B \ .
\end{array}
$$

The reaction velocities are assumed to be of the following form:

$$v_1 = k_1ABX$$
$$v_2 = k_2X^2$$
$$v_3 = k_3ABY$$
$$v_4 = k_4X$$
$$v_5 = k_5Y$$
$$v_6 = k_6$$
$$v_7 = k_7$$
$$v_{-7} = k_{-7}A$$
$$v_8 = k_8 \ .$$

At steady state, the following relationships among the reaction rates hold:

$$0 = v_8^\circ - v_1^\circ - v_3^\circ$$
$$0 = v_7^\circ - v_8^\circ - v_{-7}^\circ$$
$$0 = v_1^\circ + 2v_3^\circ + v_6^\circ - 2v_2^\circ - v_4^\circ$$
$$0 = v_8^\circ + v_6^\circ - v_4^\circ - v_5^\circ$$

from which the following expressions for the steady states are found:

$$A^\circ = (k_7 - k_8)/k_{-7}$$
$$Y^\circ = (k_6 + k_8 - k_4X)/k_5$$
$$B^\circ = k_8/[A(k_1X + k_3Y)]$$

where X is solved from the cubic

$$f_3(X,\beta) = X^3+\beta_2X^2+\beta_1X+\beta_0 = 0$$

with

$$\beta_2 = (k_4/2k_2) + k_3(k_6+k_8)/(k_1k_5-k_3k_4)$$

$$\beta_1 = k_3k_4(k_6+2k_8)/[2k_2(k_1k_5-k_3k_4)] - (k_6+k_8)/2k_2$$

$$\beta_0 = -k_3(k_6{}^2+3k_6k_8+2k_8{}^2)/2k_2(k_1k_5-k_3k_4) \ .$$

From the expressions above, we can establish a priori from the rate constants the following bounds of the steady states:

$$0 < A^\circ = (k_7-k_8)/k_{-7}$$

$$0 < B^\circ_m < B^\circ < +\infty$$

$$0 < X^\circ < (k_6+k_8)/k_4$$

$$0 < Y^\circ < (k_6+k_8)/k_5$$

where

$$B^\circ_m = k_{-7}k_8\delta/[(k_7-k_8)(k_6+k_8)]$$

$\delta = (k_4/k_1)$ or (k_5/k_3) whichever is smaller.

Note that, above all, it is necessary that $k_7>k_8$ for the steady state of A to be positive. This condition will be assumed in the phrase "for every k" used below. The following conclusions can be seen to follow immediately from figure 3.5:

(i). A positive steady state within the a priori bounds given above is unique whenever

$(k_5/k_3) > (k_4/k_1)$.

This condition implies $\beta_2>0$ and $\beta_0<0$ and the statement readily follows from figure 3.5(a).

(ii). Let $(k_5/k_3)<(k_4/k_1)$. This condition implies $\beta_0>0$ and $\beta_1<0$ for every **k**. If $K_3>0$ then no positive steady state for the network exists. This conclusion agrees with the definition of the nilstate set $\mathbf{N}_1$ given in Table III.1. However, if $K_3<0$ then there can be 0,1 or 2 positive steady states as shown by figure 3.5(c).

$K_3=0$ is the equation for the 2,0-bifurcation set. The necessary conditions that the corresponding steady states are always positive can also be written down immediately by referring to figure 3.5.

F. The Fold Catastrophe

For completeness, this section summarizes the results of the analysis on the fold catastrophe manifold defined by the quadratic polynomial

$$f_2(X,\beta) = X^2+\beta_1X+\beta_0 = 0 \quad . \tag{3.11}$$

Following the steps used in the analysis of the cusp catastrophe manifold, we find that the transformation

$$X' = X + (\beta_1/2)$$
$$\rho_0 = \beta_0 - (\beta_1/2)^2$$

gives

$$f_2(X',\rho_0) = (X')^2 + \rho_0 = 0.$$

The regions on the ρ_0-line where there are 2, 1 or 0 positive real roots of $f_2(X,\beta)$ are shown in figure 3.6. The singular points of the manifold are given by the equation

$$K_2 = \beta_0 - (\beta_1/2)^2 = 0 \ . \qquad (3.12)$$

The state sets and bifurcation sets for the quadratic are summarized in Tables III.3 and III.4.

Example III.2

The following network gives a quadratic reduced steady state equation and can have 0,1 or 2 positive steady states.

Network N_{12}

$$\begin{array}{ll}
R_1 & \rightarrow X \\
R_2, R_3 & X \rightleftarrows Y \\
R_4 & X \rightarrow Y + X \\
R_5 & 2Y \rightarrow X \\
R_6 & Y \rightarrow
\end{array}$$

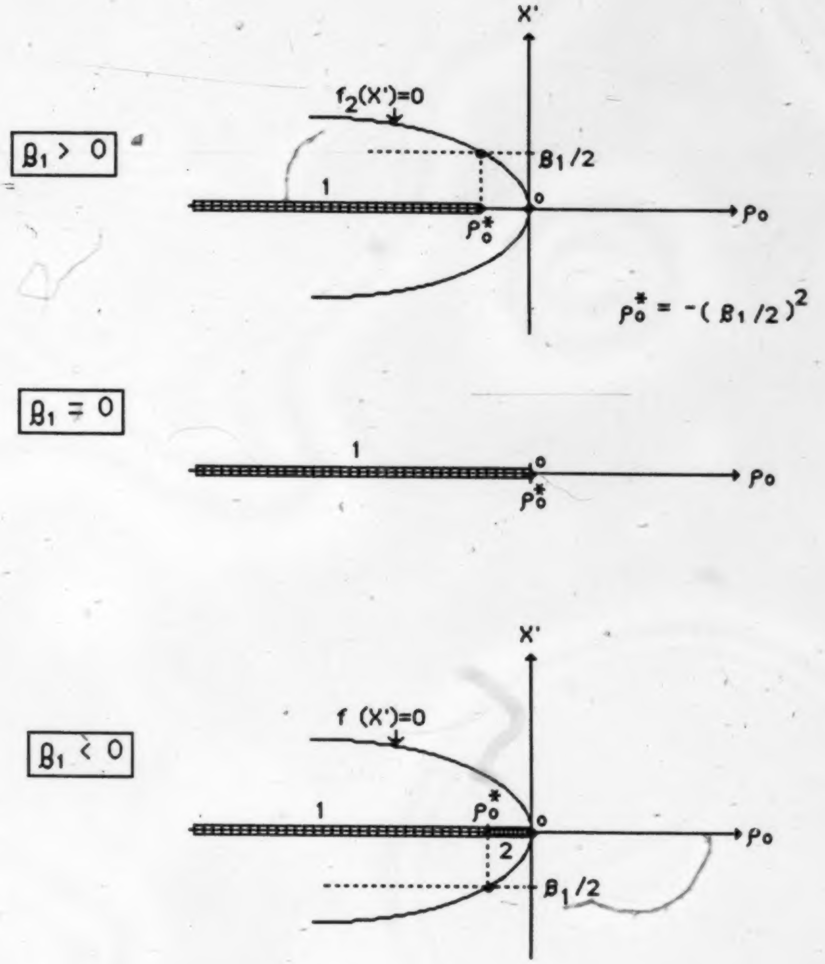
$\beta_1 > 0$
X'
$f_2(X')=0$
$\beta_1/2$
1
0
ρ_o
ρ_o^*
$\rho_o^* = -(\beta_1/2)^2$
$\beta_1 = 0$
1
0
ρ_o
ρ_o^*
$\beta_1 < 0$
X'
$f(X')=0$
1
ρ_o^*
0
ρ_o
2
$\beta_1/2$

Figure 3.6

The positive roots of the quadratic polynomial $f_2(X,\beta)$ correspond to the portion of the manifold $f_2(X')=0$ above the line $X'=\beta_1/2$. The state sets are : N ▭0 , U ▨1 and D ■2 .

TABLE III.3

STATE SETS OF QUADRATIC STEADY STATE EQUATIONS

State Set	Defining Conditions
D	$\beta_1<0,\ \beta_0>0,\ K_2<0$
U	$\beta_0<0$
$\mathbf{N}_1$	$K_2>0$
$\mathbf{N}_2$	$\beta_1>0,\ \beta_0>0,\ K_2<0$

TABLE III.4

BIFURCATION SETS OF QUADRATIC STEADY STATE EQUATIONS

$\mathbf{B}_{10}$	$\beta_0=0$	$\beta_1\geq 0$
$\mathbf{B}_{12}$	$\beta_0=0$	$\beta_1<0$
$\mathbf{B}_{20}$	$K_2=0$	$\beta_1<0$
$\mathbf{O}_{210}$	$\beta_0=\beta_1=0$	

It can easily be shown, using the definition of the bistate set D in Table III.3, that the following relationship among the rate constants is necessary for the existence of 2 positive steady states :

$$k_3/k_6 < k_2/k_4 < 1 \quad .$$

The existence and uniqueness of the steady state is ensured whenever $k_2/k_4 > 1$ regardless of the values of the other rate constants. This simple condition is necessary and sufficient. The rest of the state and bifurcation sets can likewise be written down easily once the β's are found.

The following network, on the other hand, can only have either 0 or 2 positive steady states for all parameter values.

Network N_{13}

R_1	$\rightarrow X$
R_2, R_3	$X \rightleftarrows 2Y$
R_4	$Y \rightarrow X$
R_5	$X \rightarrow 2X$
R_6	$Y \rightarrow$

$\beta_0 > 0$ for all positive parameters and therefore only the state sets **D** or **N** can be non-empty. Note that it is sufficient that $k_5 \geq k_2$ or $k_4 \geq k_6$ to satisfy $\mathbf{N}_1$, i.e. the absence of positive steady states. ■

G. Complete Linear Stability Regions and Hopf Bifurcation Sets of Dynamical Systems with $d \leq 3$

An immediate application of the algebro-geometric analysis on the cuspoid catastrophe manifolds is on linear stability analysis leading to a complete analysis of the characteristic polynomial. Also, it turns out that the Hopf bifurcation sets can be defined explicitly for dynamical systems with up to 3 independent state variables. A Hopf bifurcation set contains the parameters that delineate parameters leading to oscillations from those that do not.

For $d=3$, let the characteristic polynomial be given by

$$P_3(\lambda) = \lambda^3+\alpha_1\lambda^2+\alpha_2\lambda+\alpha_3 = 0.$$

This can be transformed to

$$P_3(\lambda') = \lambda'^3+\rho_1\lambda'+\rho_0 = 0$$

using the following equations:

$$\lambda' = \lambda + (\alpha_1/3)$$

$$\rho_1 = \alpha_2 - 3(\alpha_1/3)^2$$

$$\rho_0 = \alpha_3 - \alpha_2(\alpha_1/3) + 2(\alpha_1/3)^3 \ .$$

Figure 3.7 gives all the regions on the ρ_1-ρ_0 plane where the eigenvalues, including complex ones, have positive or negative real parts. The equation for the line L_c is given below. The details of the derivation of this equation are given in appendix D.

$$L_c : \qquad \rho_1 = \rho_0/[2(\alpha_1/3)] - 4(\alpha_1/3)^2 \qquad (3.13)$$

Part of this line gives the parameter points where the real parts of a pair of complex conjugate eigenvalues change sign. Recall that the equation for L_ρ is

$$L_\rho : \qquad \rho_1 = -\rho_0/(\alpha_1/3) - (\alpha_1/3)^2 \ . \qquad (3.14)$$

Observe from figure 3.7 that if $\alpha_1 \leq 0$, then at least one eigenvalue has a positive real part (either real or a complex pair) except along the lines L_ρ and L_c where some eigenvalues have zero real parts. Recall that along L_ρ, α_3 vanishes leading to a zero eigenvalue. For $\alpha_1=0$, the eigenvalues along L_ρ with $\rho_1>0$ are zero and a pair of pure imaginary numbers.

The above picture should agree with the well-established Routh-Hurwitz Theorem(14). This theorem states that the number of eigenvalues with positive real parts is equal to the number of sign changes in the two sequences of

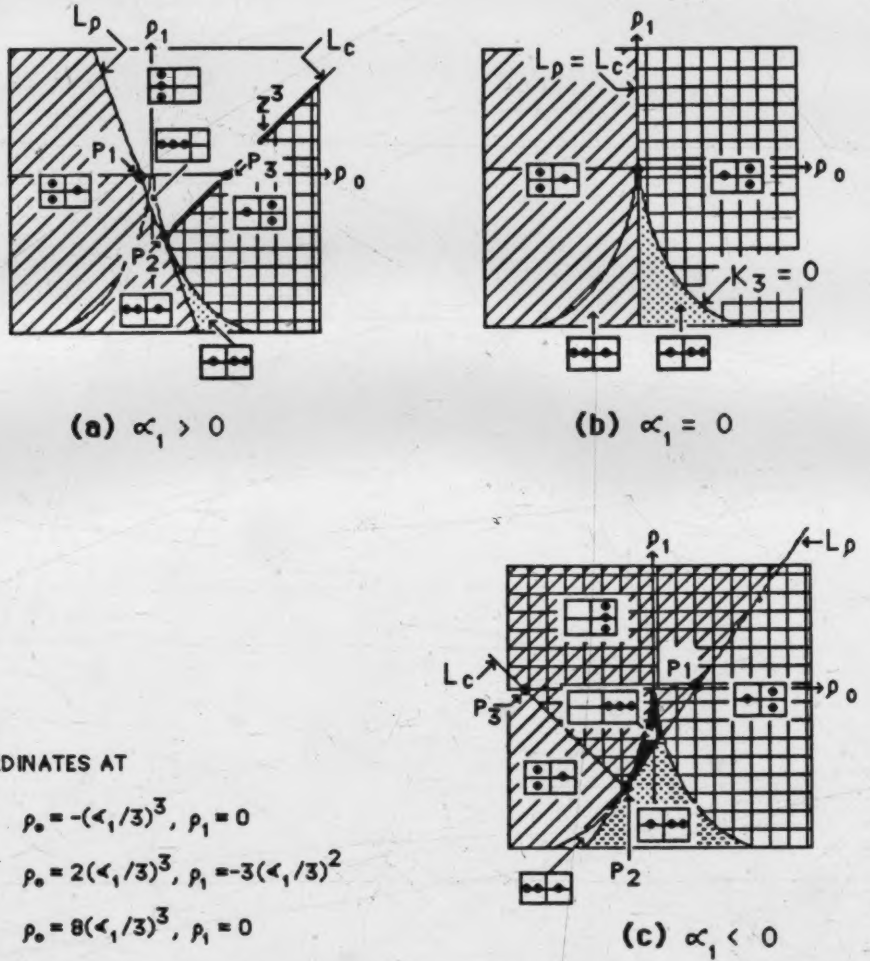

(a) $\alpha_1 > 0$

(b) $\alpha_1 = 0$

(c) $\alpha_1 < 0$

COORDINATES AT

P1 : $\rho_0 = -(\alpha_1/3)^3$, $\rho_1 = 0$

P2 : $\rho_0 = 2(\alpha_1/3)^3$, $\rho_1 = -3(\alpha_1/3)^2$

P3 : $\rho_0 = 8(\alpha_1/3)^3$, $\rho_1 = 0$

Figure 3.7

Regions on the $\rho_1 - \rho_0$ plane where different roots (eigenvalues) of the characteristic polynomial $P_3(\lambda)$ lie. ⊞ is the complex plane, and for example : ⊞ 2 negative real and 1 positive real eigenvalues ; ⊞ 1 positive real and a pair of complex conjugate eigenvalues with positive real parts. The half-ray Z^3 emanating from P2 for $\alpha_1 > 0$ is the Hopf Bifurcation set.

Hurwitz determinants, $\{1,\Delta_1,\Delta_3,\ldots\}$ and $\{1,\Delta_2,\Delta_4,\ldots\}$. The first three Hurwitz determinants are

$$\Delta_1 = \alpha_1$$
$$\Delta_2 = \alpha_1\alpha_2-\alpha_3$$
$$\Delta_3 = \alpha_3\Delta_2 \ .$$

A linearly stable region exists only if $\alpha_1>0$. This is the region to the right of L_ρ and to the left of L_c shown in figure 3.7, $\alpha_1>0$. In this region, all the real parts of the eigenvalues are negative. Let us now compare the defining conditions for this stable region with the prediction of the Routh-Hurwitz Theorem. This region according to the theorem is identified by

$$\Delta_1>0,\Delta_2>0,\Delta_3>0.$$

A little algebra shows that the equation for L_c corresponds exactly to $\Delta_2=0$, and the left side of this line to $\Delta_2>0$. The line L_ρ corresponds to $\alpha_3=0$, and the right side of it to $\alpha_3>0$. Hence, the same result arises. But there is an important advantage of being able to visualize the regions in parameter space where complex and real eigenvalues are. We know that when a real eigenvalue changes sign, *M* folds back and there is a change in the number of positive steady states. Furthermore, we could expect that the point P2 where the lines L_ρ and L_c intersect is interesting because it is where the different parameter regions corresponding to different eigenvalue signs meet. (From the coordinates given in figure 3.7, it follows that P2 corresponds to $\alpha_2 = \alpha_3 = 0$.)

Figure 3.7 also shows the points where some eigenvalues become pure imaginary and the rest have strictly negative real parts. This points can be Hopf bifurcation points where periodic solutions for the dynamical equations start to emerge. In appendix E, one finds a full statement of the Hopf Bifurcation Theorem. Here, it is only necessary to mention in addition to those requirements just stated above that the steady state must be isolated. Therefore, cases where α_d vanishes identically implying a continuum of steady states are excluded. The direction of the bifurcation of the periodic solutions will not be considered in the present discussion.

Referring to figure 3.7(a), the requirements of the Hopf bifurcation theorem are satisfied by the line L_c (Δ_2=0) with the following restrictions:

$$\alpha_1 > 0, \ \alpha_3 > 0 \text{ and } da/d\mu \neq 0$$

where μ is the bifurcation parameter and a is the real part of the complex eigenvalue. Since Δ_2=0, the above restrictions also imply α_2>0. The requirement that $da/d\mu \neq 0$ is called the transversality condition.[3//] This condition

---

[3//] A degenerate Hopf bifurcation may occur when this condition is not satisfied. Reference 28 gives an example of merely states how the bifurcation set is crossed using a particular bifurcation parameter μ, and does not affect the fact that the bifurcation set demarcates stability regions. Hence, we drop this condition in the following definition of the Hopf bifurcation set Z^d for d=3:

$$Z^3 = \{ p \mid \Delta_2=0 \text{ and } \alpha_i>0 \ (i=1,2,3) \} . \tag{3.15}$$

From the above definition of Z^3, a convenient negative test for Hopf Bifurcation can be stated : if for a given set of parameters satisfying $\Delta_2=0$ leads to a non-positive coefficient α_i (i=1,2,3), then no Hopf bifurcation occurs.

The characteristic polynomial for d=2 is

$$P_2(\lambda) = \lambda^2+\alpha_1\lambda+\alpha_2 = 0 .$$

Figure 3.8 shows the regions on the α_1-α_2 plane corresponding to different real or complex roots. The positive α_2-axis represents the Hopf bifurcation set in this case. Thus, the Hopf bifurcation set Z^2 is defined as

$$Z^2 = \{ p \mid \Delta_1=0 \text{ and } \alpha_2>0 \} \tag{3.16}$$

Again, in all calculations, one must check that for the parameters satisfying Z^d, the corresponding steady state values are positive. The use of these results will now be

---

[3] (cont'd) this case using a model of glycolytic oscillations.

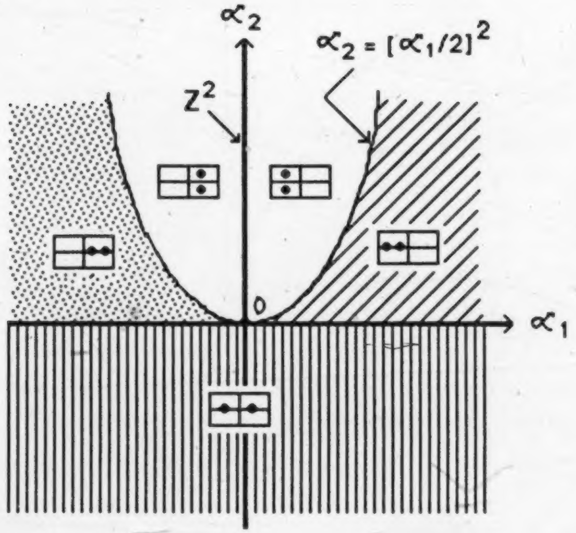
α_2
$\alpha_2 = [\alpha_1/2]^2$
Z^2
0
α_1

Figure 3.8

Roots of the quadratic characteristic polynomial (eigenvalues) on the α_1-α_2 plane. ⊞ is the complex plane and, for example, ⊞ means complex pair of eigenvalues with positive real parts and ⊞ means 1 positive real and 1 negative real. The half-ray Z^2 emanating from the origin is the Hopf bifurcation set.

illustrated by a few examples.

Example III.3 Proof that the Edelstein Network can not have a Hopf Bifurcation

The reactions of the Edelstein network are given in example II.3. For this network, the coefficients of the characteristic equation are

$$\alpha_1 = k_2E + (k_2+2k_{-1})S + k_{-2}+k_{-3}B+k_3 - k_1A$$

$$\alpha_2 = (k_{-2}+k_{-3}B+k_3)(k_2E+2k_{-1}S-k_1A) - k_2k_{-2}E + 2k_2k_{-1}S^2 - k_2k_1AS .$$

After substituting the value of k_1 resulting from the condition $\alpha_1=0$, one gets

$$\alpha_2 = -k_2E(k_{-2}+k_2S)-(k_2S+k_{-2}+k_{-3}B+k_3)^2 < 0.$$

Thus, the definition of Z^2 will never be satisfied for any set of positive parameters. In fact, the network has not been shown to exhibit sustained oscillations.■

Example III.4 Z^2 for the Brusselator

The following network called the Brusselator(29) possesses a stable limit cycle for some appropriate values of the rate constants.

Network N_{14}

$$R_1, R_4 \qquad \rightleftarrows X$$

$$R_2 \qquad 2X + Y \rightarrow 3X$$

$$R_3 \qquad X \rightarrow Y \, .$$

The kinetic equations are

$$dX/dt = k_1 - k_4X + k_2X^2Y - k_3X$$

$$dY/dt = -k_2X^2Y + k_3X \; ,$$

possessing a unique steady state given by

$$X^\circ = k_1/k_4 \quad , \quad Y^\circ = k_3k_4/k_1k_2 \; .$$

The Hopf bifurcation set is given by the equation

$$Z^2 : \qquad k_3k_4^2 = k_4^3 + k_1^2k_2$$

Figure 3.9 shows the dynamics on both sides of the Hopf bifurcation set. In these plots,[4] the rate constants used are $k_1 = k_2 = k_4 = 1$ and the bifurcation parameter is k_3. The Hopf bifurcation value is $k_3^c = 2$. At this value, $d\alpha_1/d\mu < 0$ and the stable limit cycle occurs when $k_3 > k_3^c$.■

---

[4] Throughout this work, integration of systems of first order ordinary differential equations is carried out using the IMSL Routine DGEAR which is based on Gear's stiff methods.

Example III.5 Z^3 for the Oregonator

The Oregonator⁽³⁰⁾ was proposed as a model to simulate the sustained oscillations observed in the Belousov-Zhabotinsky reaction⁽²⁶⁾. The reactions are

Network N_{15}

$$
\begin{array}{ll}
R_1 & Y \to X \\
R_2 & X + Y \to \\
R_3 & X \to 2X + 2Z \\
R_4 & 2X \to \\
R_5 & 2Z \to Y .
\end{array}
$$

The kinetic equations are

$$dX/dt = k_1Y-k_2XY+k_3X-2k_4X^2$$

$$dY/dt = k_5Z-k_1Y-k_2XY$$

$$dZ/dt = 2k_3X-2k_5Z .$$

Note that R_5 is first order with respect to Z. The reader can easily check that the network has a unique steady state for any given set of positive parameters. This steady state can be expressed explicitly in terms of these parameters and so are the coefficients of the characteristic polynomial. For the sake of illustration, let the bifurcation

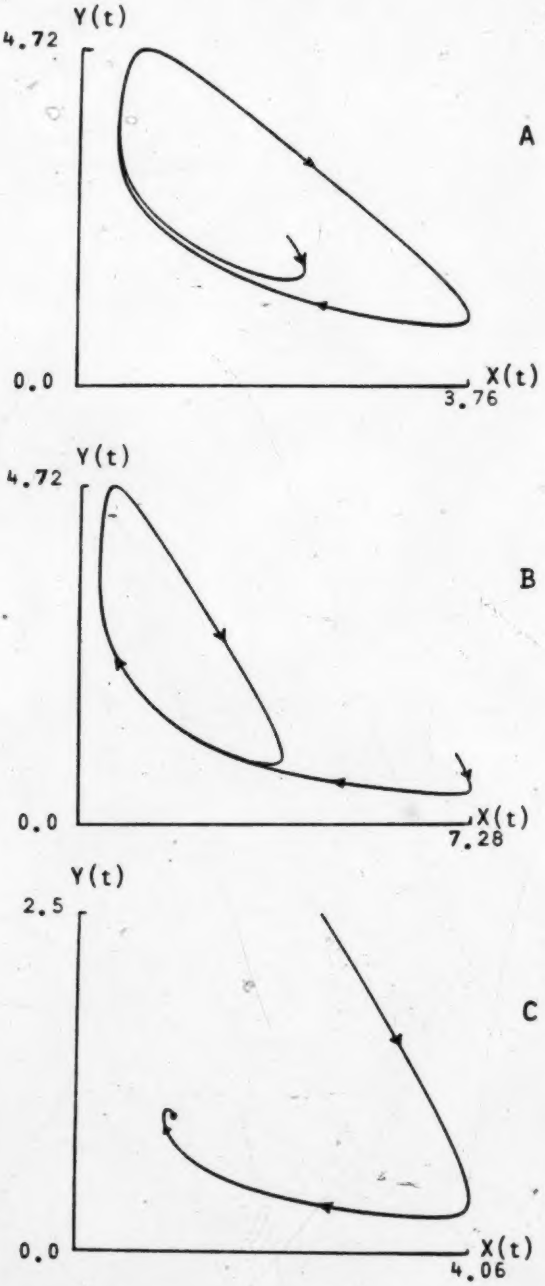

Figure 3.9

A and B show the approach to the limit cycle that is exhibited by the Brusselator (Network N_{14}) when $k_1 = k_2 = k_4 = 1$ and $k_3 = 3$. This limit cycle collapses into a stable focus (C) when $k_3 = 1$.

parameter $\mu = k_3$ and let $k_1 = k_2 = k_4 = k_5 = 1$. Then the coefficients of the characteristic polynomial are

$$\alpha_3 = 2[4(X^\circ)^2+4X^\circ+Y^\circ-\mu]$$
$$\alpha_2 = 4(X^\circ)^2+(14-\mu)X^\circ+3Y^\circ-3\mu+2$$
$$\alpha_1 = 5X^\circ+Y^\circ-\mu+3$$
$$\alpha_0 = 1 \ .$$

The Hopf bifurcation set Z^3 is defined by

$$\Delta_2 = 2(3\mu+Y^\circ)-(5X^\circ+Y^\circ-\mu+3)[(10-\mu)X^\circ+3Y^\circ+\mu+2] = 0$$

along with the condition that $\alpha_i>0$, $i=1,2,3$. When $\Delta_2<0$, a stable limit cycle exists as figure 3.10 demonstrates.■

H. The Swallowtail Catastrophe

The quartic polynomial

$$f_4(X,\beta) = X^4+\beta_3X^3+\beta_2X^2+\beta_1X+\beta_0 = 0 \qquad (3.17)$$

can be transformed into a 3-parameter quartic by translating X to X', that is

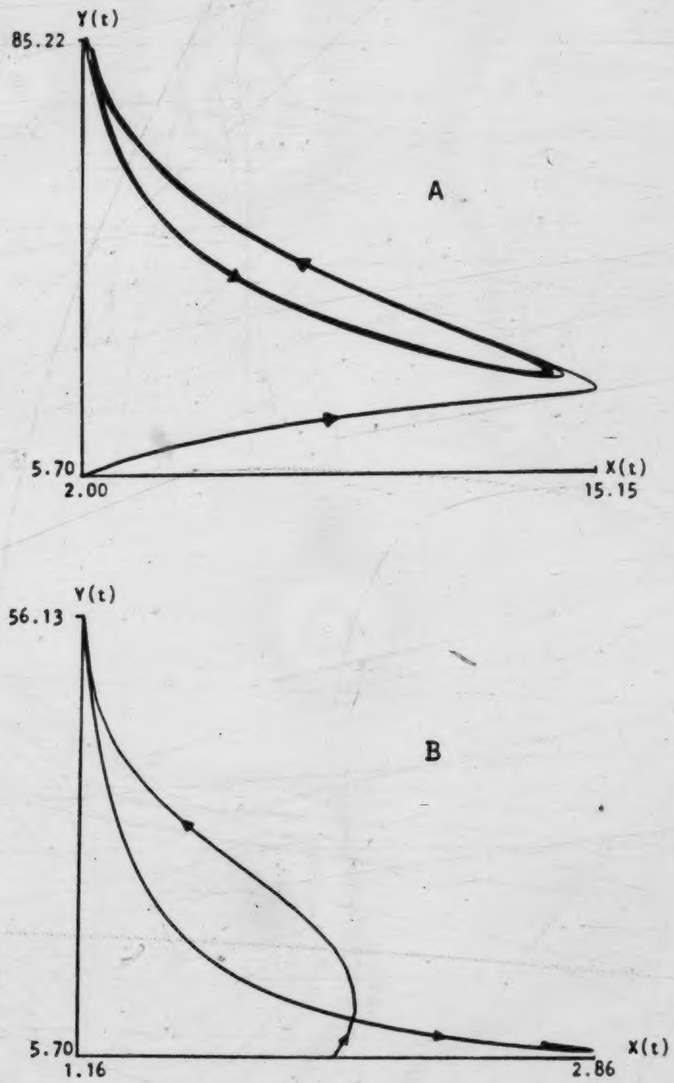

Figure 3.10

A -The stable limit cycle shown by the Oregonator (Network N_{15}) when $k_1 = k_2 = k_4 = k_5 = 1$ and $k_3 = 5$.
B -The limit cycle disappears and the trajectories approach the stable steady state when k_3 is changed to 1.0.

$$\begin{aligned} X' &= X+(\beta_3/4) \\ \rho_2 &= \beta_2-6(\beta_3/4)^2 \\ \rho_1 &= \beta_1-2\beta_2(\beta_3/4)+8(\beta_3/4)^3 \\ \rho_0 &= \beta_0-\beta_1(\beta_3/4)+\beta_2(\beta_3/4)^2-3(\beta_3/4)^4 \end{aligned} \tag{3.18}$$

giving

$$f_4(X',\rho) = (X')^4+\rho_2(X')^2\rho_1X'+\rho_0 = 0 \ .$$

The swallowtail catastrophe set is defined by

$$\Sigma^0 = \{ (\rho_2,\rho_1,\rho_0) \in R^3 \mid K_4 = 0 \} \tag{3.19}$$

where

$$K_4 = 27\rho_1^4-144\rho_0\rho_1^2\rho_2+4\rho_1^2\rho_2^3-256\rho_0^3+128\rho_0^2\rho_2^2-16\rho_0\rho_2^4 \ . \tag{3.20}$$

Σ^0 gives the set of (ρ_2,ρ_1,ρ_0) satisfying $f_4(X') = \partial f_4/\partial X' = 0$. It is a connected surface in ρ_2-ρ_1-ρ_0 space and is shown in figure 3.11. The following sets corresponding to degenerate singular points of $f_4(X',\rho_2,\rho_1,\rho_0)= 0$ are also shown in fig. 3.11:

$$\Sigma^1 = \{(\rho_2,\rho_1,\rho_0) \mid f_4(X')=\partial f_4/\partial X'=\partial^2 f_4/\partial X'^2=0 \}$$

$$\Sigma^2 = \{(\rho_2,\rho_1,\rho_0) \mid f_4(X')=\partial f_4/\partial X'=\partial^2 f_4/\partial X'^2=\partial^3 f_4/\partial X'^3=0 \} \ .$$

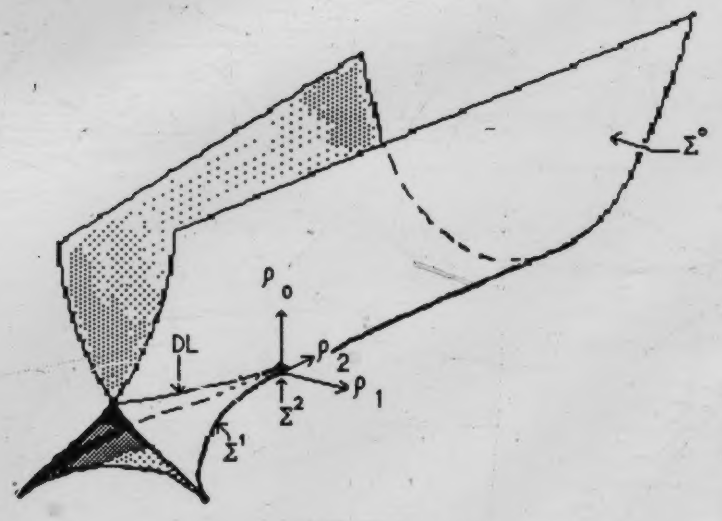

Figure 3.11

The swallowtail catastrophe set (Σ^0). Σ^1 is a curve of cusp points with two branches meeting at the swallowtail point, Σ^2. Note that $\Sigma^2 \subset \Sigma^1 \subset \Sigma^0$. DL is a curve corresponding to the double limit point variety (see chapter IV).

Note that Σ^2 is a subset of Σ^1 which in turn is a subset of Σ^0. In terms of the ρ parameters, Σ^1 and Σ^2 are defined below:

$$\Sigma^1=\{(\rho_2,\rho_1,\rho_0)\,|\,\rho_1=\pm(2/9)\rho_2(-6\rho_2)^{1/2},\ \rho_0=-\rho_2^2/12,\ \rho_2\leq 0\} \tag{3.21}$$

$$\Sigma^2 = \{(\rho_2,\rho_1,\rho_0)=(0,0,0)\}\ . \tag{3.22}$$

Figure 3.11 suggests separating two cases, $\rho_2\geq 0$ and $\rho_2<0$, to give two qualitatively different bifurcation sets on the ρ_1-ρ_0 plane as shown in figure 3.12(a) and (b).

The manifold $f_4(X',\rho_2,\rho_1,\rho_0)=0$ for each of these bifurcation sets are also shown in figure 3.12.

Now that the singularity structure of $f_4(X',\rho_2,\rho_1,\rho_0)=0$ is known in detail, the regions in ρ_2-ρ_1-ρ_0 space where there are 4,3,2,1 or 0 distinct real and positive roots of $f_4(X,\ \beta_3,\ \beta_2,\ \beta_1,\ \beta_0) = 0$ can be identified exactly. The region with 4 distinct real positive roots will be called the Quadristate set, Q.

From equation (3.18), $X > 0$ if and only if $X' > \beta_3/4$. The intersection of the plane

$$P(\rho_2,\beta_3) = \{\ (X',\rho_1,\rho_0)\ |\ X' = \beta_3/4\ \}$$

for fixed ρ_2, is always a straight line whose equation is

$$L(\rho_2,\beta_3)\ :\qquad \rho_0 = -(\beta_3/4)\rho_1-[\rho_2+(\beta_3/4)^2](\beta_3/4)^2 \tag{3.23}$$

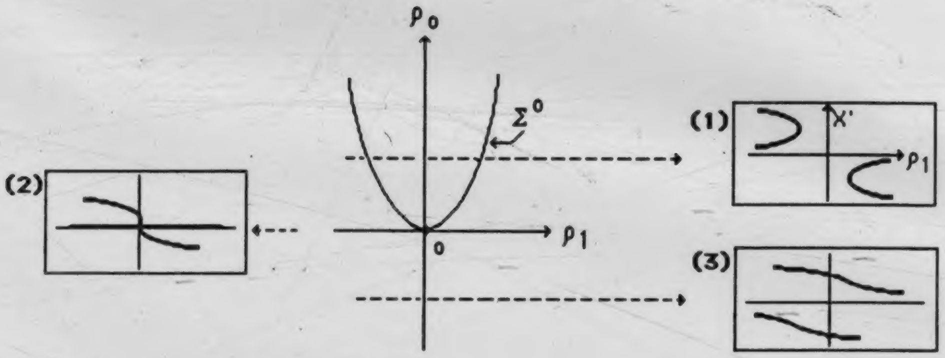
ρ0
Σ0
(1)
X'
ρ1
(2)
0
ρ1
(3)

(a) $\rho_2 \geq 0$

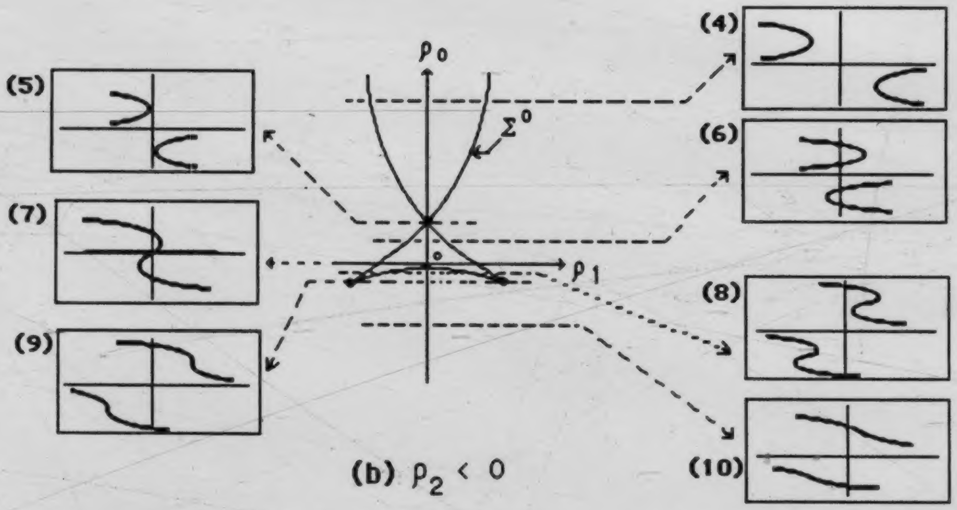
(4)
ρ0
(5)
Σ0
(6)
(7)
o
ρ1
(8)
(9)
(10)

(b) $\rho_2 < 0$

Figure 3.12

Two types of bifurcation sets (a) and (b) depending on the sign of ρ_2 for the quartic polynomial. The graphs of the real roots X' as functions of ρ_1 are shown for 10 different fixed values of ρ_0.

In fact, the envelope of these lines for various β_3 values is one of the bifurcation sets shown in figure 3.12 depending on the sign of ρ_2. With this picture in hand and the diagrams given in figure 3.12, the state sets **Q**, **T**, **D**, **U** and **N** are determined. All the possibilities are exhausted in figure 3.13.

In order to identify the state and bifurcation sets, the coordinates of the points labeled as (ρ_1',ρ_0'), (ρ_1',ρ_0') and (ρ_1'',ρ_0'') must be determined. Unlike the cusp, there are no explicit expressions for the coordinates of these points. The explicit definitions for the various state sets can be made but their application is quite cumbersome. Instead, we list down some general tests that are sufficient to prove the absence of some state sets.

First, note that the kind of bifurcation set on the ρ_1-ρ_0 plane, i.e. either (a) or (b) in figure 3.12, and the slope of $L(\rho_2,\beta_3)$ are immediately determined by β_3 and β_2. Figure 3.13 will be of help in understanding the following tests. Below, **P** is the constrained parameter space where the constraints are specified in each test.

Test 1. No more than 2 Steady States

If $8\beta_2-3\beta_3^2\geq 0$, then $\mathbf{Q}=\mathbf{T}=\emptyset$ and $\mathbf{P} = \{ \mathbf{N}\ U\ \mathbf{U}\ U\ \mathbf{D} \}$.

(U means 'union')

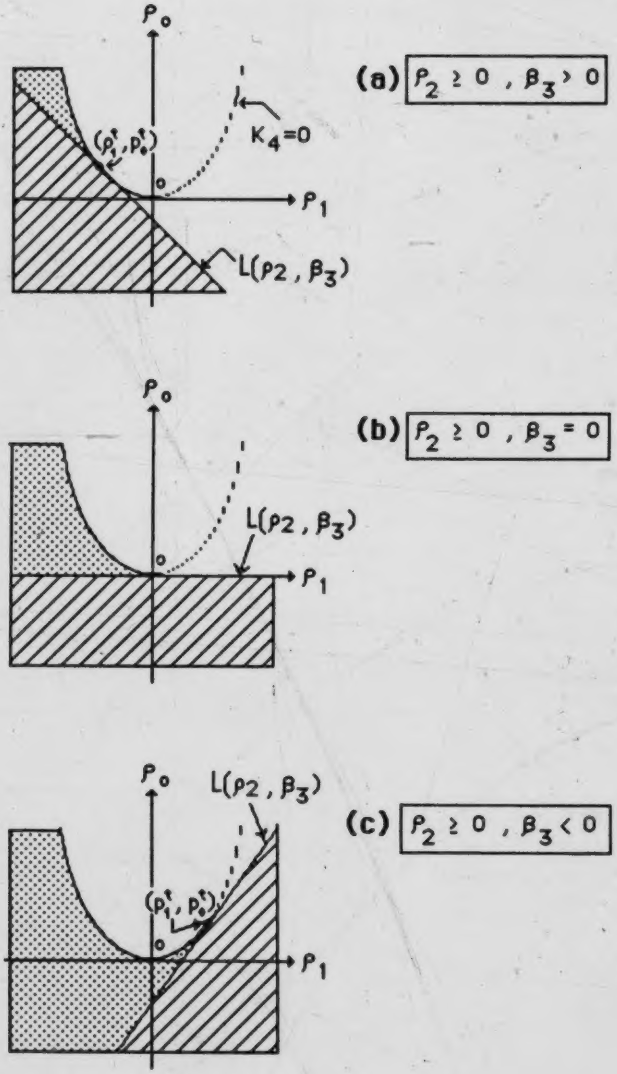
(a) $\rho_2 \geq 0$, $\beta_3 > 0$
ρ_0
ρ_1
(ρ_1^*, ρ_0^*)
$K_4=0$
0
$L(\rho_2, \beta_3)$
(b) $\rho_2 \geq 0$, $\beta_3 = 0$
ρ_0
ρ_1
0
$L(\rho_2, \beta_3)$
(c) $\rho_2 \geq 0$, $\beta_3 < 0$
ρ_0
ρ_1
(ρ_1^*, ρ_0^*)
0
$L(\rho_2, \beta_3)$

Figure 3.13

State sets for the quartic polynomial $f_4(X,\beta) = 0$ according to the signs of ρ_2 and β_3 : N ☐ 0, U ▨ 1, D ░ 2, T ■ 3, Q ▦ 4

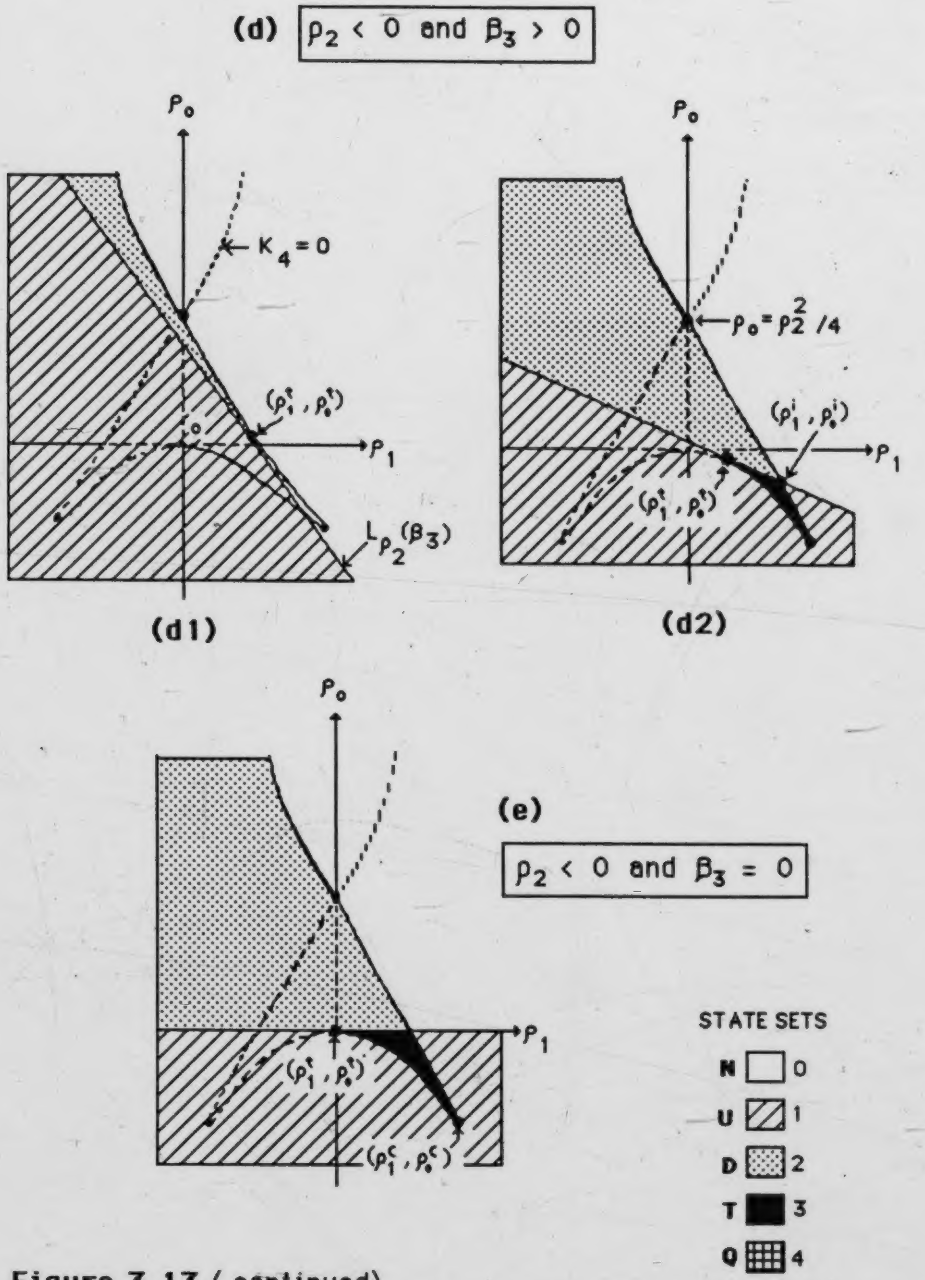
(d) $\rho_2 < 0$ and $\beta_3 > 0$
ρ_0
$K_4 = 0$
(ρ_1^t, ρ_0^t)
ρ_1
$L_{\rho_2}(\beta_3)$
(d1)
ρ_0
$\rho_0 = \rho_2^2/4$
(ρ_1^i, ρ_0^i)
ρ_1
(ρ_1^t, ρ_0^t)
(d2)
ρ_0
(e)
$\rho_2 < 0$ and $\beta_3 = 0$
ρ_1
(ρ_1^t, ρ_0^t)
(ρ_1^c, ρ_0^c)
STATE SETS
N ☐ 0
U ▨ 1
D ░ 2
T ■ 3
Q ▦ 4

Figure 3.13 (continued)

(f) $\boxed{\rho_2 < 0 \text{ and } \beta_3 < 0}$

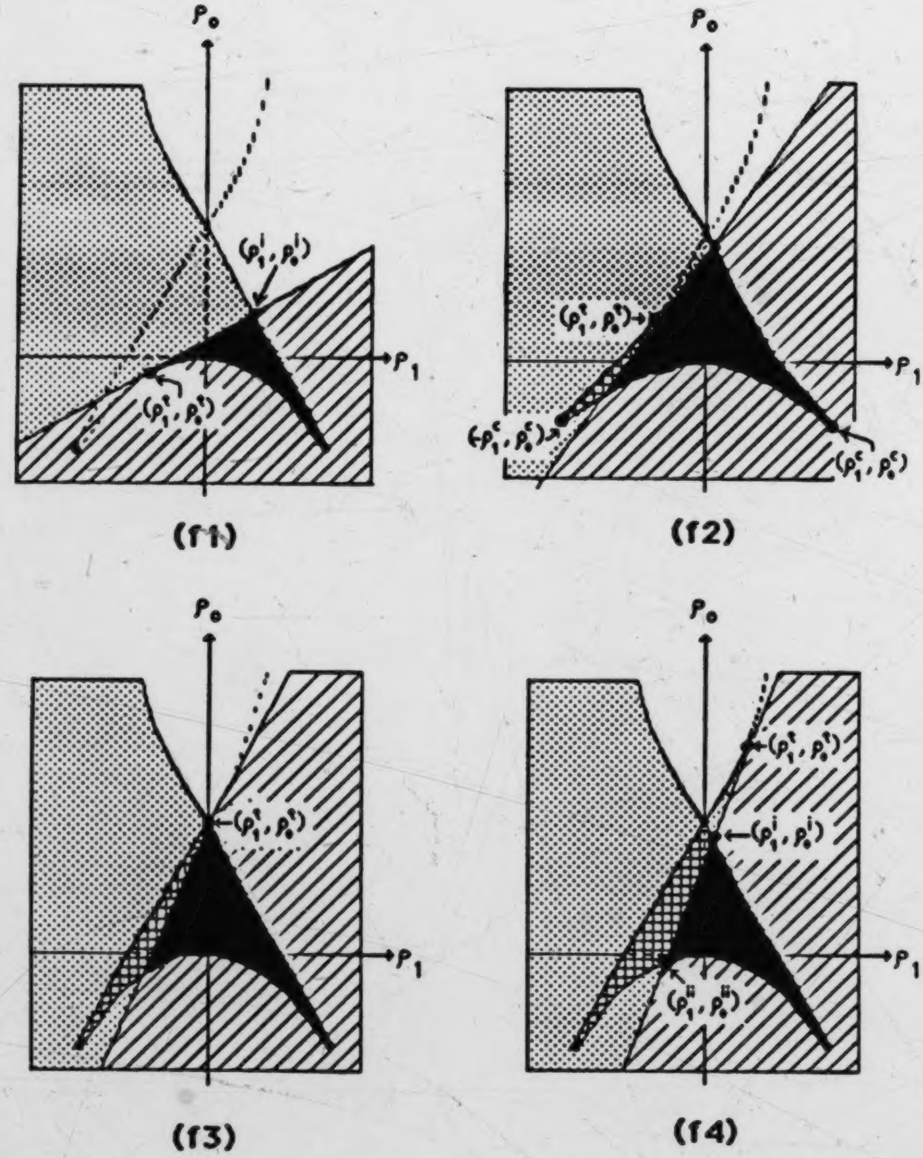
ρ_o
ρ_1
(ρ_1^i, ρ_o^i)
(ρ_1^s, ρ_o^s)
(ρ_1^c, ρ_o^c)
$(\rho_1^{ii}, \rho_o^{ii})$

(f1) (f2)

(f3) (f4)

Figure 3.13 (cont'd) STATE SETS: N ☐ 0, U ▨ 1, D ▒ 2, T ■ 3, Q ▦ 4

Test 2. Sufficient Condition for Uniqueness

If $8\beta_2-3\beta_3^2\geq 0$ and $\beta_0<0$, then $\mathbf{Q}=\mathbf{T}=\mathbf{D}=\mathbf{N}=\emptyset$ and $\mathbf{P} = \{\mathbf{U}\}$.

Tests 1 and 2 correspond to cases (a), (b) and (c) in figure 3.13. The condition $8\beta_2-3\beta_3^2\geq 0$ is equivalent to $\rho_2\geq 0$. The condition $\beta_0<0$ is equivalent to $\rho_0<\rho_0^L$ where ρ_0^L is given by equation (3.23).

In cases (a)-(c) of figure 3.13, there are no positive real roots when $K_4<0$. Likewise, in all of cases (d)-(f) as long as $K_4 < 0$ and $\rho_0>\rho_2^2/4$, there are no positive real roots. These are the contents of tests 3 and 4.

Test 3. Absence of Steady States

If $8\beta_2-3\beta_3^2\geq 0$ and $K_4<0$, then $\mathbf{Q}=\mathbf{T}=\mathbf{D}=\mathbf{U}=\emptyset$ and $\mathbf{P} = \{\mathbf{N}\}$.

Test 4. Absence of Steady States

If all of the following conditions are satisfied, then $\mathbf{Q}=\mathbf{T}=\mathbf{D}=\mathbf{U}=\emptyset$ and $\mathbf{P} =\{\mathbf{N}\}$.

(i) $8\beta_2-3\beta_3^2<0$

(ii) $K_4<0$

(iii) $4\rho_0-\rho_2^2>0$.

Regardless of β_2 and β_3, the region 'below' the line $L(\rho_2,\beta_3)$, that is $\rho_0<\rho_0^L$, has always an odd number of steady states. This is stated in test 5. Test 6 gives the complementary case.

Test 5. Odd number of Steady States

If $\beta_0<0$ then $\mathbf{Q}=\mathbf{D}=\mathbf{N}=\emptyset$ and $\mathbf{P} = \{ \mathbf{T} \cup \mathbf{U} \}$.

Test 6. Even Number of Steady States

If $\beta_0>0$ then $\mathbf{T}=\mathbf{U}=\emptyset$ and $\mathbf{P} = \{ \mathbf{Q} \cup \mathbf{D} \cup \mathbf{N} \}$.

Test 7 extends the claim of Test 5. It is to be understood that Test 7 is not a necessary condition for the uniqueness of a positive real root.

Test 7. Uniqueness of Steady States

If $\beta_0<0$ and $K_4>0$, then $\mathbf{Q}=\mathbf{T}=\mathbf{D}=\mathbf{N}=\emptyset$ and $\mathbf{P}=\{\mathbf{U}\}$.

The following test concerns itself with the necessary conditions for Q to be non-empty.

Test 8. Necessary condition for the existence of Q

If any of the following conditions is not satisfied, then $\mathbf{Q} = \emptyset$.

(i) $8\beta_2-3\beta_3^2<0$

(ii) $\beta_3<\beta_3^C<0$

(iii) $\beta_0>0$

β_3^C is given implicitly (as a function of β_2) in appendix F, equation (F.1).

Lastly, we want to include the following well known algebraic rule for counting positive roots of polynomials:

Test 9. Descartes' Rule of Signs(62)

Consider the polynomial $f_n(X) = X^n+\beta_{n-1}X^{n-1}+...+\beta_0$. Let N be the number of sign changes in the sequence $\{1, \beta_{n-1}, \beta_{n-2}, ..., \beta_0\}$ ignoring any zeroes. Then there are at most N real positive roots of $f_n(X)$. Furthermore, there are exactly either N, or (N-2), or (N-4),... real positive roots.

The above tests can also be applied to the analysis of the characteristic polynomial for dynamical systems with four independent variables, as was done in the previous section.

This concludes the analysis on the fold, cusp and swallowtail catastrophes. The higher order catastrophes can, in principle, be analyzed in a similar way.

One finds in the chemical engineering literature several examples of simple networks occurring in a non-isothermal continuously stirred tank reactor (CSTR) that exhibit higher order catastrophes. Some examples are given by Balakotaiah and Luss(32). The emergence of these highly degenerate singularities is mainly due to the highly non-linear dependence of the rate constants to the temperature (e.g. the Arrhenius exponential dependence). Near these singularities, the steady state equations can be shown to be equivalent to some high ordered polynomials. This point will be further discussed in the next chapter.

IV. BIFURCATION VARIETIES AND DIAGRAMS

A. Cross-sections of *M*

In chapter III, we studied the projection of the steady state manifold *M* onto the (C,k) parameter space because we were interested in the number of steady states for a given set of parameters. In this chapter, we shall look at cross-sections of *M* along some path indicated by a *bifurcation parameter*, μ. This parameter is usually an externally controlled experimental condition like the flow rate used in a CSTR, total enzyme concentration in biochemical networks, or the concentrations of certain external species. Some of the current parameters j_i used in Clarke's (h,j)-parametrization of *M* may also be used as μ when the experimentalist can manipulate in some way the velocities of corresponding reactions. Taking cross-sections of *M* is a convenient way of visualizing this manifold which is usually of high dimension. It must also be emphasized that a steady state study under one varying parameter of an experimental reaction system corresponds to a cross-section of the *M* of the general network that encompasses the particular system.

The graph of the steady state concentrations of the species X_i° (i=1,..,n) versus μ is called a *bifurcation diagram*. It is very important to remember that the qualitative features of a bifurcation diagram for a certain μ is affected by the values of the other parameters. In concrete terms, let the steady state parameter be represented as $\mathbf{p}=(\mu,\mathbf{p}^-)$. When $\mathbf{p}_1^- \neq \mathbf{p}_2^-$, it may happen that the bifurcation diagrams for the species X_i in each case are 'inequivalent'. For example, one may have folds while the other may be straight. The next section will introduce a precise definition of equivalence between two diagrams. Closely associated with the concept of equivalence is the stability of a diagram. We will soon realize that a connected region in $\mathbf{p}^-$-space induces a set of equivalent diagrams. Sets of inequivalent diagrams are separated in $\mathbf{p}^-$-space by what we will call the *bifurcation varieties*. The problem of classifying and enumerating all possible bifurcation diagrams (for a given μ) can now be understood as the problem of determining these bifurcation varieties.

The above ideas represent an intuitive overview of recent mathematical results on 'Imperfect Bifurcation Theory' mainly due to Golubitsky and co-workers(18). Their work has already found important applications in chemical engineering as evidenced by a series of articles published by Balakotaiah and Luss(32-34) where they have analyzed very simple reactions (but under non-isothermal conditions) occurring in a CSTR. In this chapter, we consider the applications to realistically complex reaction networks.

B. Equivalence and Stability of Bifurcation Diagrams

Let there be a total of *m* parameters in a system of *d* independent steady state equations represented by the vector equation

$$F(X,p) = 0 \tag{4.1}$$

with $X \epsilon R^d$ and $p \epsilon R^m$. It is emphasized that X here is considered to be a vector of independent state variables unless otherwise mentioned. One of the parameters will be distinguished as the bifurcation parameter, denoted as μ, and write $p=(\mu,p^-) \epsilon RxR^{m-1}$. The remaining parameters p^- are referred to as 'perturbation parameters'(18). A steady state bifurcation problem is defined for every fixed p^-:

$$F(X,\mu;p^-) = F_{p^-}(X,\mu) = 0 \ . \tag{4.2}$$

Thus, there is a family of steady state bifurcation problems, one member for each p^-. The bifurcation diagram associated with (4.2) can be defined as the set

$$D(F_{p^-}) = \{ \ (X,\mu) \ | \ F_{p^-}(X,\mu) = 0 \ \} \ . \tag{4.3}$$

Two bifurcation diagrams $D(F_a)$ and $D(F_b)$ are said to be equivalent if the mappings F_a and F_b are contact equivalent(18). Contact equivalence is a local notion and will now be introduced briefly.

Let $\mathbf{F}(0,0) = 0$ and $\mathbf{G}(0,0) = 0$. The two mappings $\mathbf{F},\mathbf{G}$: $(R^d \mathrm{x} R,0) \rightarrow (R^d,0)$ [5] are said to be contact equivalent if there exists a smoothly parameterized family of invertible matrices $\tau_{X\mu}$ on R^d and a diffeomorphism on $R^d \mathrm{x} R$ of the form

$$(\mathbf{X},\mu) \rightarrow (\mathbf{Y}(\mathbf{X},\mu),\Lambda(\mu)) \tag{4.4}$$

such that

$$\mathbf{F}(\mathbf{X},\mu) = \tau_{X\mu}\mathbf{G}(\mathbf{Y}(\mathbf{X},\mu),\Lambda(\mu)) \ . \tag{4.5}$$

It is required that $\mathbf{Y}(\cdot,\mu)$ and $\Lambda(\cdot)$ are orientation preserving , i.e. $\det[d_x\mathbf{Y}] > 0$ and $d\Lambda/d\mu > 0$. Furthermore, $(\mathbf{Y}(0,0),\Lambda(0)) = (0,0)$ which means that $(\mathbf{X},\mu)$ and $(\mathbf{Y},\Lambda)$ are 'in contact' at the origin. It is also noteworthy that in the diffeomorphism, Λ is only a function of μ. The physical reason for this is the view that μ is an external parameter and therefore not affected by the state of the system represented by $\mathbf{X}$.

The next aim is to partition the set of perturbation parameters $\mathbf{p}^-$ into open sets $\{A_i\}$ such that $\mathbf{F}_{p1^-}$ and $\mathbf{F}_{p2^-}$ are contact equivalent if and only if $\mathbf{p}_1^- \in A_i$ and $\mathbf{p}_2^- \in A_i$. Denote the set of bifurcation diagrams induced by A_i as

---

[5] This notation is used to indicate that these functions need be defined only for $(\mathbf{X},\mu)$ in some small neighborhood of the origin (reference 18).

$$D(F\{A_i\}) = \{ \, D(F_{p^-}) \mid p^- \in A_i \, \} \, . \tag{4.6}$$

Each $D(F_{p^-}) \in D(F\{A_i\})$ is a stable bifurcation diagram in the sense that a sufficiently small perturbation on F_{p^-} (e.g. perturbing p^- to $p^{-\prime}=p^-+\epsilon$, ϵ small) will give rise to a contact equivalent bifurcation problem F_{p^-}, containing all the qualitative features of the bifurcation diagram $D(F_{p^-})$. It has been shown that all diagrams associated with a given A_i are equivalent (Corollary 2.16, p.37 of reference 18). Needless to say, the hypersurfaces separating different A_i's correspond to unstable bifurcation diagrams. Next, it will be shown how to find these hypersurfaces which are called by the collective name bifurcation varieties.

C. Calculating Bifurcation Varieties

If a bifurcation diagram $D(F_{p^-})$ is unstable, then p^- must lie on at least one of 3 algebraic surfaces in R^{m^--1}. (Stewart(35) has referred to these surfaces as 'accidents'). These surfaces divide p^--space into several regions, and any two bifurcation problems associated with different values of p^- lying in the same region are equivalent(18). These surfaces are called

---

'// Golubitsky and Schaeffer(18) gave the term 'Bifurcation Variety' which we refrain from using because of the general sense that we take for the word 'bifurcation'. Balakotaiah and Luss(32) have used instead the term 'Isola' which we

(1). Isola variety[*], I_μ

(2). Hysteresis variety, H_μ

(3). Double Limit variety, DL_μ

They correspond to the three basic ways by which a diagram can fail to be stable as shown in figure 4.1.

Isola Variety, I_μ

Slight deviation from the value of p^- corresponding to the diagram shown in fig.4.1(a) will in general cause a splitting of the diagram into two smooth isolated pieces. Since the zero set of **F** is not a manifold, we must have

$$\text{rank } d_{X\mu}\mathbf{F} < d$$

where $d_{X\mu}\mathbf{F}$ is the differential of **F** with respect to **X** and μ but not p^-. Thus a diagram with an isola point $(\mathbf{X},\mu;p^-)$ can occur only if p^- belongs to the set called the Isola Variety:

$$I_\mu = \{\ p^-\ |\ \exists\ (\mathbf{X},\mu) \text{ with } \mathbf{F}(\mathbf{X},\mu;p^-)=0 \text{ and rank } d_{X\mu}\mathbf{F} < d\ \}\ . \tag{4.7}$$

The set above is the minimal definition of the Isola variety; later (section G), using further conditions on the second derivatives of **F**, we shall be able to point out the different types of isola points.

---

[*] (cont'd) also adopt here.

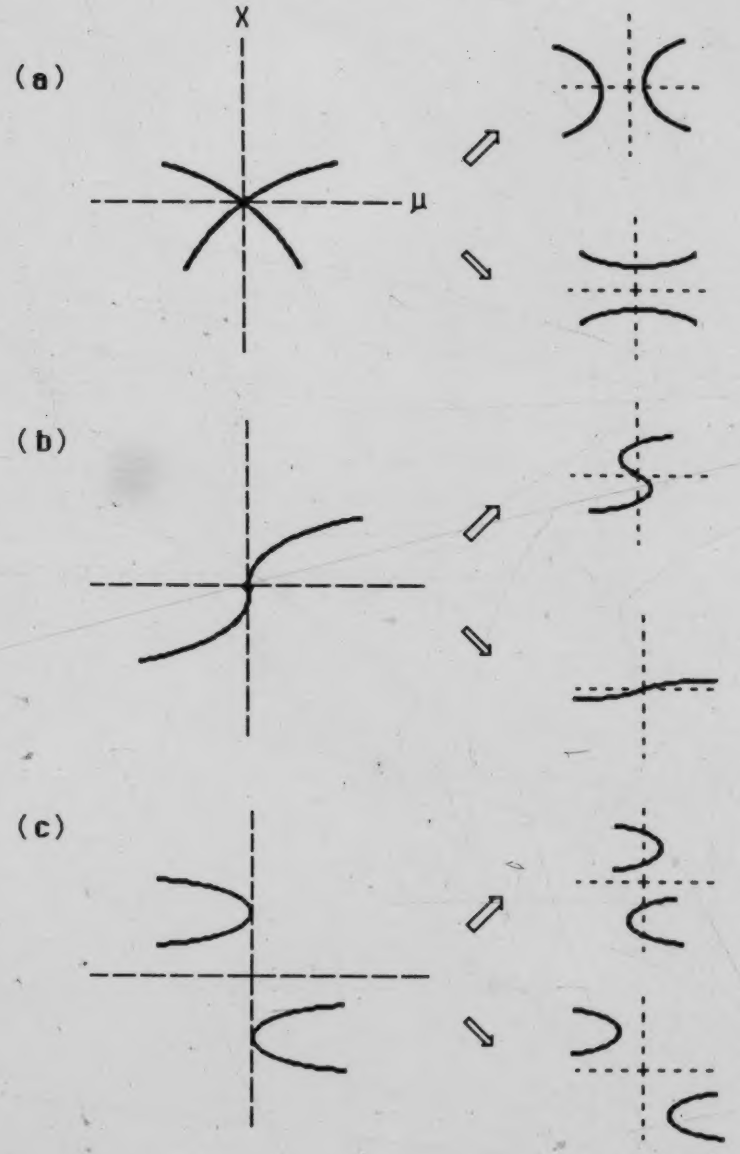

Figure 4.1

Three ways by which a diagram can fail to be stable : (a) isola point, (b) hysteresis point, and (c) double limit point. Their perturbations to inequivalent diagrams are shown on the right.

Example IV.1

For $d=1$, $d_{x\mu}F = [\partial F/\partial X, \partial F/\partial \mu]$ and the rank condition implies $\partial F/\partial X = \partial F/\partial \mu = 0$. When $d=2$,

$$d_{x\mu}F = \begin{bmatrix} \partial F_1/\partial X_1 & \partial F_1/\partial X_2 & \partial F_1/\partial \mu \\ \partial F_2/\partial X_1 & \partial F_2/\partial X_2 & \partial F_2/\partial \mu \end{bmatrix}$$

and rank $d_{x\mu}F = 1 < d$ means only one of the columns of this matrix is independent and

$$\det\begin{bmatrix} \partial F_1/\partial X_1 & \partial F_1/\partial X_2 \\ \partial F_2/\partial X_1 & \partial F_2/\partial X_2 \end{bmatrix} = 0$$

$$\det\begin{bmatrix} \partial F_1/\partial X_1 & \partial F_1/\partial \mu \\ \partial F_2/\partial X_1 & \partial F_2/\partial \mu \end{bmatrix} = 0$$

$$\det\begin{bmatrix} \partial F_1/\partial X_2 & \partial F_1/\partial \mu \\ \partial F_2/\partial X_2 & \partial F_2/\partial \mu \end{bmatrix} = 0$$

Only 2 of the above equations are independent. ■

The rank condition on a $d\text{x}(d+1)$ matrix is equivalent to two scalar equations. Thus the defining equations in (4.7) is a system of $(d+2)$ equations in $(d+m)$ variables $(\mathbf{X},\mathbf{p})$. On elimination of $\mathbf{X}$ and μ, a single equation in $\mathbf{p}^{-}\in R^{m-1}$ is obtained.

Example IV.2

Let $\mathbf{F}(\mathbf{X},\mu;\mathbf{p}^{-}) = 0$ represent the full set of steady state equations for a chemical reaction network, including the dependent equations if there are conservation constraints. Let d be the rank of ν.

We have $d_{X\mu}\mathbf{F} = [\mathbf{M},\mathbf{F}_{\mu}]$. Observe that each column of $\mathbf{M}$ is always equal to a non-negative linear combination of the columns of the matrix $[\nu(\mathrm{diag}\ \mathbf{v}^{\circ})] = \nu'$. Since each component of $\mathbf{v}^{\circ}$ is strictly positive, rank ν = rank ν' = d. Now, let $\mathbf{v}$ be of the form $\mathbf{v} = (\mathrm{diag}\ \mathbf{k})\mathbf{u}(\mathbf{X},\mathbf{p})$ and let the bifurcation parameter μ be equal to the rate (or pseudo-rate) constant of the m-th reaction, k_m. Then $\mathbf{F}_{\mu} = (1/k_m)\nu'_m$ where ν'_m is the m-th column of ν'. ■

Hysteresis Variety, H_{μ}

In figure 4.1(b), although there is precisely one solution $\mathbf{X}$ for each μ, an arbitrarily small perturbation of the right sign will produce an S-shaped bifurcation diagram for which there are three solutions for each μ close to the origin.

When no isola point is present, rank $d_{X\mu}\mathbf{F}$ = d. The bifurcation diagram is thus a smooth curve ι :

$$\iota(\tau) = \{ (\mathbf{X}(\tau),\mu(\tau)) \mid \tau \in R \} .$$

At the origin,

$$d\mu(0)/d\tau = d^2\mu(0)/d\tau^2 = 0 \tag{4.8}$$

and we require that

$$d\mathbf{X}(0)/d\tau = \mathbf{q} \neq 0 .$$

On differentiating the relation $\mathbf{F}(\mathbf{X}(\tau),\mu(\tau);\mathbf{p}^-) = 0$, we obtain

$$[d_x\mathbf{F}]\mathbf{q} = 0 \tag{4.9}$$

$$d_x^2\mathbf{F}(\mathbf{q},\mathbf{q}) \in \text{range } [d_x\mathbf{F}] \tag{4.10}$$

where $d_x\mathbf{F}$ and $d_x^2\mathbf{F}$ refer, respectively, to the first and second differentials of $\mathbf{F}$ with respect to $\mathbf{X}$. The hysteresis variety for a given μ is defined by the set

$$H_\mu = \{ \mathbf{p}^- \mid \exists\ (\mathbf{X},\mu) \text{ with } \mathbf{F} = \det[d_x\mathbf{F}] = 0, \text{ and } d_x^2\mathbf{F}(\mathbf{q},\mathbf{q}) \in \text{range } [d_x\mathbf{F}] \ ;\ 0\neq\mathbf{q}\in\ker[d_x\mathbf{F}] \} \tag{4.11}$$

where 'ker' means kernel.

Example IV.3

For clarity, this example demonstrates explicitly how the range condition (4.10) arises. Let

$$\mathbf{F} = \begin{pmatrix} f_1(X(\tau), Y(\tau), \mu(\tau)) \\ f_2(X(\tau), Y(\tau), \mu(\tau)) \end{pmatrix} = \begin{matrix} 0 \\ 0 \end{matrix}$$

and

$$[d_x\mathbf{F}] = \begin{bmatrix} \partial f_1/\partial X & \partial f_1/\partial Y \\ \partial f_2/\partial X & \partial f_2/\partial Y \end{bmatrix}$$

$$\mathbf{q} = \begin{bmatrix} dX/d\tau \\ dY/d\tau \end{bmatrix}$$

$$\mathbf{F}_\mu = \begin{bmatrix} \partial f_1/\partial \mu \\ \partial f_2/\partial \mu \end{bmatrix}$$

$$\mathbf{F}_\tau = \begin{bmatrix} \partial f_1/\partial \tau \\ \partial f_2/\partial \tau \end{bmatrix}$$

The first total derivative of **F** with respect to τ is

$$[d_x\mathbf{F}]\mathbf{q} + \mathbf{F}_\mu(d\mu/d\tau) + \mathbf{F}_\tau = 0 \ . \qquad (4.12)$$

which therefore leads to (4.9) when (4.8) is used. Now, let

$$F_{xx} = (\partial^2 f_1/\partial X^2 \ , \ \partial^2 f_2/\partial X^2)'$$
$$F_{xy} = (\partial^2 f_1/\partial X\partial Y \ , \ \partial^2 f_2/\partial X\partial Y)'$$
$$F_{yy} = (\partial^2 f_1/\partial Y^2 \ , \ \partial^2 f_2/\partial Y^2)'$$

and

$$q' = (d^2X/d\tau^2 \ , \ d^2Y/d\tau^2)' \ .$$

Getting the derivative of (4.12) further, and using (4.8) again, results to

$$q'[d_x^2 F]q + [d_x F]q' = 0.$$

where

$$[d_x^2 F] = \begin{bmatrix} F_{xx} & F_{xy} \\ F_{xy} & F_{yy} \end{bmatrix}$$

Thus, the range condition is now explicitly

$$d_x^2 F(q,q) = [d_x F](-q') \in \text{range } [d_x F] \ . \ \blacksquare \qquad (4.13)$$

The range condition corresponds to one equation if the dimension of $\ker[d_x F]$ is 1. Thus the defining equations in (4.11) is a system of (d+2) equations in (d+m) unknowns.

Eliminating $\mathbf{X}$ and μ leaves a single equation in $\mathbf{p}^{-} \epsilon R^{m-1}$.

For convenience in further applications, the equation corresponding to the range condition will now be determined explicitly. Let $\mathbf{z}$ be in the left null space of $[d_x\mathbf{F}]$, that is

$$\mathbf{z}[d_x\mathbf{F}] = 0 \ . \tag{4.14}$$

The range of $[d_x\mathbf{F}]$ is given by the set

$$\mathcal{W} = \{ \mathbf{w} \in R^d \mid [d_x\mathbf{F}]\mathbf{a} = \mathbf{w} \text{ for some } \mathbf{a} \in R^d \} \ .$$

Using (4.14), $\mathbf{w} \in \mathcal{W}$ if and only if

$$\mathbf{z} \cdot \mathbf{w} = 0 \ . \tag{4.15}$$

Hence,

$$\mathbf{z} \cdot d_x^2\mathbf{F}(\mathbf{q},\mathbf{q}) = 0 \tag{4.16}$$

where $\mathbf{q}$ and $\mathbf{z}$ are vectors in the right and null spaces of $[d_x\mathbf{F}]$, respectively.

Example IV.4

The independent steady state equations for chemical reaction networks is found from equation (2.25) to be

$$\mathbf{F} = \nu_I(\text{diag } \mathbf{v}^\circ)[\kappa^t-(1/2)\kappa^t(\text{diag } \zeta)+(1/2)(\text{diag } \kappa^t\zeta)\kappa^t]\zeta = 0 \qquad (4.17)$$

where $\zeta = (\zeta_I{}^t, \zeta_D{}^t)^t = \mathbf{x}-\mathbf{e}_n$. Equation (4.17) assumes that all reactions in the network are utmost bimolecular. The expression for ζ_D in terms of ζ_I is given by equation (2.24). Note that the origin $\zeta=0$ is a particular steady state solution of (4.17). The Jacobian matrix associated with **F** is

$$[d_x\mathbf{F}] = \nu_I(\text{diag } \mathbf{v}^\circ)\kappa_g{}^t \qquad (4.18)$$

where $\kappa_g{}^t$ is defined in equation (2.28). Finally, the second differential has the expression

$$d_x^2\mathbf{F}(\zeta,\zeta) = \nu_I(\text{diag } \mathbf{v}^\circ)[(\text{diag } \kappa^t\zeta)\kappa^t-\kappa^t(\text{diag } \zeta)]\zeta. \qquad (4.19)$$

■

Double Limit Variety, DL_μ

If, as in figure 4.1(c), two (or more) fold points occur on the same plane (μ = constant), an unstable diagram exists. It is clear that there can be two fold points on the same μ-slice only if $\mathbf{p}^-$ belongs to the set

$$DL_\mu = \{\ p^- \mid \exists\ (X,\mu) \text{ and } (Y,\mu),\ X\neq Y, \text{ with}$$
$$F(X,\mu;p^-) = 0 = F(Y,\mu;p^-) \text{ and} \qquad (4.20)$$
$$\det[d_x F(X,\mu;p^-)]=0=\det[d_x F(Y,\mu;p^-)]\ \}$$

This is the Double Limit Variety. There ~~are (d+2) equ~~ations in (d+m) unknowns giving a single equation in $p^- \epsilon R^{m-1}$.

Example IV.5

For one-variable steady state equations, DL_μ starts to occur in a quartic polynomial. In figure 3.11, the swallowtail catastrophe set is shown and $DL\mu$ is defined by a parabolic curve as given below:

$$DL_\mu = \{(\rho_0,\rho_1,\rho_2) \mid \rho_0=\rho_2{}^2/4\ ,\ \rho_1=0\ ,\ \rho_2\leq 0\}. \ \blacksquare \qquad (4.21)$$

D. A Hysteresis Variety of the Edelstein Network

We now see how the general methods in the calculation of the bifurcation varieties discussed above can be applied to a chemical reaction network. In particular, we calculate a hysteresis variety of the Edelstein network (see Example II.3). Let the parameters for this network be $(k_1{}',k_2,k_{-2},k_{-1},E_{-2t},k_3,E_{-23t}) \epsilon R^7$ where

$$k_1{}' = k_1 A$$

$$E_{-2t} = k_{-2}E_t.$$
$$k_s = k_{-3}'+k_{-2}+k_3 \quad (k_{-3}'=k_{-3}B)$$
$$E_{-23t} = (k_{-2}+k_3)E_t\ .$$

Distinguishing k_1' as the bifurcation parameter, we write the independent steady state equations as follows

$$F(X_I,\mu;p^-) = (\ f_1(X_I,\mu;p^-),\ f_2(X_I,\mu;p^-)\ )' = 0$$

where

$$f_1(X_I,\mu;p^-) = (\mu-k_2E)S - k_{-2}E - k_{-1}S^2 + E_{-2t} \tag{4.22}$$
$$f_2(X_I,\mu;p^-) = -(k_2S+k_s)E + E_{-23t} \tag{4.23}$$

$$X_I = (S,E)'$$
$$p^- = (k_2,k_{-2},k_{-1},E_{-2t},k_s,E_{-23t}) \in R_+^6\ .$$

The Jacobian matrix M_I is

$$M_I = \begin{bmatrix} \mu-k_2E-2k_{-1}S & -k_2S-k_{-2} \\ -k_2E & -k_2S-k_s \end{bmatrix}$$

and $\det(M_I) = 0$ gives

$$f_3(X_I,\mu;p^-) = 2k_{-1}k_2S^2+(2k_{-1}k_s-k_2\mu)S+(k_2k_s-k_2k_{-2})E-k_s\mu = 0. \tag{4.24}$$

We now find $\mathbf{q} \in \ker \mathbf{M}_I$, $\mathbf{q} = (q_1,q_2)' \neq 0$, i.e.

$$\mathbf{M}_I\mathbf{q} = 0 \ .$$

This gives

$$q_1 = -(k_2S+k_3)q_2/(k_2E)$$

and we let

$$\mathbf{q} = (\ k_2S+k_3,\ -k_2E\ )' \neq 0 \ .$$

To find the single equation corresponding to the range condition (4.10), let

$$\mathbf{w} = d_x^2\mathbf{F}(\mathbf{q},\mathbf{q})$$

that is,

$$\mathbf{w} = (q_1\ \ q_2) \begin{bmatrix} \mathbf{F}_{SS} & \mathbf{F}_{SE} \\ \mathbf{F}_{SE} & \mathbf{F}_{EE} \end{bmatrix} \begin{matrix} q_1 \\ q_2 \end{matrix}$$

where

$$\mathbf{F}_{SS} = (\ -2k_{-1},\ 0)'$$
$$\mathbf{F}_{SE} = (\ -k_2,\ -k_2\ )'$$
$$\mathbf{F}_{EE} = (\ 0,\ 0\ )'$$

giving

$$w = -2q_1 \begin{bmatrix} k_{-1}q_1+k_2q_2 \\ k_2q_2 \end{bmatrix} .$$

It is now necessary to find z such that $z \cdot w = 0$ holds (equation 4.15). Let $z = (z_1, z_2)'$.

$$zM_I = 0 \quad \text{gives}$$
$$z_1 = -(k_2S+k_3)z_2/(k_2S+k_{-2})$$

and we let

$$z = (\ k_2S+k_3,\ -k_2S-k_{-2}\ ) .$$

Finally, the range condition (4.10) is equivalent to the following equation :

$$f_4(X_I,\mu;p^-) = k_{-1}k_2^2S^2+2k_{-1}k_2k_3S-k_2^2(k_3-k_{-2})E+k_{-1}k_3^2 = 0 . \tag{4.25}$$

Eliminating μ, E and S from $f_1=f_2=f_3=f_4=0$ given by equations (4.22)-(4.25) will now provide the equation for H_μ in the parameters p^-. The result is given in Table IV.1. The tedious algebra was performed using a program called *REDUCE2 (reference 36). The sum of the 53 terms equals 0

TABLE IV.1

Hysteresis Variety of the Edelstein Network with k_1' as the Bifurcation Parameter

$$
\begin{aligned}
H_\mu = \; & - k_{-1}^3 k_{-3}'^6 \\
& -6k_{-1}^3 k_3 k_{-3}'^5 \\
& -6k_{-1}^3 k_{-2} k_{-3}'^5 \\
& +3k_{-1}^2 k_2^2 k_3 k_{-3}'^4 E_0 \\
& -15k_{-1}^3 k_3^2 k_{-3}'^4 \\
& -30k_{-1}^3 k_{-2} k_3 k_{-3}'^4 \\
& -15k_{-1}^3 k_{-2}^2 k_{-3}'^4 \\
& +12\, k_{-1}^2 k_2^2 k_3^2 k_{-3}'^3 E_0 \\
& +12\, k_{-1}^2 k_2^2 k_{-2} k_3 k_{-3}'^3 E_0 \\
& -20k_{-1}^3 k_3^3 k_{-3}'^3 \\
& -60k_{-1}^3 k_{-2} k_3^2 k_{-3}'^3 \\
& -60k_{-1}^3 k_{-2} k_3^2 k_{-3}'^3 \\
& -20k_{-1}^3 k_{-2}^3 k_{-3}'^3 \\
& -3k_{-1} k_2^4 k_3^2 k_{-3}'^2 E_0^2 \\
& -27k_{-1} k_2^4 k_{-2} k_3 k_{-3}'^2 E_0^2 \\
& -27k_{-1} k_2^4 k_{-2}^2 k_{-3}'^2 E_0^2 \\
& +18k_{-1}^2 k_2^2 k_3^3 k_{-3}'^2 E_0 \\
& +36k_{-1}^2 k_2^2 k_{-2} k_3^2 k_{-3}'^2 E_0 \\
& +18k_{-1}^2 k_2^2 k_{-2}^2 k_3 k_{-3}'^2 E_0 \\
& -15k_{-1}^3 k_3^4 k_{-3}'^2 \\
& -60k_{-1}^3 k_{-2} k_3^3 k_{-3}'^2 \\
& -90k_{-1}^3 k_{-2}^2 k_3^2 k_{-3}'^2 \\
& -60k_{-1}^3 k_{-2}^3 k_3 k_{-3}'^2 \\
& -15k_{-1}^3 k_{-2}^4 k_{-3}'^2 \\
& -6k_{-1} k_2^4 k_3^3 k_{-3}' E_0^2 \\
& -33k_{-1} k_2^4 k_{-2} k_3^2 k_{-3}' E_0^2 \\
& -27k_{-1} k_2^4 k_{-2}^2 k_3 k_{-3}' E_0^2 \\
& +12k_{-1}^2 k_2^2 k_3^4 k_{-3}' E_0 \\
& +36k_{-1}^2 k_2^2 k_{-2} k_3^3 k_{-3}' E_0 \\
& +36k_{-1}^2 k_2^2 k_{-2}^2 k_3^2 k_{-3}' E_0 \\
& +12k_{-1}^2 k_2^2 k_{-2}^3 k_3 k_{-3}' E_0 \\
& -6k_{-1}^3 k_3^5 k_{-3}' - 30k_{-1}^3 k_{-2} k_3^4 k_{-3}' \\
& -60k_{-1}^3 k_{-2}^2 k_3^3 k_{-3}' - 60k_{-1}^3 k_{-2}^3 k_3^2 k_{-3}' \\
& -30k_{-1}^3 k_{-2}^4 k_3 k_{-3}' - 6k_{-1}^3 k_{-2}^5 k_{-3}' \\
& + k_2^6 k_3^3 E_0^3 - 3k_{-1} k_2^4 k_3^3 E_0^2 \\
& -6k_{-1} k_2^4 k_{-2} k_3^3 E_0^2 - 3k_{-1} k_2^4 k_{-2}^2 k_3^2 E_0^2 \\
& +3k_{-1}^2 k_2^2 k_3^5 E_0 + 12k_{-1}^2 k_2^2 k_{-2} k_3^4 E_0 \\
& +18k_{-1}^2 k_2^2 k_{-2}^2 k_3^3 E_0 + 12k_{-1}^2 k_2^2 k_{-2}^3 k_3^2 E_0 \\
& +3k_{-1}^2 k_2^2 k_{-2}^4 k_3 E_0 - k_{-1}^3 k_3^6 \\
& -6k_{-1}^3 k_{-2} k_3^5 - 15k_{-1}^3 k_{-2}^2 k_3^4 \\
& -20k_{-1}^3 k_{-2}^3 k_3^3 - 15k_{-1}^3 k_{-2}^4 k_3^2 \\
& -6k_{-1}^3 k_{-2}^5 k_3 - k_{-1}^3 k_{-2}^6 \\
& \\
= \; & 0.
\end{aligned}
$$

and defines H_μ for $\mu=k_1A$. Note that the parameters are the original ones: $(k_{-1}, k_2, k_{-2}, k_3, k_{-3}', E_t)$.

E. Enumeration of Bifurcation Diagrams

Observe that the definitions of the bifurcation varieties are based on the local degenerate singularities of *M*. It is possible that there exist singularities more degenerate than those used in defining the 3 bifurcation varieties above; however, we know that the former are subsets of the latter. It is also quite possible that these bifurcation varieties can intersect each other. What this leads to is the creation of more connected regions in p^--space, regions that correspond to inequivalent bifurcation diagrams. Points of intersection among (or possibly, self-intersections of) the bifurcation varieties induce unstable diagrams that exhibit multilocal singularities and perturbations on the p^-'s lead to several inequivalent stable diagrams. Some bifurcation problems may in fact possess an intersection point among the bifurcation varieties wherein all the connected regions in p^--space meet. Thus, perturbing this highly singular bifurcation problem in all directions should generate all the bifurcation diagrams possible. Golubitsky et al.(37-38) call this singularity an organizing center.

Example IV.6

The hysteresis and isola varieties intersect at a point $p_{\bar{0}}$ when there exist (X_1,μ_1) and (X_2,μ_2) such that

$$F(X_i,\mu_i;p_{\bar{0}}) = \partial F(X_i,\mu_i;p_{\bar{0}})/\partial X = 0 \qquad i=1,2$$

and

$$\partial^2 F(X_1,\mu_1;p_{\bar{0}})/\partial X^2 = 0 \ ,$$

$$\partial F(X_2,\mu_2;p_{\bar{0}})/\partial \mu = 0.$$

If $\mu_1 \neq \mu_2$, then the singularity is described as 'multilocal'. The following example illustrates the case where $X_1 = X_2$ and $\mu_1 = \mu_2$. This example also illustrates an 'organizing center'.

Consider the following one-dimensional steady state bifurcation problem:[7//]

$$\begin{aligned} F(X,\mu;p^{-}) &= (1/3)\mu X^3 - (1/2)p_2 X^2 + (1-2\mu)X \\ &\quad + (p_2-p_1) \\ &= 0 \end{aligned}$$

where $p^{-} = (p_1,p_2) \in R^2$ and $(X,\mu) \in R^2$. The hysteresis variety is given by

$$\begin{aligned} H_\mu : \quad & p_1 = p_2(1 + p_2^2/24\mu^2) \\ & -4/(3[2]^{1/2}) < p_1 < 4/(3[2]^{1/2}) \\ & -(2^{1/2})/2 < p_2 < (2^{1/2})/2 \end{aligned}$$

[7//] This equation actually arises out of the finite element analogue of the Euler beam problem.(18)

$$\mu = (1 \pm [1-2p_2^2]^{1/2})/4 , \quad 0 < \mu < 1/2$$
$$X = p_2/2\mu , \quad -\infty < X < +\infty .$$

The above limits on p_1 and p_2 are required because the corresponding values of μ and X must be real.

The isola variety is

$$I_\mu : \quad p_1 = p_2$$

and the corresponding values for μ and X are 1/2 and 0, respectively. (There is actually another branch of the isola variety defined by $p_1 = -2p_2+(6)^{1/2}$ which is not considered here because it does not intersect H_μ within its allowed range given above). The two varieties intersect at the origin $(p_1,p_2) = (0,0)$ where the corresponding values of X and μ are 0 and 1/2, respectively. Figure 4.2 illustrates the origin as an organizing center where 4 regions on the p_1-p_2 plane meet, each region corresponding to a different bifurcation diagram. ■

The problem of enumerating all possible bifurcation diagrams for a given bifurcation parameter is seen to involve a local problem and a global one. The local problem is to determine the singularities of the steady state manifold *M*. In effect, this will give the equations for the

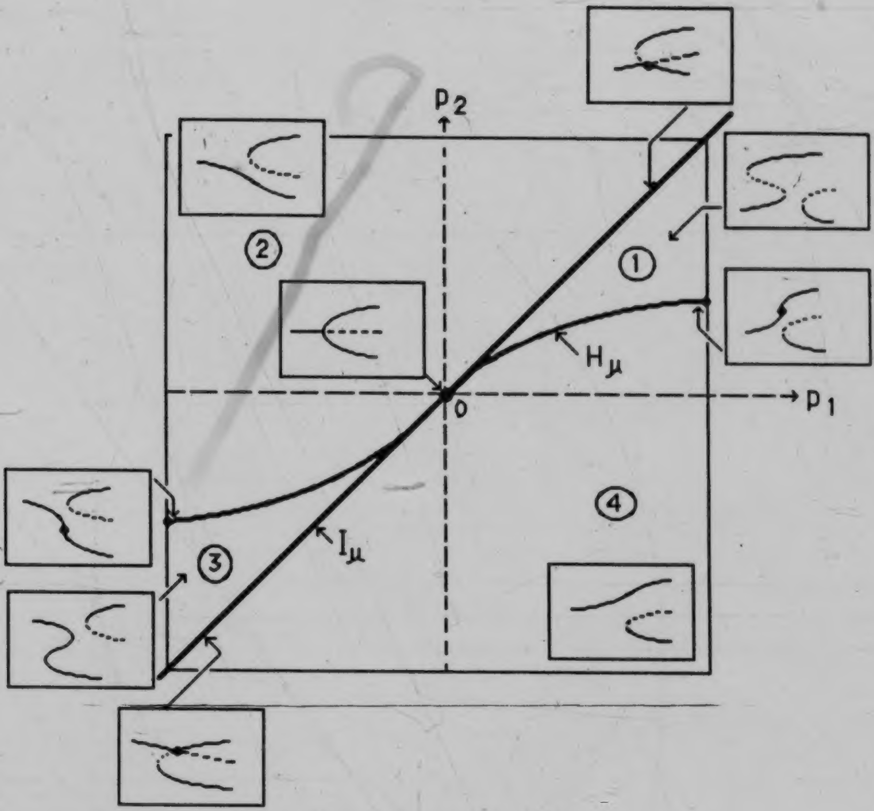

Figure 4.2

Bifurcation varieties for the finite element analogue of the Euler beam problem (see example IV.6). The hysteresis variety (H_μ) and the isola variety (I_μ) intersect at the origin and divide the plane into 4 regions that induce 4 inequivalent bifurcation diagrams as shown. Also shown are the unstable diagrams corresponding to the varieties.

bifurcation varieties. The global problem is to find all the connected regions in p^--space and figuring out the global shape of the diagram associated with each connected region.

The succeeding discussion is restricted to the case where the state variable is one-dimensional. The ideas are based mainly on a recent work of Golubitsky and Schaeffer(18). To understand their results, a few mathematical concepts will now be introduced very briefly. The reader is encouraged to consult reference 18 for more details.

$F(X,\mu;\tilde{\alpha})$, $\alpha \in R^t$, is a *t*-parameter unfolding of $G(X,\mu)$ if $F(X,\mu;0) = G(X,\mu)$ for all (X,μ). Think of F as a perturbation of the problem G. It is desirable to have an unfolding F containing the minimum number of perturbation parameters (sometimes called the 'unfolding' parameters) which generates all possible inequivalent bifurcation diagrams when G is perturbed in all directions. Such an F is called a universal unfolding. For one-dimensional problems, procedures for finding universal unfoldings are available (for example, see references 18 and 40). The minimum number of unfolding parameters necessary for a universal unfolding is called the codimension of a bifurcation problem. For G defined near (0,0), we let rank G = n if the Taylor expansion of G(X,0) at X=0 starts with terms of degree n.

Example IV.7

Consider a one-dimensional bifurcation problem F. Let $(X_0,\mu_0;\mathbf{p}_{\bar{o}})$ be a degenerate singular point satisfying the following conditions:

$$F(X_0,\mu_0;\mathbf{p}_{\bar{o}}) = 0$$

$$\partial^i F(X_0,\mu_0;\mathbf{p}_{\bar{o}})/\partial X^i = 0 \ , \quad i = 1,\ldots k$$

$$\Delta \equiv \partial^{k+1}F(X_0,\mu_0;\mathbf{p}_{\bar{o}})/\partial X^{k+1}\cdot\partial F(X_0,\mu_0;\mathbf{p}_{\bar{o}})/\partial\mu \neq 0 \ .$$

Then in the neighborhood of $\mathbf{p}_{\bar{o}}$, $F(X,\mu)$ is contact equivalent to

$$G(X,\mu) = X^{k+1} \pm \mu \qquad (+\text{ if } \Delta>0,\ -\text{ if } \Delta<0)$$

whose universal unfolding is

$$G(X,\mu,a) = X^{k+1}-a_{k-1}X^{k-1}-a_{k-2}-\ldots-a_1X\pm\mu \ .$$

This result is a special case of a general theorem proved by Golubitsky and Schaeffer(18). It has been extensively applied by Balakotaiah and Luss(32) in their steady state analysis of simple but exothermic reactions in a CSTR. If a singular point such as $(X_0,\mu_0;\mathbf{p}_{\bar{o}})$ exists, then the maximum number of steady state solutions next to the singular point is (k+1) and the universal unfolding enables one to find all the possible local bifurcation diagrams. ■

F. A Flowchart for Determining Bifurcation Diagrams

Golubitsky, Keyfitz and Schaeffer(37) has given a theorem that lists a complete classification of local bifurcation problems of codimension < 4 and rank ≤ 3. Their results are incorporated in the flowchart diagram (Figure 4.3) along with other results already contained in the diagram given by Stewart (reference 35, p.279). In the notation of the singularities in figure 4.3, S^r_c refers to a singularity of codimension c and rank r. Note that the rank of G obviously restricts the existence of some of the bifurcation varieties as summarized in Table IV.2. The detailed definitions of the singularities given in the flowchart should also be regarded as refinements on the definitions of the bifurcation varieties in one dimension. The defining conditions of the singularities give algebraic equations in terms of the unfolding parameters after elimination of X and μ. Table IV.3 lists the singularities against their respective bifurcation varieties. Note that S^3_2 and S^3_3 are intersection points of the Isola and Hysteresis Varieties for rank 3 bifurcation problems. Since S^3_0 is a non-degenerate singularity, it does not belong to any bifurcation variety.

It has already been mentioned that in some bifurcation problems, there may exist highly degenerate singular points

Figure 4.3

A flowchart for determining singularity types of a bifurcation problem $G(x,\mu) = 0$.$^{(35,37)}$ S_c^r refers to a singularity with codimension c and rank r.

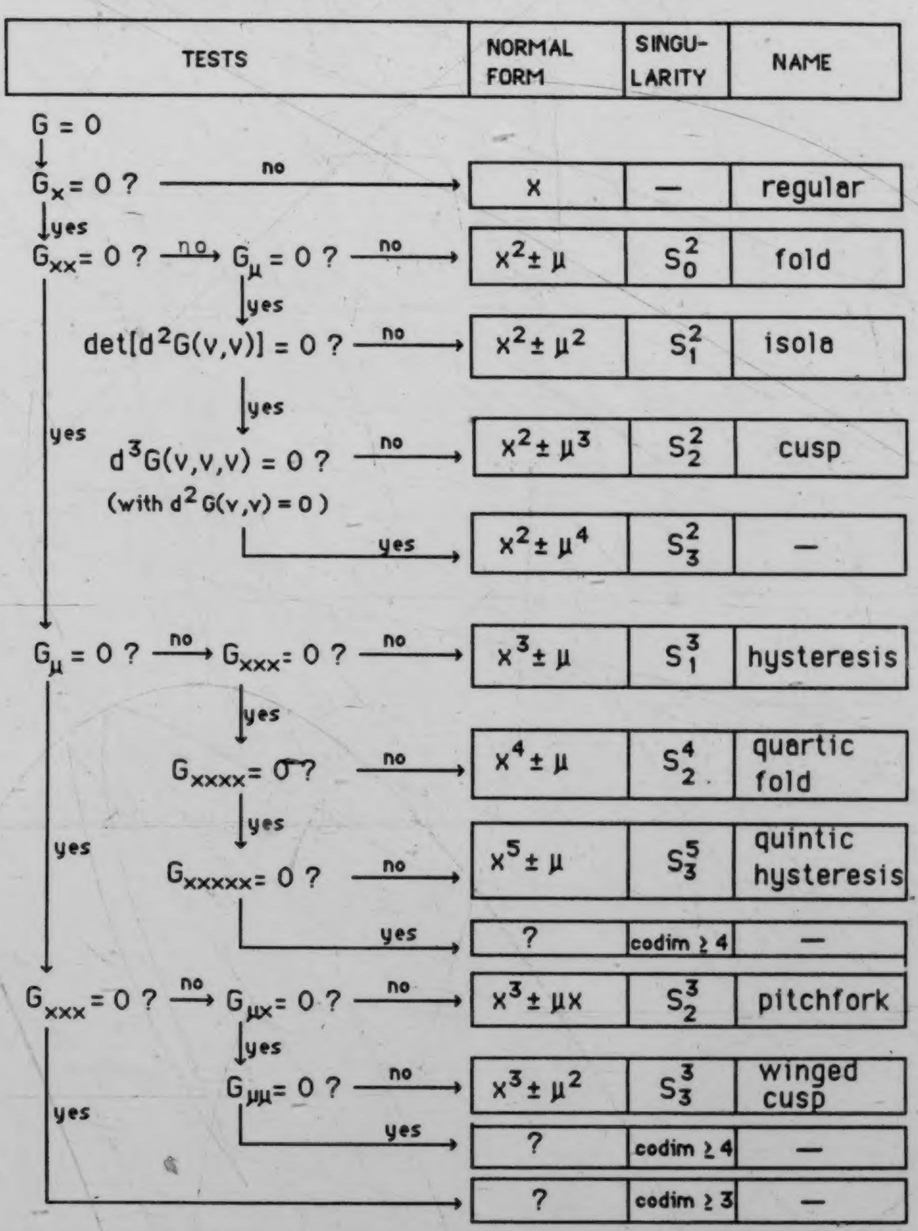
TESTS
NORMAL FORM
SINGULARITY
NAME
G = 0
Gx = 0 ?
no
x
—
regular
yes
Gxx = 0 ?
no
Gμ = 0 ?
no
x² ± μ
S₀²
fold
yes
det[d²G(v,v)] = 0 ?
no
x² ± μ²
S₁²
isola
yes
d³G(v,v,v) = 0 ?
(with d²G(v,v) = 0)
no
x² ± μ³
S₂²
cusp
yes
x² ± μ⁴
S₃²
—
yes
Gμ = 0 ?
no
Gxxx = 0 ?
no
x³ ± μ
S₁³
hysteresis
yes
Gxxxx = 0 ?
no
x⁴ ± μ
S₂⁴
quartic fold
yes
Gxxxxx = 0 ?
no
x⁵ ± μ
S₃⁵
quintic hysteresis
yes
?
codim ≥ 4
—
yes
Gxxx = 0 ?
no
Gμx = 0 ?
no
x³ ± μx
S₂³
pitchfork
yes
Gμμ = 0 ?
no
x³ ± μ²
S₃³
winged cusp
yes
?
codim ≥ 4
—
yes
?
codim ≥ 3
—

TABLE IV.2

Bifurcation Varieties that may exist for a given Rank of G

Rank G	Variety
2	I_μ
3	I_μ, H_μ
4	I_μ, H_μ, DL_μ

TABLE IV.3

Some Types of Singularity for the Isola and Hysteresis Varieties ($S_c{}^r$ is a singularity with codimension c and rank r)

I_μ : S_1^2, S_2^2, S_3^2, S_2^3, S_3^3
H_μ : S_1^3, S_2^3, S_3^3, S_2^4, S_3^5

(X_0,μ_0) whose perturbations will give rise to all or most of the bifurcation diagrams possible. Golubitsky and Keyfitz(38) found an ~~organizing cen~~ter for the steady state bifurcation problem associated with a single, first-order exothermic reaction in a CSTR. They have called this the 'winged cusp' (S_3^3 in the flowchart, figure 4.3). Balakotaiah and Luss(33) then verified the work of Golubitsky and Keyfitz(38) using physical parameters and were able to elucidate more details on the multiplicity patterns. A beautiful example of multilocal singularities as well as another organizing center is also given by Golubitsky, Keyfitz and Schaeffer(37) in their analysis of the thermal-chainbranching model for the reaction between H_2 and O_2.

G. Bifurcation Varieties of Reduced Steady State Problems

In this section, we again exploit the possibility of reducing the system of steady state equations into one dimension and the consequent ability to exactly express the state sets (including the lower or upper bounds of the steady states if they exist). The primary aim here is to come up with ready formulas that are convenient for practical applications.

Isolas

It has already been mentioned that the steady state manifold *M* is a simply connected hypersurface. Isolas can occur only as crossections of *M*. Physical reality usually corresponds to a cross-section of *M*. For this reason, a detailed treatment on isolas giving the different types and their defining conditions is given below.

Let the steady state bifurcation problem in one dimension be

$$F(X,\mu;p^-) = 0, \quad (X,\mu;p^-) \in R_+ x R_+ x R_+^{m-1} .$$

The isola variety is defined as

$$I_\mu = \{p^- \in R_+^{m-1} | \exists (X,\mu) \text{ such that } F=\partial F/\partial X=\partial F/\partial \mu=0\} . \qquad (4.26)$$

We will see that due to the vanishing of the first derivatives of F, there are in general four different types of isolas. The following discussion is not restricted to the rank of F. A further reference is G. Iooss and D. Joseph's book (reference 41).

Let (X^0,μ_0) be an isola point. The curves passing through (X^0,μ_0) satisfy the following equation near that point:

$$2F(X,\mu) = F_{xx}(\delta X)^2+2F_{x\mu}\delta X\delta\mu+F_{\mu\mu}(\delta\mu)^2 + o[(|\delta X|+|\delta\mu|)^2] = 0$$

where

$$o[z^n] \text{ means } \lim\{o[z^n]/z^n\}=0 \text{ as } z\to 0$$

and

$$\delta X = X-X^{\circ}$$

$$\delta\mu = \mu-\mu_0 \ .$$

As (X,μ) approaches (X°,μ_0), the equation for the curves $F(X,\mu)=0$ reduces to the characteristic quadratic:

$$F_{xx}(dX)^2+2F_{x\mu}dXd\mu+F_{\mu\mu}(d\mu)^2 = 0 \ . \qquad (4.27)$$

Thus,

$$d\mu/dX = -(F_{x\mu}/F_{\mu\mu}) \pm (H^{1/2}/F_{\mu\mu}) \qquad (4.28)$$

where $H = F_{x\mu}{}^2-F_{xx}F_{\mu\mu}$.

Equation (4.28) give the slopes of the tangents to the curve(s) at the isola point (X°,μ_0). Note that H is the negative of the determinant of the Hessian matrix of F.

When not all of the second derivatives of F vanish simultaneously, then the isola point is referred to as a 'double point' because only two curves possessing distinct tangents may pass through the point. If the tangents are not defined, that is when $H<0$, then the point is called a 'conjugate point'. In order for more than two distinct curves to pass through the isola point, it is necessary that at least all of the second derivatives of G vanish simultaneously.

The classification now to be given assumes that the isola points are either double or conjugate points. The classification is mainly based on the sign of H. The four types of isolas are shown in figure 4.4.

Quadratic Steady State Equations

Let

$$F_2(X,\mu,p^-) = X^2+\beta_1(\mu,p^-)X+\beta_0(\mu,p^-) = 0 .$$

Since rank = 2, only an isola variety is possible. In the discussion that follows, we will refer to the isola variety of a bifurcation problem of rank r as ${}^rI_\mu$. The Isola variety for r=2 is written down immediately as

$$ {}^2I_\mu = \{ p^- \mid \beta_0=(\beta_1/2)^2,\ \partial\beta_0/\partial\mu=(\beta_1/2)\partial\beta_1/\partial\mu,\ \beta_1\le 0 \} . \tag{4.28}$$

The condition $\beta_0=(\beta_1/2)^2$ comes from eliminating X from F = $\partial F/\partial X = 0$. The second condition arises out of the elimination of X from $\partial F/\partial X = \partial F/\partial\mu = 0$. The last condition $\beta_1\le 0$ ensures that X and μ are non-negative for the corresponding p^- of the isola variety. To determine which type of isola, one then applies the conditions defined in the preceding

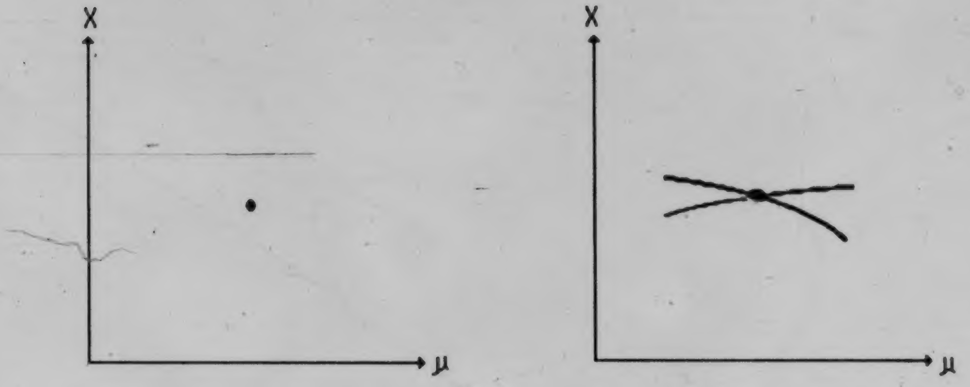

(a) $F = F_x = F_\mu = 0$
$H < 0$ and $F_{\mu\mu}F_{xx} > 0$

(b) $F = F_x = F_\mu = 0$
$H > 0$, $F_{xx}F_{x\mu} \neq 0$

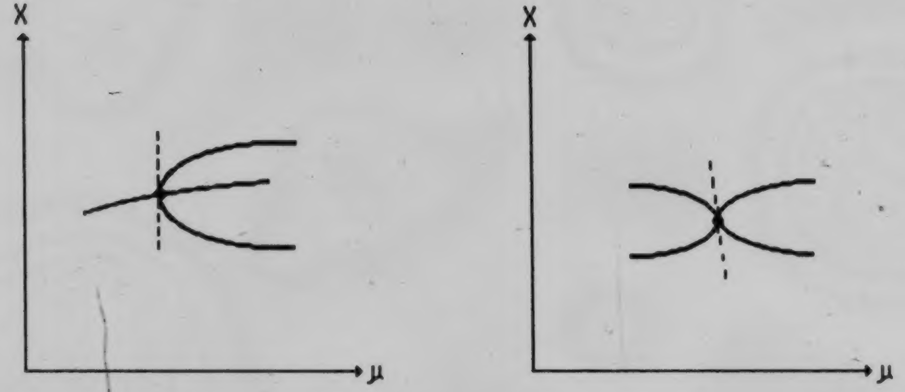

(c) $F = F_x = F_\mu = 0$
$H > 0$, $F_{xx} = 0$, $F_{x\mu} \neq 0$

(d) $F = F_x = F_\mu = 0$
$H = 0$

Figure 4.4

Four types of Isola points based on the second partial derivatives. $H = F^2_{x\mu} - F_{xx}F_{\mu\mu}$.

section.

Cubic Steady State Equations

Let

$$F_3(X,\mu,p^-) = X^3+\beta_2(\mu,p^-)X^2+\beta_1(\mu,p^-)X+\beta_0(\mu,p^-) = 0 \ .$$

The Hysteresis variety for a given μ, ${}^rH_\mu$, is defined for rank r=3 as

$$ {}^3H_\mu = \{ \ p^- \ | \ \rho_1(\mu,p^-)=\rho_0(\mu,p^-)=0, \ \beta_2(\mu,p^-)<0 \ \} \ . \qquad (4.29)$$

where ρ_1 and ρ_0 are defined below (equation 3.5) in terms of β_2,β_1 and β_0.

$$\begin{aligned} \rho_1 &= \beta_1 - 3(\beta_2/3)^2 \qquad (3.5) \\ \rho_0 &= \beta_0 - \beta_1(\beta_2/3) + 2(\beta_2/3)^3 \ . \end{aligned}$$

Eliminating μ from $\rho_1=\rho_0=0$ gives the defining equation for the algebraic variety in p^--space. The additional condition $\beta_2<0$ ensures that for the particular (μ,p^-) where $\rho_1=\rho_0=0$, the corresponding state variable X is positive. This condition is a necessary test for the existence of the Hysteresis Variety for the cubic.

Note that it is not right to say that ${}^3H_\mu$ is the cusp point (the origin) itself. This is because ρ_1 and ρ_0 are also functions of μ and ${}^3H_\mu$ is defined by p^- only. For $p^- \epsilon\, {}^3H_\mu$, a curve $\tau(\mu)$ is traced on the ρ_1-ρ_0 plane as the bifurcation parameter μ is varied. All curves $\tau(\mu)$ on this plane passing through the origin have a set of perturbation parameters p^- that belongs to ${}^3H_\mu$. In figure 4.5, p_1^- and p_3^- do not belong to ${}^3H_\mu$ while $p_2^- \epsilon\, {}^3H_\mu$. The corresponding bifurcation diagrams are also shown in figure 4.5.

The isola variety for the cubic can occur in several ways as shown in figure 4.6. Note that the curves Γ_1 have $p^- \epsilon\, {}^3I_\mu$ only if they are tangent to the cusp curve to the right of the tangency point between the line L_ρ and the cusp curve. This tangency point between L_ρ and the cusp curve occur at $\rho_0 = 2(\beta_2/3)^3$. Thus, it is clear that there exists an isola point only if

$$\rho_0 > 2(\beta_2/3)^3$$

or equivalently (using the definition of ρ_0 above),

$$3\beta_0 - \beta_1\beta_2 > 0\ . \tag{4.30}$$

Condition (4.30) is a necessary test for the existence of an isola point for the cubic.

The isola variety ${}^3I_\mu$ has the following explicit definition:

$${}^3I_\mu = \{\ p^-\ |\ K_3(\mu,p^-) = K_1(\mu,p^-) = 0,\ 3\beta_0 - \beta_1\beta_2 > 0\ \} \tag{4.31}$$

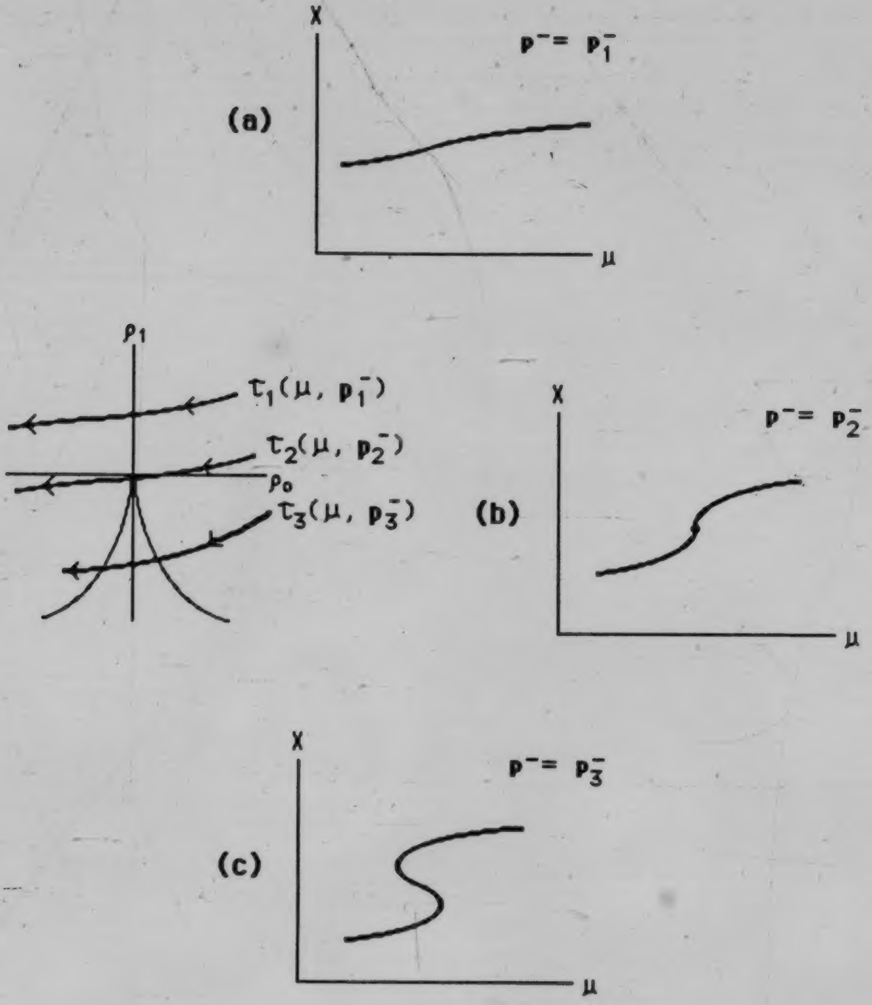
X
p⁻ = p₁⁻
(a)
μ
ρ₁
τ₁(μ, p₁⁻)
τ₂(μ, p₂⁻)
ρ₀
τ₃(μ, p₃⁻)
(b)
X
p⁻ = p₂⁻
μ
X
p⁻ = p₃⁻
(c)
μ

Figure 4.5

Curves $\tau_i(\mu, p_i^-)$ traced on the $\rho_1 - \rho_o$ plane as μ varies but p_i^- fixed. Since $\tau_2(\mu, p_2^-)$ passes through the cusp point (the origin), p_2^- belongs to the Hysteresis variety and induces an unstable diagram shown in (b). Perturbations of p_2^- give rise to either stable diagram (a) or (c).

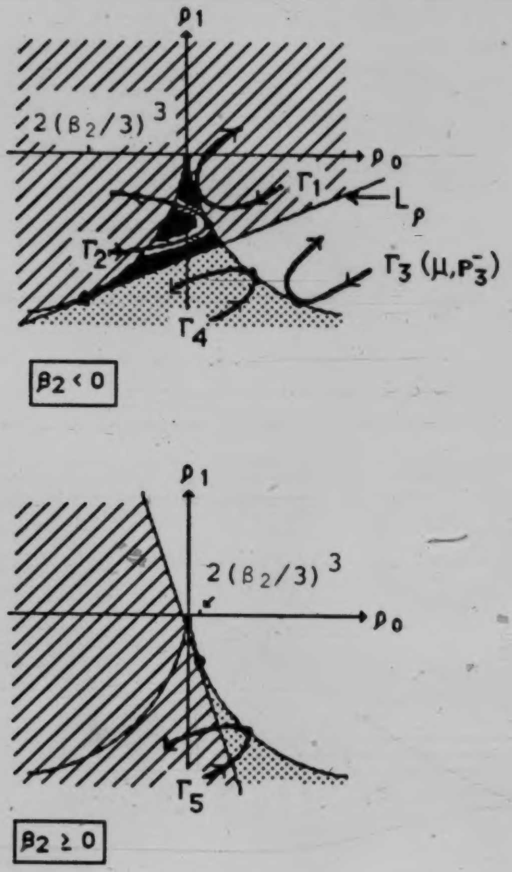
ρ_1
$2(\beta_2/3)^3$
ρ_0
Γ_1
L_ρ
Γ_2
$\Gamma_3(\mu, P_3^-)$
Γ_4
$\beta_2 < 0$
ρ_1
$2(\beta_2/3)^3$
ρ_0
Γ_5
$\beta_2 \geq 0$

Figure 4.6

For $P_i^- \in I_\mu$, possible curves $\Gamma_i(\mu, P_i^-)$ traced on the $\rho_1 - \rho_0$ plane as μ varies. It is assumed that the line L_ρ is fixed as μ changes.

where K_1 is given by

$$K_1(\mu,p^-) = \rho_1(\partial\rho_1/\partial\mu)^2+3(\partial\rho_0/\partial\mu)^2 \tag{4.32}$$

and K_3 is given by equation (3.8). Recall that $K_3 = 0$ corresponds to the condition $\partial F/\partial X = 0$ while $K_1 = 0$ is for the condition $\partial F/\partial\mu = 0$. Figure 4.7 gives the corresponding bifurcation diagrams for the curves shown in figure 4.6.

${}^3H_\mu$ and ${}^3I_\mu$ are the only possible bifurcation varieties for a cubic steady state equation. We emphasize that these varieties are exclusive to the chosen bifurcation parameter μ. Assigning another parameter as μ will change the definition of the perturbation parameters p^- and therefore of ${}^3H_\mu$ and ${}^3I_\mu$.

Figure 4.8 shows how multilocal singularities can occur. Their perturbations are also shown.

Quartic Steady State Equations

In the following treatment of the quartic, the constraint X>0 is dropped for simplicity. The hysteresis variety is given by Σ' shown in figure 3.11. Hence,

$${}^4H_\mu = \{\ p^-\ |\ \rho_0=-\rho_2^2/12,\ \rho_1=\pm(2/9)\rho_2(-6\rho_2)^{1/2},\ \rho_2\leq 0\ \}. \tag{4.33}$$

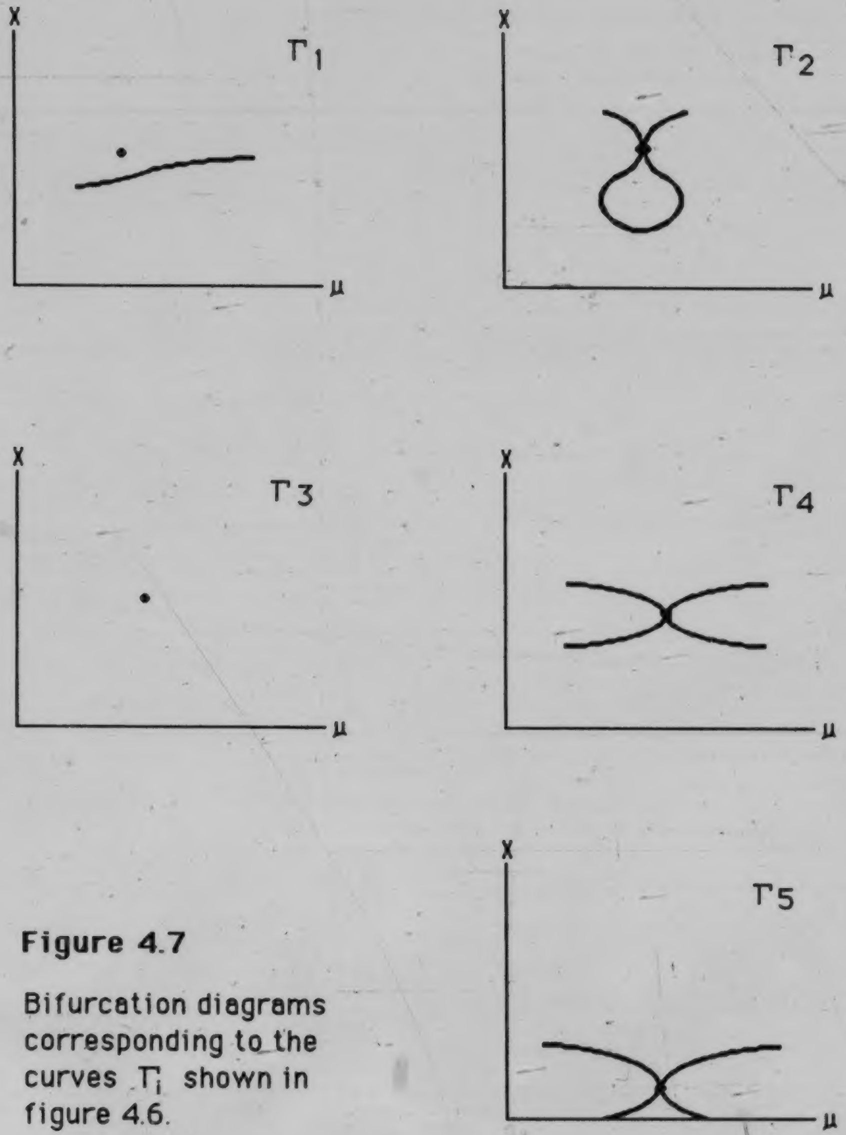

Figure 4.7

Bifurcation diagrams corresponding to the curves Γ_i shown in figure 4.6.

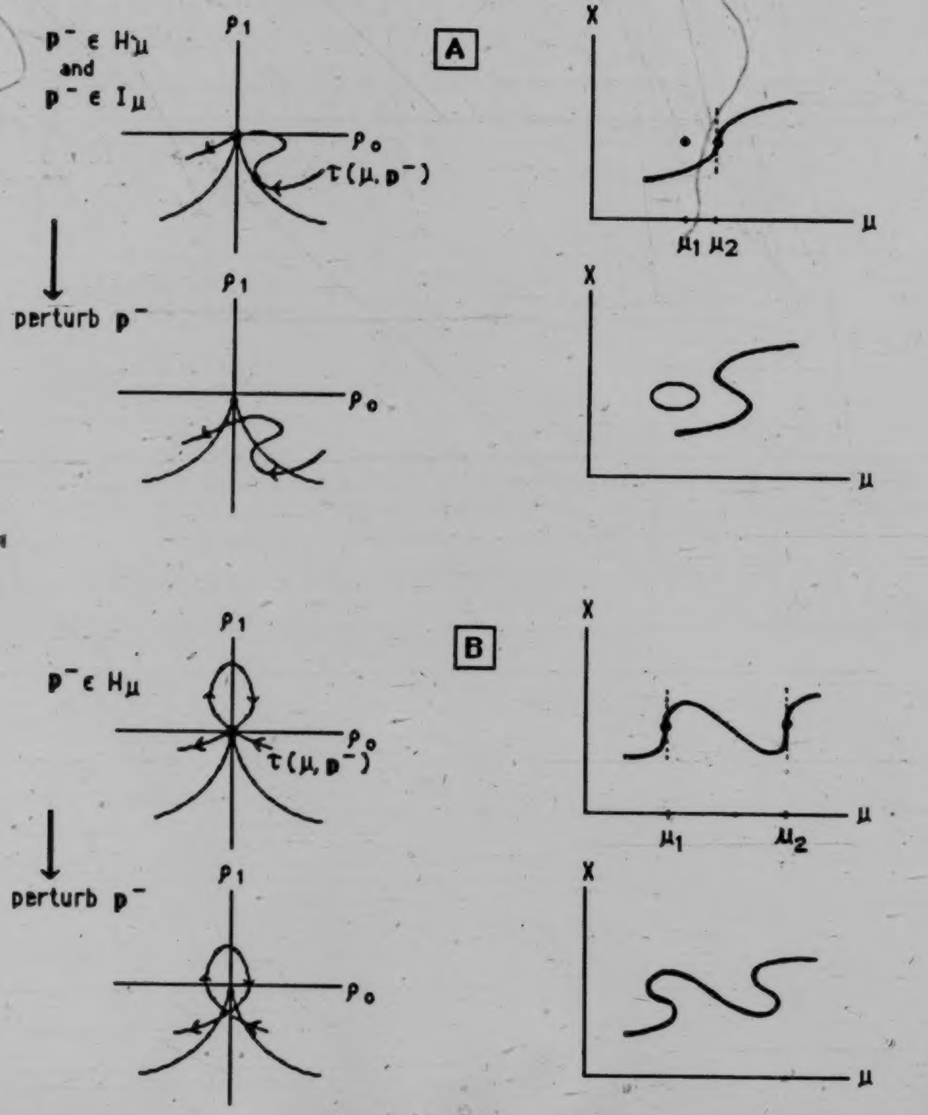
p⁻ ∈ H_μ
and
p⁻ ∈ I_μ
p₁
A
p₀
τ(μ, p⁻)
X
μ
μ₁ μ₂
perturb p⁻
p₁
p₀
X
μ
p⁻ ∈ H_μ
p₁
B
p₀
τ(μ, p⁻)
X
μ
μ₁
μ₂
perturb p⁻
p₁
p₀
X
μ

Figure 4.8

Examples of how multilocal singularities arise in bifurcation diagrams. In A, p^- belongs to both the Hysteresis and Isola varieties. In B, p^- is a member of the Hysteresis variety. In both cases, the singularities occur at two different values of μ, $\mu_1 \neq \mu_2$. Shown also are the curves τ and the corresponding diagrams when p^- is perturbed.

where $\rho_0(\mu,\mathbf{p}^-)$, $\rho_1(\mu,\mathbf{p}^-)$ and $\rho_2(\mu,\mathbf{p}^-)$ are given in equation (3.18) repeated below:

$$\begin{aligned} \rho_2 &= \beta_2-6(\beta_3/4)^2 \\ \rho_1 &= \beta_1-2\beta_2(\beta_3/4)+8(\beta_3/4)^3 \\ \rho_0 &= \beta_0-\beta_1(\beta_3/4)+\beta_2(\beta_3/4)^2-3(\beta_3/4)^4 \ . \end{aligned} \tag{3.18}$$

The double limit variety exists in the quartic. It is shown as the curve labeled *DL* in figure 3.11 and has a simple set of describing equations:

$$^4DL_\mu = \{ \ \mathbf{p}^- \ | \ \rho_1=0, \ \rho_0=\rho_2{}^2/4, \ \rho_2\leq 0 \ \} \ . \tag{4.34}$$

Referring to figures 3.11 and 3.13 , it is seen that two of the necessary conditions for the existence of $^4DL_\mu$ when the constraint X>0 is included are $\beta_3<0$ and $\rho_2<0$ (see figure 3.13(f4)).

Regarding the isola variety, no simple explicit defining conditions were found except for $K_4=0$ (given in equation 3.20) which results from the elimination of X' from the equations $f_4(X')=\partial f_4/\partial X'=0$.

Example IV.8

The iodate-arsenous acid reaction in a CSTR was introduced previously in Example I.1 including a 2-variable model (Network N_1) analyzed by Ganapathisubramanian and Showalter(7). For the convenience of the reader, the network is repeated below:

Network N_1

$R_1, R_{-1} \qquad \rightleftarrows X$
$R_2, R_{-2} \qquad \rightleftarrows B$
$R_3 \qquad B + X \rightarrow 2X$
$R_4 \qquad B + 2X \rightarrow 3X$.

The reduced steady state equation is a cubic polynomial and therefore the results of this section can be applied directly after finding the β coefficients of the cubic. In reference 7, the bifurcation parameter is $\mu = k_0 + k_0'$ where $k_0 = k_1' = k_2'$. In our notation, $\mu = k_{-1}' = k_{-2}'$. Using exactly the same parameter values used in Table I of the reference, the bifurcation diagrams were generated as well as the corresponding 'paths through the cusp'(18) as μ is increased. The results are given in figure 4.9. The hysteresis (H_μ) and isola (I_μ) varieties are also shown along k_0'~~. The~~ parameters ρ_0 and ~~ρ_1~~ are defined in equation (3.5) in terms of the β coefficients of the cubic steady state equation. ■

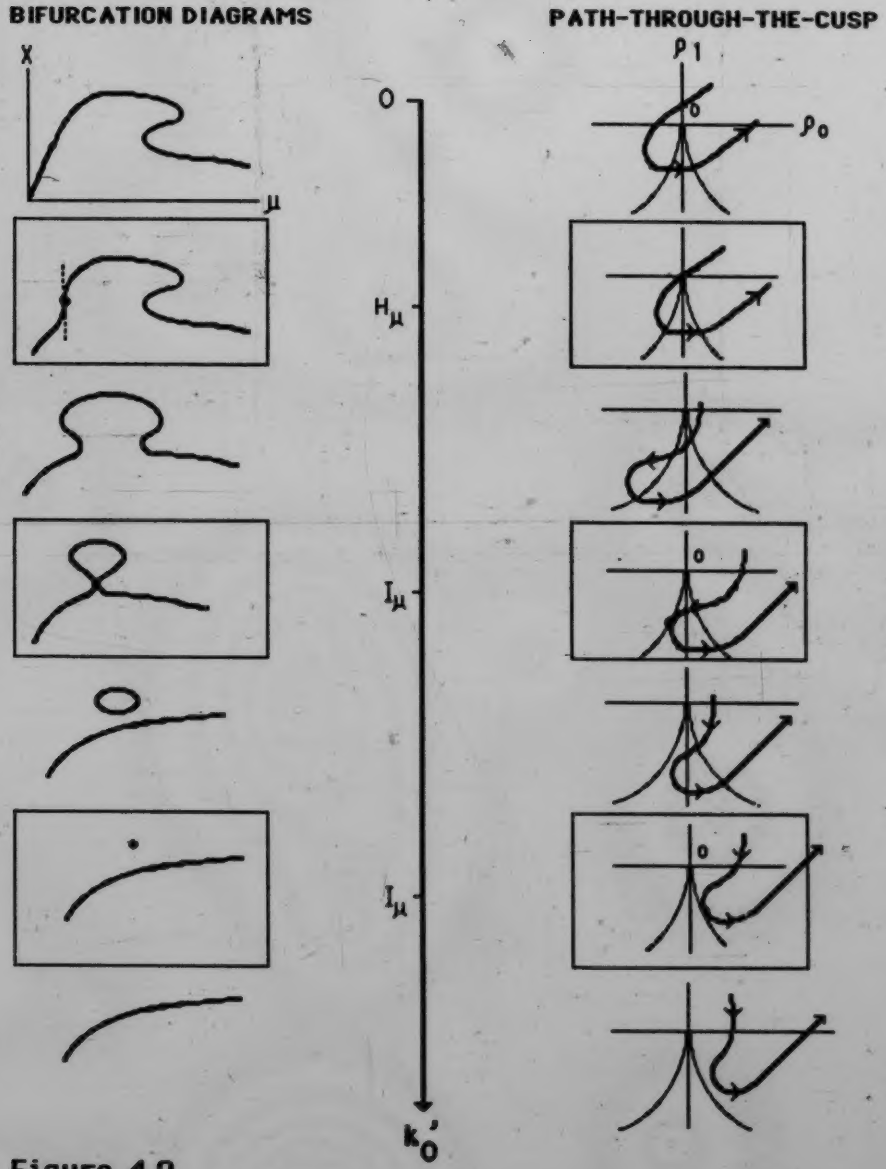
BIFURCATION DIAGRAMS
PATH-THROUGH-THE-CUSP
X
μ
ρ1
ρ0
0
Hμ
Iμ
Iμ
k0'
o

Figure 4.9

Sequence of bifurcation diagrams (left column) as the perturbation parameter k_0' is increased from 0. The right column shows the corresponding path through the cusp as μ is increased. The The network is N_1 which is a model used for the IO_3^-- H_3AsO_3 system by Ganapathisubramanian and Showalter (ref. 7).

V. SYSTEMATIC MODELING OF BISTABILITY IN CHEMICAL REACTION SYSTEMS

A. Introduction

There is an added bonus in knowing the geometry of the set of steady states of a network. Through the structure of the current polytope Π_v, the mechanism of any complex network can be sorted out systematically.

In Chapter II, we have seen that the general steady state of a chemical reaction network is a superposition of its extreme currents and all steady states are found in the current cone C_v. It was also discussed that a cross-section of C_v, the current polytope Π_v, is sufficient to represent all the information contained in C_v. A very important result of our ability to find the structure of Π_v is the construction of a 'topology' for the set of extreme currents, or one can say ultimately, the set of reactions. Two currents are 'far away from each other' if they belong to distant vertices in Π_v.

One must bear in mind that the whole of C_v represents all the possible steady states of an ensemble (of infinite count) of reaction systems whose network structure (or stoichiometry) are the same. A particular reaction system has fixed parameters; and more often than not, the rate constants have widely ranging magnitudes. As a consequence, the steady state of the system will often be found near a low-dimensional face of Π_v. This would mean further that at steady state there are only few extreme currents that are significant. The identification of these dominant extreme currents are aided by experimental information. Using the topology offered by the Π_v of the network, certain reactions will be found to be inessential for the study of certain features of the chemical system. With this view of Π_v in mind, it is realized that we should be able to use it as a modeling tool for complex reaction systems. Given the mechanism of a reaction system, no matter how complex, which is known to exhibit different dynamical or static features. A prerequisite to the understanding of how these features come about is the identification of the 'elementary processes' or reaction 'pathways'. These words, so often used in textbooks and journal articles, now have their concrete definition in terms of extreme currents. The structure of Π_v for the network offers us a systematic approach in deciding which pathways are most important and which ones can be definitely ignored. These ideas will be pursued in this chapter.

We shall consider the problem of identifying the dominant extreme currents when a reaction network is capable of exhibiting bistability. For a given network, we will see that we are able to identify a minimal subset of reactions that is necessary for the emergence of bistability. The next section is devoted to the development of the criteria that determines whether or not a given network has potential to have multiple steady states at all, and whether or not a given extreme current is dominant when the conditions favor bistability.

The conclusion of this work is the identification of the extreme currents responsible for the bistability observed experimentally in the peroxidase-oxidase (PO) reaction(42,51) in an open system. In order to understand the complex mechanism of this system, a much simpler 'prototype' network is fully analyzed with the hope that we will be able to discover some basic ingredients that would lead to bistability. This simple model is the classical substrate-inhibition enzyme mechanism which is fully analyzed in section C. Section D introduces the reader to the mechanism of the peroxidase-oxidase reaction. Finally, section E presents a bistable model of this reaction with its full analysis and correlation with experimentally observed features.

B. A Modeling Approach to Bistability

Different dynamical or static behaviors usually occur under different sets of conditions. The modeling can therefore be simplified by considering each dynamic behavior separately. In this chapter we focus on bistability. The purpose is to propose a systematic approach to modeling bistability not only in the PO reaction but in general to all complex reaction networks that are capable of having multiple steady states. As in the PO reaction, the list of elementary steps in the mechanism is often a long one and one wants to determine a minimal reaction subset, a 'model', that is sufficient to generate bistability.

Below, we enumerate the proposed steps in the procedure for extracting a minimal model for the bistability in a network :

(i). The first important step is to determine the extreme currents composing the steady state of the network, that is, find the current matrix **E**.

(ii). The second step requires a consideration of the 'topology' of the network, that is, how one extreme current is coupled to another and what reactions are involved. This is accomplished by determining the structure of the current polytope, Π_v, whose vertices represent the extreme currents.

(iii). The third step involves elucidation of the inner structure of Π_v. The details of this test will be discussed in this section.

The reactions composing the dominant extreme currents are taken as the minimal model. Reactions that belong exclusively to the insignificant extreme currents are thrown away and considered as inessential.

In Chapter II, we saw that a necessary condition for the existence of multiple steady states is the vanishing of the Jacobian of the set of independent kinetic equations. By multiple steady states here we mean at least 2 isolated steady states. The Jacobian vanishes for some (h,j) if and only if

$$\alpha_d(h,j) = 0 \qquad (5.1)$$

which results to one vanishing eigenvalue. The test is not sufficient because the singular points of *M* may happen to be degenerate. This usually does not happen and we do not need to worry about it here. We have seen in Chapter II, section K that if α_d is always positive for all sets of steady state parameters then no multiplicity of steady states is possible.

Example V.1

The following enzyme network with product inhibition was claimed by Aarons and Gray(50) to be capable of having 3 steady states. Using the $\{\alpha_d=0\}$-test given above, that claim is easily proven to be false.

Network N_{16}

$$\begin{array}{rc}
R_1, R_{-1} & (\ ) \rightleftarrows S \\
R_2 & E + S \rightarrow ES \\
R_3 & ES \rightarrow E + P \\
R_4, R_{-4} & 2P + E \rightleftarrows PEP \\
R_5 & P \rightarrow (\ )
\end{array}$$

There are only 4 independent dynamical species due to the conservation constraint $[E]+[ES]+[PEP]=E_t$, constant. One finds that

$$\alpha_d = k_{-4}k_3k_5(k_2E_t+k_{-1}) > 0$$

and therefore multiplicity of steady states is impossible. It can be shown that it is necessary that reactions R_2 and R_3 should be reversible for α_d to be able to change sign for some feasible parameters. One can also check that the stoichiometric coefficient of the species P in reaction R_4 must indeed be at least 2 for multiple steady states to be possible. ∎

We now develop an additional criterion which turns out to be very helpful in the PO model. Our criterion is that an experimental system with bistability lies on a two-dimensional face of Π_v and that this face will contain part of the surface defined by $\alpha_d=0$. The reasons for this will be developed in the discussion which follows.

The condition $\alpha_d=0$ is an equation of a hypersurface Σ° which can be drawn inside Π_v for a given h. If there is no conservation constraint, then Σ° has a fixed position in Π_v regardless of the value of the parameter h. An example of this has already been given by Clarke (reference 4,p.38) for the 1-dimensional Schlogl model. However, if there are conservation conditions, then the position of Σ° will depend on the value of h. In either case, this hypersurface must exist if there is the possibility of multiple steady states at all.

The sign of α_d is related to stability. In a bistable system, there is a middle unstable steady state that corresponds to the region in Π_v where α_d is negative and two stable steady states that correspond to nearby regions where α_d is positive. Thus, the parameters of an experimental bistable system must place the system in the vicinity of the hypersurface Σ°.

Another important ingredient is the proposition that an experimental system will probably correspond to the lowest dimensional face of Π_v that is consistent with the observed experimental behavior. The reasoning behind this statement involves the fact that chemical reaction rates vary over many orders of magnitude. Usually the rates of the less important reactions in a chemical system at steady state are many orders of magnitude smaller than the rates of the dominant reactions. It would be improbable for a large number of independent currents to be equal at steady state. Thus, the center of Π_v is the least probable location to find an experimental system because in this region all currents are equal. Π_v has faces that are of one lower dimension than the polytope itself. The centers of these faces are also improbable because all but one current in a set of independent currents must be equal. The most probable locations for finding an experimental system are near the lowest dimensional faces, with vertices having the highest probability of all.

We now consider the lowest dimensional face of Π_v that is consistent with bistability. A vertex is unacceptable. It represents an extreme current where the reaction rates are locked into fixed ratios. To have several steady states at a vertex, the only thing that can vary is the flow in this single current. Mathematically this is possible if the reaction kinetics is of high order but it seems unlikely that any realistic chemical network would meet the required mathematical conditions. Our view of bistability is that the three steady states (2 stable, 1 unstable) differ in that each state has a different combination of important reactions. Thus there should be three independent combinations of reactions involved. Three independent currents span a three dimensional cone, which corresponds to a two dimensional face of Π_v. In order to have bistability on this face, the curve $\{\alpha_6=0\}$ must also pass through the interior of the face.

C. Elements in the Substrate-Inhibition Mechanism Essential for Bistability

It is believed by Degn et al.(42,61) that the major cause of the experimentally observed bistability in the peroxidase-oxidase reaction is the inhibition of the enzyme at high oxygen concentrations. A subset of the reactions of the network now to be analyzed has actually been suggested by Degn(61) as a crude model for this bistability. For this reason, we present a full steady state analysis of the reversible substrate-inhibition enzyme mechanism and show how to extract the important reactions for the occurrence of bistability. We find that we are able to list down the essential extreme currents and take this list as our guide in the analysis of the PO reaction mechanism.

The reactions are given below. Reactions 1 and 2 represent the reversible flux of the substrate S from a constant reservoir denoted by (A). E represents the free enzyme, ES and SES are enzyme-substrate complexes. The symbol (P) also means a constant product reservoir.

Network N_{17}

R_1, R_2	$(A) \rightleftarrows S$
R_3, R_7	$S + E \rightleftarrows ES$
R_4, R_8	$ES \rightleftarrows E + (P)$
R_5, R_6	$S + ES \rightleftarrows SES$

The current matrix **E** is

$$\mathbf{E} = \begin{bmatrix} 1 & 1 & 0 & 0 & 0 & 0 \\ 1 & 0 & 0 & 0 & 0 & 1 \\ 0 & 1 & 0 & 1 & 0 & 0 \\ 0 & 1 & 0 & 0 & 1 & 0 \\ 0 & 0 & 1 & 0 & 0 & 0 \\ 0 & 0 & 1 & 0 & 0 & 0 \\ 0 & 0 & 0 & 1 & 0 & 1 \\ 0 & 0 & 0 & 0 & 1 & 1 \end{bmatrix}$$

and the 6 extreme current diagrams are shown in figure 5.1. Π_v is 4 dimensional and there are 14 edges, 15 two-faces and 7 three-faces as given in detail below. (The APL programs published by von Hohenbalken(11) were used). The numbers identifying each face correspond to those of the extreme currents given in figure 5.1 (or column numbers of **E**).

```
1-FACES : 14

  1 2
  1 3
  1 4
  1 5
  1 6
  2 3
  2 4
  2 5
  3 4
  3 5
  3 6
  4 5
  4 6
  5 6

2-FACES : 15

  1 2 3
  1 2 4
  1 2 5
  1 3 4
  1 3 5
  1 3 6
  1 4 6
  1 5 6
  2 3 4
  2 3 5
  2 4 5
  3 4 5
  3 4 6
  3 5 6
  4 5 6

3-FACES : 7

  1 2 3 4
  1 2 3 5
  1 2 4 5 6
  1 3 4 6
  1 3 5 6
  2 3 4 5
  3 4 5 6
```

Table V.1 lists all the two-faces in terms of the component extreme currents. The signs of α_d for each face are also given ('+' means it is always positive and cannot change sign, while '+-' means it can change sign). There are only three possible 2-faces that can have their α_d's vanish for some parameters (h,j). It can be easily checked that the 2-faces (2 3 4) and (2 3 5) can have either 2 or 0 steady states for all parameters (*M* in these cases has a non-degenerate fold singularity). Only the face (1 2 3) can generate 3 steady states. Thus, we can take reactions R_1-R_6

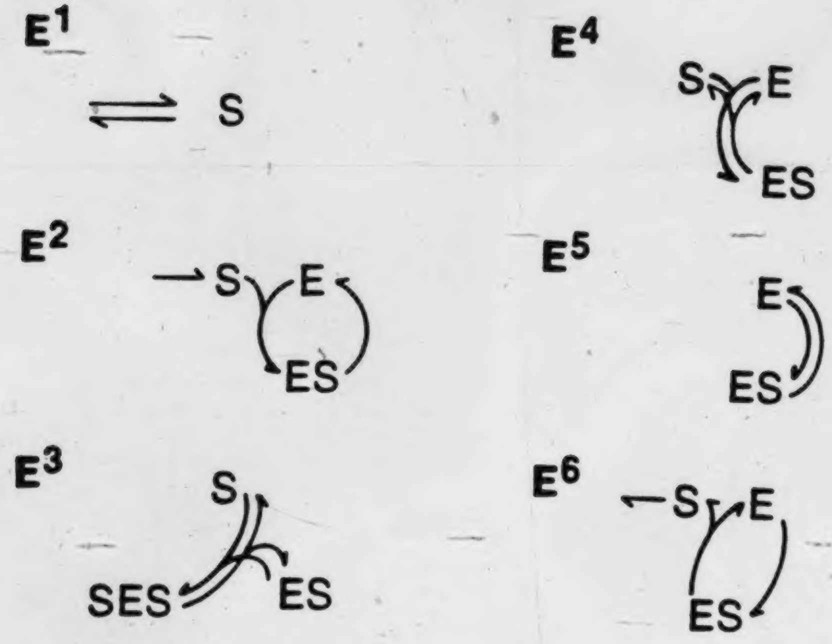
E1
S
E2
S
E
ES
E3
S
SES
ES
E4
S
E
ES
E5
E
ES
E6
S
E
ES

Figure 5.1

The six extreme subnetworks corresponding to the columns of the current matrix E for the reversible classical substrate-inhibition enzyme mechanism.

TABLE V.1

Two-dimensional Faces of the Current Polytope Π_v of Network N_{17} (substrate-inhibition mechanism)

(Numbers in the 1st column give the column numbers of the current matrix **E**; n is the number of species in each 2-face, and d is the number of independent species)

Two-face	n	d	α_d
1 2 3	4	3	+-
1 2 4	3	2	+
1 2 5	3	2	+
1 3 4	4	3	+
1 3 5	4	3	+
1 3 6	4	3	+
1 4 6	3	2	+
1 5 6	3	2	+
2 3 4	4	3	+-
2 3 5	4	3	+-
2 4 5	3	2	+
3 4 5	4	3	+
3 4 6	4	3	+
3 5 6	4	3	+
4 5 6	3	2	+

as the minimal reaction set for a bistable model. Reactions R_7 and R_8 are inessential.

The current polytope for the model is given in figure 5.2. The $\{\alpha_d=0\}$-curve is also given for a fixed **h** = $(1/E^\circ, 1/S^\circ, 1/ES^\circ, 1/SES^\circ)'$. The coefficient α_d (d=3) for the model is

$$\alpha_d(h,j) = j_2 j_3 h_2 \cdot [j_1(h_1h_3+h_1h_4+h_3h_4)+j_2h_3(h_4-h_1)]$$

which vanishes when

$$j_1(h_1h_3+h_1h_4+h_3h_4) + j_2h_3(h_4-h_1) = 0$$

for $j_2j_3h_2 \neq 0$. Using the conservation condition for the total enzyme concentration E_t, the above equation implies

$$j_1/j_2 = (h_4^{-1}-h_1^{-1})/E_t$$

from which we conclude that multiplicity of steady states occurs when $[SES]^\circ > [E]^\circ$. (In example II.8, the variation of $[S]^\circ$ and α_d as a function of E_t was given for some fixed values of the rate constants).

The steady state manifold for this minimal model possesses a degenerate singularity which is the cusp. From the analysis of the cusp catastrophe manifold in Chapter III, we can express exactly the set of parameters that lead to 3 distinct steady states given by the tristate set T

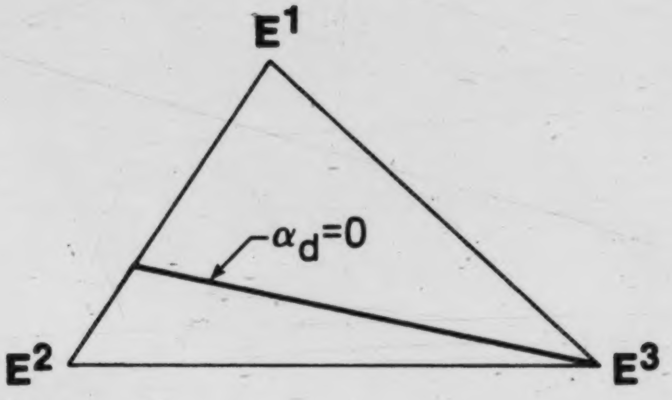

Figure 5.2

The current polytope Π_v of the reduced substrate-inhibition mechanism involving currents E^1, E^2, E^3 given in figure 5.1. For a fixed parameter h, $\alpha_d=0$ is a straight line as shown.

$$\mathbf{T} = \{ (\beta_2, \beta_1, \beta_0) \mid \beta_2 < 0, \beta_1 > 0, \beta_0 < 0 \text{ and } K_3 < 0 \}$$

where

$$K_3 = 27\beta_0^2 + 4\beta_0\beta_2^3 - 18\beta_0\beta_1\beta_2 - \beta_1^2\beta_2^2 + 4\beta_1^3$$
$$\beta_0 = -k_1k_4k_6/k_2k_3k_5$$
$$\beta_1 = (k_4k_6/k_3k_5) + (k_4k_6E_t/k_2k_5) - (k_1k_6/k_2k_5)$$
$$\beta_2 = (k_6/k_5) - (k_1/k_2).$$

Thus,

$$\mathbf{T} = \{(k, E_t) \mid k_2k_6 < k_1k_5,\ k_4(k_2 + k_3E_t) > k_1k_3,\ K_3 < 0\}.$$

The analysis above tells us that $\mathbf{E}^2$, the pathway corresponding to the catalytic cycle, and $\mathbf{E}^3$ which is the enzyme inhibition pathway, are sufficient to generate a fold on *M*. For bistability or 3 steady states, *M* must fold twice and $\mathbf{E}^1$, the reversible flux of substrate, is a necessary addition. The three elements $\mathbf{E}^1$, $\mathbf{E}^2$ and $\mathbf{E}^3$ in this minimal model will have their counterparts in the bistable model for the PO reaction.

Example V.2

Briefly, we demonstrate the existence of the 3 steady states in the model for a specified set of parameters and give a simple way of explaining why the highest and lowest steady state values are stable and the middle one unstable. Focus the attention on substrate S. The rate of 'production' of S due to the exchange with the reservoir is $v_{in}(S) = k_1 - k_2S$; the rate of 'consumption' of S due to the enzymatic reactions is given by $v_{out}(S) = k_3k_4k_6E_tS/(k_4k_6+k_3k_6S+k_3k_5S^2)$ (assuming that the enzymic species E, ES and SES are at steady state).

Figure 5.3 gives a network diagram of the model and a plot of $v_{in}(S)$ and $v_{out}(S)$. These two functions intersect at three points corresponding to the 3 steady state values of S labeled as SS(I), SS(II) and SS(III) in the figure. The stability of SS(I) and SS(III) could be understood easily as follows. If S is increased beyond SS(I) (but less than SS(II)), v_{out} predominates, that is, S is consumed, bringing the system back to SS(I). On the other hand, if S is decreased below SS(I), then v_{in} predominates, i.e. more S flows in and the system goes back to SS(I). The same argument can be followed to show the local stability of SS(III). Now, consider SS(II). If S is increased above SS(II), v_{in} predominates and S is increased further. Similarly, if S is decreased below SS(II), v_{out} predominates and S is decreased further. Small perturbations on SS(II) are magnified thus making it unstable. ■

D. Mechanism and Models of the Peroxidase-Oxidase Reaction

The aerobic oxidation of NADH (nicotinamide adenine dinucleotide) catalyzed by the enzyme horseradish peroxidase, referred to in this work as the peroxidase-oxidase (PO) reaction, has the following overall reaction

$$2NADH + 2H^{+} + O_2 \rightarrow 2NAD^{+} + 2H_2O \ . \qquad (5.2)$$

Only some pertinent features of the PO mechanism will be pointed out here. For more details, the reader is referred to the series of papers written by Yamazaki and co-workers (e.g. reference 43) and by Degn and Olsen (e.g. reference 47). Table V.2 gives a listing of the individual reaction steps that have been studied or postulated previously for the PO reaction. In particular, most of the reactions are taken from the table given by Olsen and Degn(47) and some are from Yokota and Yamazaki(43).

It is now widely agreed that the PO reaction is a free radical branched chain reaction. At acidic pH (e.g. < 6), superoxide ($O_2^{\cdot -}$) is believed to be mainly involved in the branching through reactions R_{12} and R_{10}(58). For example, the branch initiated by R_{12} produces 3NAD$\cdot$ radicals through reactions R_{12}, R_1, R_2 and R_3 while the branch initiated by reaction R_{10} has a gain of only one NAD$\cdot$ radical if we

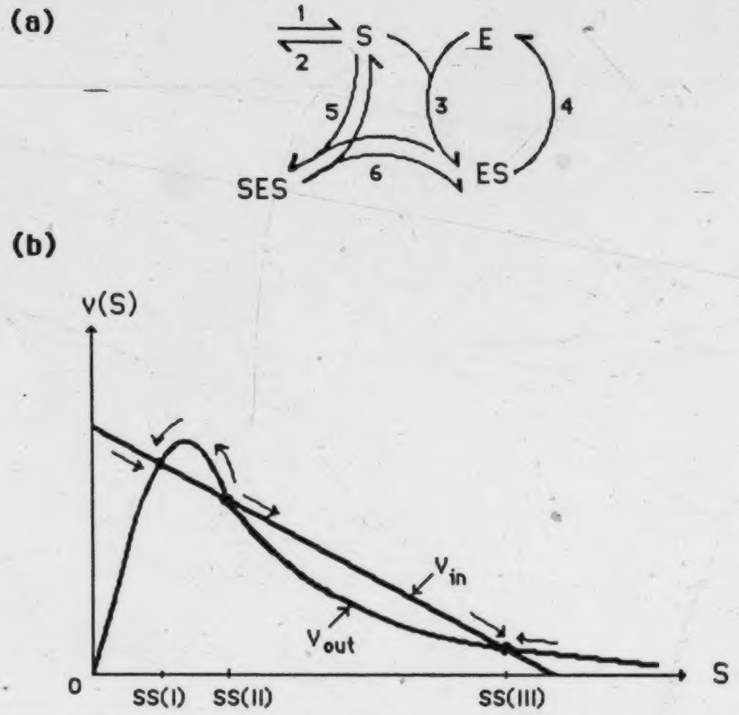
(a)
1
2
S
E
3
4
5
6
SES
ES
(b)
v(S)
v_{in}
v_{out}
0
SS(I)
SS(II)
SS(III)
S

Figure 5.3

(a) The minimal subset of reactions (model) for the enzyme substrate-inhibition mechanism capable of bistability.

(b) With the enzymic species E, ES and SES at steady state, the rate of production, v_{in} ($= k_1 - k_2 S$), and the rate of consumption due to the ezymatic reactions, v_{out}, are plotted. S is at steady state where v_{in} and v_{out} intersect, in the above case at 3 points. SS(II) is unstable while SS(I) and SS(III) are stable.

consider the reaction sequence R_{10}, R_8, R_2 and R_3. We note here that reaction R_8 has not been confirmed experimentally but Yokota and Yamazaki(43) has postulated its occurrence. The reaction between NADH and Compound III (R_7) has actually been observed and is found to be slow(57). In contrast to some models proposed by other authors (e.g. reference 44), the termination reaction R_{13} will be considered as second (not first) order kinetically.*//

The reaction system we are interested in is an open system where oxygen is diffusing from the gas phase into a well-stirred solution. The rate of oxygen transport into the liquid is represented by the pseudo-reactions R_{16} and R_{17} given in Table V.2. Reference 42 gives a diagram of a corresponding experimental system. This PO reaction system is known to exhibit damped and sustained oscillations, bistability and even chaos (42). Simple models to account for these observed behaviors have been proposed. Observing that some autocatalytic reactions are occurring, Degn and Mayer(45) investigated 2-species models derived from the old Lotka model(51) to simulate the damped oscillations in the PO reaction. Olsen and Degn(42,47) concocted a 4-species model based on the main features of the complex mechanism (e.g. branching of the chain reaction) and successfully reproduced the qualitative forms of the sustained

---

*// Another possible second order termination reaction aside from the disproportionation reaction R_{13} is the dimerization reaction(58) $2NAD\cdot \rightarrow NAD\text{-}NAD$. In our further analysis of the mechanism, the case where NADH will be in stoichiometric excess is assumed and the choice of which termination reaction to consider does not matter.

TABLE V.2 Elementary Processes in the Peroxidase-Oxidase Reaction Mechanism(43,47)

R_1 $\quad Per^{3+} + H_2O_2 \rightarrow CoI$

R_2 $\quad CoI + NADH \rightarrow CoII + NAD\cdot$

R_3 $\quad CoII + NADH \rightarrow Per^{3+} + NAD\cdot$

R_4 $\quad CoII + H_2O_2 \rightarrow CoIII$

R_5 $\quad Per^{3+} + NAD\cdot \rightarrow Per^{2+} + NAD^+$

R_6 $\quad Per^{2+} + O_2 \rightarrow CoIII$

R_7 $\quad CoIII + NADH \rightarrow CoI + NAD\cdot + H^+$

R_8 $\quad CoIII + NAD\cdot \rightarrow CoI + NAD^+$

R_9 $\quad CoI + O_2^{\overline{\cdot}} \rightarrow CoII + O_2$

R_{10} $\quad Per^{3+} + O_2^{\overline{\cdot}} \rightarrow CoIII$

R_{11} $\quad NAD\cdot + O_2 \rightarrow NAD^+ + O_2^{\overline{\cdot}}$

R_{12} $\quad H^+ + O_2^{\overline{\cdot}} + NADH \rightarrow H_2O_2 + NAD\cdot$

R_{13} $\quad 2NAD\cdot + H^+ \rightarrow NADH + NAD^+$

R_{14} $\quad 2O_2^{\overline{\cdot}} + 2H^+ \rightarrow H_2O_2 + O_2$

R_{15} $\quad Per^{2+} + CoIII \rightarrow Per^{3+} + CoI$

R_{16} $\quad \rightarrow O_2$

R_{17} $\quad O_2 \rightarrow$

oscillations. Recently, Olsen(48,49) has developed a 4-species model that shows chaos for some enzyme concentrations. No model has yet been developed for the bistable behavior, although it has been suggested that bistability is probably caused by the inhibition of the enzyme due to high oxygen concentrations as supported experimentally by Degn, Olsen and Perram(42).

Sufficient information is now known about the mechanistic details of the PO reaction that computer simulations of closed systems have been claimed to agree with experimental data almost quantitatively(43,46). Recently, computer simulations done by Fed'kina et al.(44) using a detailed mechanism has produced sustained oscillations which can be taken to have the same qualitative form as the slow oscillations they have observed previously(60). The mechanism they used, however, cannot model the bistability that is easily observed in the system.

E. A Bistable Model for the PO Reaction

We consider the case where NADH is in excess and assume a constant acidic pH. Hence, the concentrations of NADH, NAD^+, H^+ are not dynamical variables. For convenience, the following symbols for the dynamical species are used:

Enzymic Species

V	ferrousperoxidase
W	ferriperoxidase
X	compound I
Y	compound II
Z	compound III

Non-enzymic species

A	H_2O_2
B	NAD·
C	$O_2^{\cdot-}$
F	O_2

There are 17 extreme currents found from all the reactions listed in Table V.2. These are coded in the current matrix given below:

$$\mathbf{E} = \begin{pmatrix}
0 & 0 & 0 & 1 & 0 & 0 & 1 & 0 & 1 & 0 & 0 & 0 & 0 & 0 & 0 & 0 & 0 \\
1 & 1 & 0 & 1 & 1 & 1 & 0 & 1 & 1 & 1 & 0 & 1 & 0 & 1 & 1 & 0 & 1 \\
1 & 1 & 0 & 1 & 1 & 0 & 1 & 1 & 1 & 0 & 1 & 1 & 1 & 1 & 0 & 0 & 0 \\
0 & 0 & 0 & 0 & 0 & 1 & 0 & 0 & 0 & 1 & 0 & 0 & 0 & 0 & 1 & 1 & 1 \\
1 & 2 & 0 & 0 & 0 & 0 & 0 & 1 & 0 & 1 & 1 & 1 & 0 & 0 & 0 & 0 & 0 \\
1 & 1 & 0 & 0 & 0 & 0 & 0 & 0 & 0 & 0 & 1 & 1 & 0 & 0 & 0 & 0 & 0 \\
0 & 0 & 0 & 0 & 0 & 0 & 0 & 0 & 0 & 0 & 1 & 1 & 1 & 1 & 1 & 1 & 1 \\
1 & 0 & 0 & 0 & 1 & 1 & 0 & 0 & 0 & 0 & 0 & 0 & 0 & 0 & 0 & 0 & 0 \\
0 & 0 & 0 & 0 & 0 & 0 & 1 & 0 & 0 & 0 & 1 & 0 & 1 & 0 & 0 & 1 & 0 \\
0 & 0 & 0 & 0 & 1 & 0 & 0 & 1 & 0 & 0 & 0 & 0 & 1 & 1 & 0 & 0 & 0 \\
0 & 0 & 0 & 2 & 1 & 1 & 2 & 1 & 1 & 1 & 1 & 0 & 2 & 1 & 2 & 2 & 1 \\
0 & 0 & 0 & 0 & 0 & 1 & 1 & 0 & 1 & 1 & 0 & 0 & 0 & 0 & 0 & 1 & 1 \\
0 & 0 & 0 & 0 & 0 & 0 & 0 & 0 & 1 & 0 & 0 & 1 & 0 & 1 & 0 & 0 & 1 \\
0 & 0 & 0 & 1 & 0 & 0 & 0 & 0 & 0 & 0 & 0 & 0 & 0 & 0 & 1 & 0 & 0 \\
0 & 1 & 0 & 0 & 0 & 0 & 0 & 1 & 0 & 1 & 0 & 0 & 0 & 0 & 0 & 0 & 0 \\
1 & 1 & 1 & 1 & 1 & 1 & 1 & 1 & 1 & 1 & 1 & 1 & 1 & 1 & 1 & 1 & 1 \\
0 & 0 & 1 & 0 & 0 & 0 & 0 & 0 & 0 & 0 & 0 & 0 & 0 & 0 & 0 & 0 & 0
\end{pmatrix}$$

Figure 5.4 shows the extreme currents represented by columns 3, 5, 9 and 14 of **E** which we will see later to be important.

The dimension of Π_v is 8 and there are 90 edges, 233 two-faces, 346 three-faces, 315 four-faces, 179 five-faces, 62 six-faces and 12 seven-faces. For possible future studies on this system, the details of these faces can be found in appendix G. It is not wise to investigate individually the large number of 2-faces. Instead, we try to identify all the possible extreme currents that fall under each of the 3 elements responsible for the bistability in the example analyzed in section C. Current $\mathbf{E}^3$ represents the reversible flux of the inhibiting substrate, O_2. The classical peroxidase catalytic cycle is given by only one extreme current namely, $\mathbf{E}^1$.

There are several choices for the inhibition pathway which should involve the formation and decay of the inactive enzyme intermediate compound III (Z). According to Yamazaki

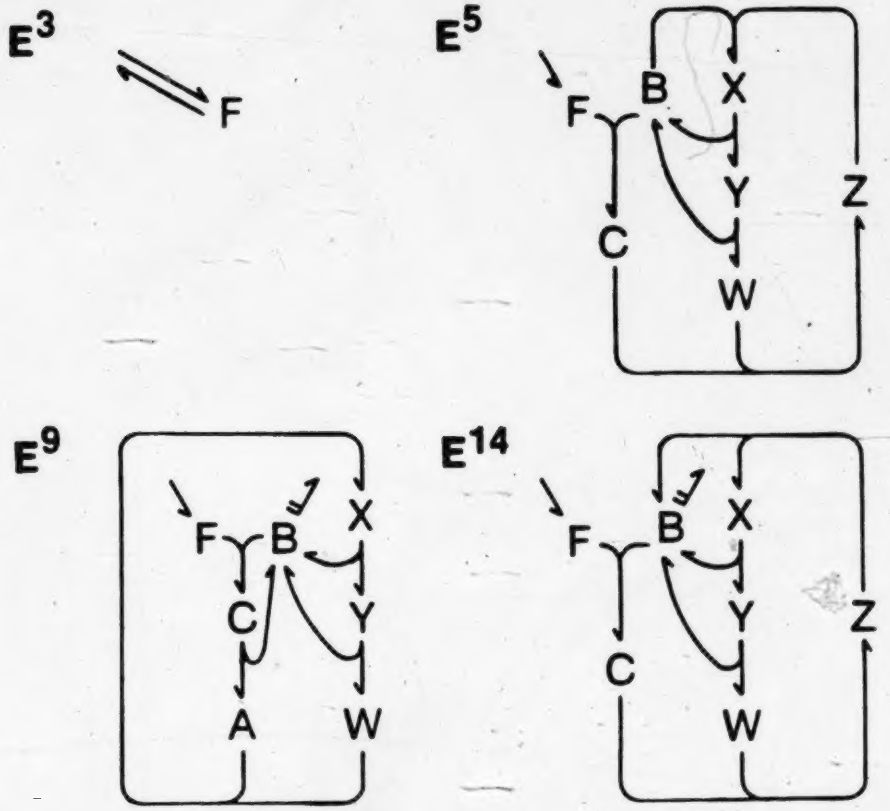

Figure 5.4

Four important extreme currents found in the peroxidase-oxidase mechanism given in Table V.2. E^3 corresponds to the reversible flux of the substrate O_2 (F), E^5 is the classical peroxidase catalytic cycle, and the two extreme currents E^9 and E^{14} are possible enzyme inhibition pathways involving the inactive intermediate Compound III (Z).

and Piette(52), the reaction between the superoxide anion radical $O_2^{\overline{\cdot}}$ (C) and ferriperoxidase (W), reaction R_{10}, appears to be the most likely path of compound III formation. This information leads us to take the currents appearing in the 10th row of **E**. Thus, we consider $\mathbf{E}^5$, $\mathbf{E}^8$, $\mathbf{E}^{13}$ and $\mathbf{E}^{14}$. Among these, the most likely choice is $\mathbf{E}^5$ for the following reasons: reaction R_7 is known to be very slow.(55-57) This eliminates $\mathbf{E}^{13}$ and $\mathbf{E}^{14}$ from consideration. It is suggested by Yokota and Yamazaki(43) and others(44) that reaction R_8 explains the characteristic compound III decay. This favors $\mathbf{E}^5$ over $\mathbf{E}^8$.

When we look at the faces of Π_v, we discover that (3 5 9), (3 9 14) and (3 8 9) are 2-faces (see appendix G). It can be shown that neither (3 9 14) nor (3 8 9) can give rise to a bistable model. A model based on (3 9 14) will always have a unique steady state for every set of parameters while (3 8 9) can only have at most 2 steady states for any set of parameters. Indeed, a model based on (3 5 9) can exhibit bistability for some parameter values. This is our proposed model and we give the network diagram in figure 5.5. We notice that this model (that we arrived at systematically) closely resembles the model proposed by Fed'kina et al.(44) for the sustained oscillations. Their model lacks R_{17} and assumes a linear termination reaction, R_{13}. Because their model has only two extreme currents, bistability cannot occur.

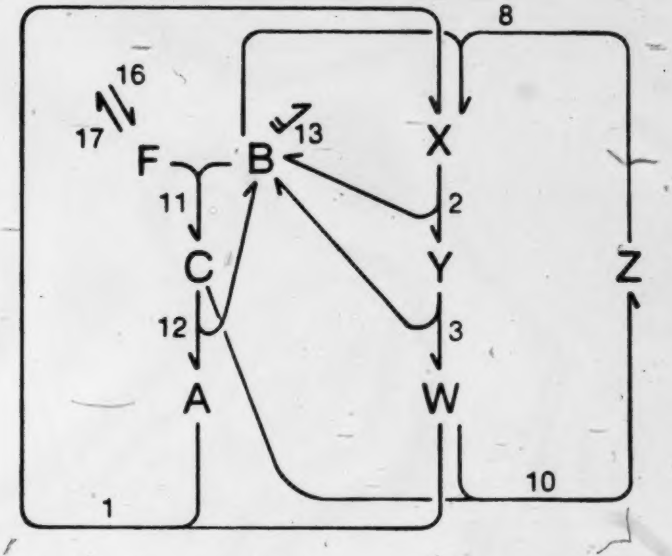
8
16
17
13
F
B
X
11
2
C
Y
Z
12
3
A
W
10
1

Figure 5.5

Network diagram of the bistable model for the peroxidase-oxidase reaction. Reaction numbers refer to those given in Table V.2. Every steady state of this model is a linear combination of the extreme currents E^3, E^5 and E^9 shown in figure 5.4.

Bistability and Damped Oscillations

The full expression for $\alpha_d(h,j)$ (d=7) for the model is given in Table V.3. One can show that $\alpha_d = 0$ if and only if

$$h_8^{-1}[j_3 j_9+(j_5+2j_9)(j_5+j_9)] + h_5^{-1}(j_3+2j_5+2j_9)(j_5+j_9)$$
$$= (h_6^{-1}+h_7^{-1})j_3 j_5$$

(note : $h^{-1} = (A^\circ, B^\circ, C^\circ, F^\circ, W^\circ, X^\circ, Y^\circ, Z^\circ)^t$)

from which we find the following exact criterion for the existence of an $\{\alpha_d=0\}$-curve in the interior of Π_V:

$$j_9/j_5 < (h_6^{-1}+h_7^{-1}-h_5^{-1})/(h_5^{-1}+h_8^{-1})$$

which in turn requires that

$$h_5^{-1} < h_6^{-1} + h_7^{-1} .$$

In other words, no bistability can occur if the steady state concentration of ferriperoxidase is greater than the sum of the steady state concentrations of compounds I and II. Π_V for the model is given in figure 5.6 with the $\{\alpha_d=0\}$-curve for a fixed **h**.

The work of solving the steady states for the model can be accomplished exactly and completely using the results of Chapter III. The equation $\mathbf{v}^\circ=\mathbf{E}'\mathbf{j}$ (where **E'** is the corresponding current matrix for the model) gives the following relationship among the steady state velocities:

TABLE V.3 $\alpha_d(h,j)$ for the PO Bistable Model (d=7)

$$
\begin{aligned}
\alpha_d(h,j) =:\ & 2h_1h_2h_3h_4h_5h_6h_7j_3j_5{}^3j_9{}^3 \\
& +4h_1h_2h_3h_4h_5h_6h_7j_3j_5{}^2j_9{}^4 \\
& +2h_1h_2h_3h_4h_5h_6h_7j_3j_5j_9{}^5 \\
& +2h_1h_2h_3h_4h_5h_6h_7j_5{}^5j_9{}^2 \\
& +10h_1h_2h_3h_4h_5h_6h_7j_5{}^4j_9{}^3 \\
& +18h_1h_2h_3h_4h_5h_6h_7j_5{}^3j_9{}^4 \\
& +14h_1h_2h_3h_4h_5h_6h_7j_5{}^2j_9{}^5 \\
& +4h_1h_2h_3h_4h_5h_6h_7j_5j_9{}^6 \\
& -2h_1h_2h_3h_4h_5h_6h_8j_3j_5{}^4j_9{}^2 \\
& -4h_1h_2h_3h_4h_5h_6h_8j_3j_5{}^3j_9{}^3 \\
& -2h_1h_2h_3h_4h_5h_6h_8j_3j_5{}^2j_9{}^4 \\
& -2h_1h_2h_3h_4h_5h_7h_8j_3j_5{}^4j_9{}^2 \\
& -4h_1h_2h_3h_4h_5h_7h_8j_3j_5{}^3j_9{}^3 \\
& -2h_1h_2h_3h_4h_5h_7h_8j_3j_5{}^2j_9{}^4 \\
& +2h_1h_2h_3h_4h_6h_7h_8j_3j_5{}^4j_9{}^2 \\
& +6h_1h_2h_3h_4h_6h_7h_8j_3j_5{}^3j_9{}^3 \\
& +6h_1h_2h_3h_4h_6h_7h_8j_3j_5{}^2j_9{}^4 \\
& +2h_1h_2h_3h_4h_6h_7h_8j_3j_5j_9{}^5 \\
& +4h_1h_2h_3h_4h_6h_7h_8j_5{}^5j_9{}^2 \\
& +16h_1h_2h_3h_4h_6h_7h_8j_5{}^4j_9{}^3 \\
& +24h_1h_2h_3h_4h_6h_7h_8j_5{}^3j_9{}^4 \\
& +16h_1h_2h_3h_4h_6h_7h_8j_5{}^2j_9{}^5 \\
& +4h_1h_2h_3h_4h_6h_7h_8j_5j_9{}^6
\end{aligned}
$$

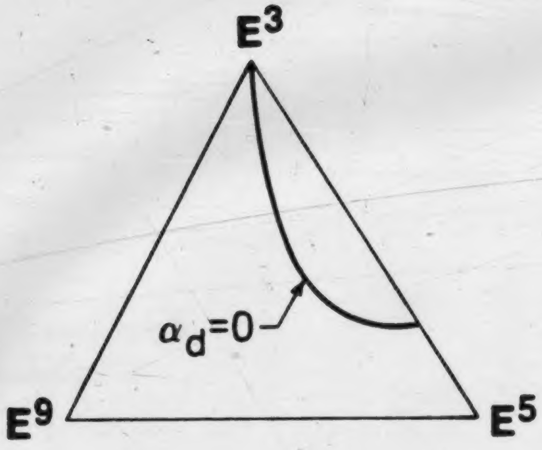

Figure 5.6

The current polytope Π_v and a curve $\alpha_d=0$ (for a fixed parameter h) of the bistable model network given in figure 5.5.

$$v_1^o = v_{12}^o = v_{13}^o$$

$$v_2^o = v_3^o = v_{11}^o$$

$$v_8^o = v_{10}^o$$

$$v_{16}^o = v_{11}^o + v_{17}^o$$

$$v_{11}^o = v_{12}^o + v_{10}^o$$

where the reaction velocities are

$$v_{16} = k_{16}$$

$$v_{17} = k_{17}F$$

$$v_{11} = k_{11}FB$$

$$v_{12} = k_{12}C$$

$$v_1 = k_1AW$$

$$v_2 = k_2X$$

$$v_3 = k_3Y$$

$$v_{10} = k_{10}CW$$

$$v_8 = k_8BZ$$

$$v_{13} = k_{13}B^2 .$$

There is one conservation condition corresponding to that of the total enzyme concentration,

$$E_t = W + X + Y + Z .$$

One can then express the steady states of 7 of the 8 species in terms of the remaining one. This last species is taken to be species B (NAD·) for convenience. Unless otherwise stated, the species symbols will also be taken as their steady state concentrations below. To determine the steady states, one first solves a cubic polynomial for the steady state value B:

$$f_3(B) = B^3+\beta_2B^2+\beta_1B+\beta_0 = 0 \tag{5.3}$$

where

$$\beta_0 = -k_8k_{16}k_{12}/k_{13}{}^2k_{10}$$

$$\beta_1 = (E_t + k_{12}/k_{10})(k_8k_{17}/k_{13}k_{11}) - (k_{16}/k_{13})$$

$$\beta_2 = (E_t + k_{12}/k_{10})(k_8/k_{13}) + (k_{17}/k_{11}) - (1/k_3 + 1/k_2)(k_{16}k_8/k_{13}) .$$

Not all positive real roots of (5.3) are allowed as steady state value for B. In order that all other species will have positive steady states, B must be less than a certain upper bound B_m:

$$B < B_m = [(k_{17}/2k_{11})^2 + (k_{16}/k_{13})]^{1/2} - (k_{17}/2k_{11}) . \tag{5.4}$$

This condition comes from the constraint that all other species must have non-negative concentrations (specifically $W>0$, see equations below). The steady states of all other species in terms of B are given by the following equations

$$C = k_{13}B^2/k_{12}$$

$$F = k_{16}/(k_{17}+k_{11}B)$$

$$X = k_{11}BF/k_2$$

$$Y = k_{11}BF/k_3$$

$$W = (k_{11}BF/k_{10}C) - (k_{12}/k_{10})$$

$$A = k_{13}B^2/k_1W$$

$$Z = k_{10}k_{13}BW/k_8k_{12} \; .$$

Our previous results on the analysis of the cusp catastrophe manifold (Chapter III) enable us to define exactly the set of parameters that will give three positive steady states for the model. The tristate set **T** is given in Table III.1 with the β coefficients given in (5.3). Some conclusions can now be made on the necessary conditions on the parameters for 3 steady states to exist - for example, $\beta_1 > 0$ implies

$$E_t > (k_{16}k_{11}/k_8k_{17})-(k_{12}/k_{10})$$

and $\beta_2 < 0$ implies

$$E_t < (k_{16}/k_3)+(k_{16}/k_2)-(k_{12}/k_{10})-(k_{17}k_{13}/k_{11}k_8).$$

Thus, the total enzyme concentration is restricted to lie within certain limits imposed by the values of the rate constants. Since E_t is positive and the above limits have to be non-negative, further constraints on the rate constants can be seen immediately. Furthermore, due to condition (5.4), there are other constraints on the parameters belonging to **T**, namely

$$\{ \; 3B_m+\beta_2 > 0 \text{ and } f_3(B_m) > 0 \; \}$$

as was shown in Chapter III (B_m is given in equation 5.4).

For the sake of demonstration, we provide the following parameter values that give 3 steady states:

$k_{11} = 1 \times 10^{8}\ M^{-1}s^{-1}$

$k_{1} = 1 \times 10^{7}\ M^{-1}s^{-1}$

$k_{10} = 1 \times 10^{9}\ M^{-1}s^{-1}$

$k_{8} = 6 \times 10^{7}\ M^{-1}s^{-1}$

$k_{13} = 1 \times 10^{7}\ M^{-1}s^{-1}$

$k_{17} = k_{12} = k_{3} = 1.0\ s^{-1}$

$k_{2} = 1.1626\ s^{-1}$

$k_{16} = 1 \times 10^{-5}\ M\ s^{-1}$

$E_{t} = 18.499\ \mu M$

Table V.4 gives the computed steady states for all species. With the initial conditions given in figure 5.7, we discover that there is a damped oscillatory approach to the steady state designated as SS(III) in Table V.4. This agrees with the presence of two pairs of complex conjugate eigenvalues for the Jacobian matrix associated with the kinetic equations. The calculated eigenvalues of this matrix evaluated at the steady state SS(III) are given in Table V.5. In this table, the vanishing first eigenvalue corresponds to the enzyme conservation constraint. All the relevant eigenvalues for the steady states SS(I) and SS(III) have negative real parts which confirm their local asymptotic stability. There is only one positive eigenvalue

TABLE V.4

Computed Steady State Concentrations of all Species in the Bistable Model for the Peroxidase-Oxidase Reaction (Parameter Values : k_{11} = 1x10^8 $M^{-1}s^{-1}$, k_1 = 1x10^7 $M^{-1}s^{-1}$, k_{10} = 1x10^9 $M^{-1}s^{-1}$, k_8 = 6x10^7 $M^{-1}s^{-1}$, k_{13} = 1x10^7 $M^{-1}s^{-1}$, k_{17} = k_{12} = k_3 = 1.0 s^{-1}, k_2 = 1.1626 s^{-1}, k_{16} = 1x10^{-8} M s^{-1}, E_t = 18.499 μM)

	Concentrations (10^{-7}M)		
Species	SS(I)	SS(II)	SS(III)
(A) H_2O_2	83.20001511	19.98949609	1.07988654
(B) NAD·	2.92627347	2.06584677	0.99251764
(C) $O_2^{\cdot-}$	8.56307643	4.26772286	0.98509127
(F) O_2	3.30439403	4.61713181	9.15317026
(W) Per^{3+}	0.10292157	0.21349827	0.91221738
(X) CoI	83.17186132	82.04272165	78.14108871
(Y) CoII	96.69560597	95.38286819	90.84682974
(Z) CoIII	5.01961114	7.35091189	15.08986416

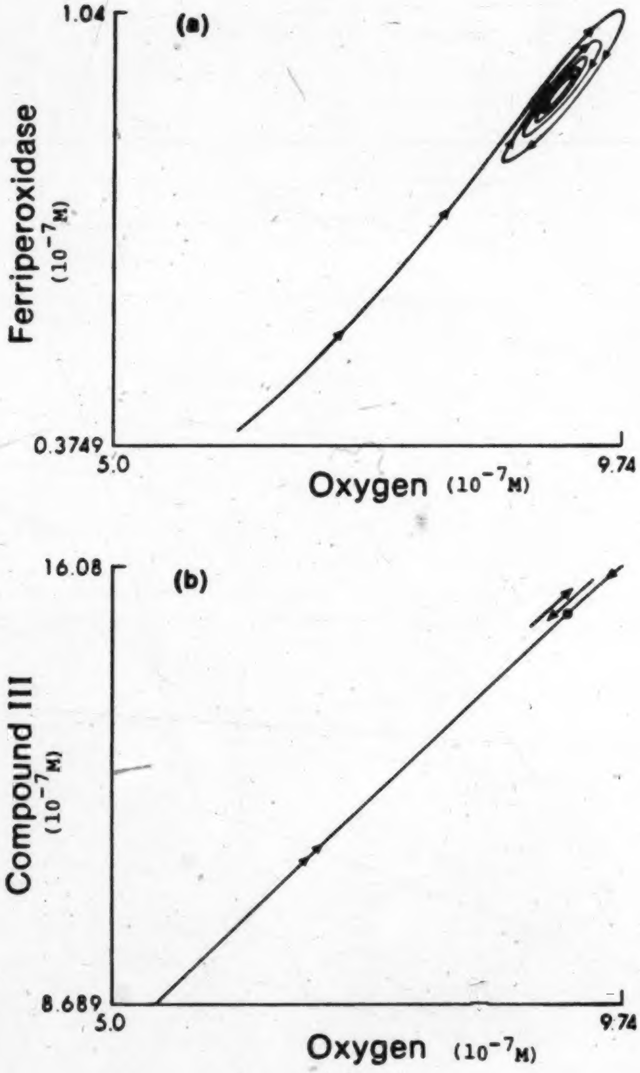

Figure 5.7

Damped oscillatory approach to the steady state designated as SS(III) in Table V.4. The damped oscillations in compound III and oxygen are synchronous as shown by the straight trajectory on the phase plot in (b). The parameter values used are given in the text. Initial conditions : A(0) = 8.5, B(0) = 1.5, C(0) = 2.0, F(0) = 5.0, W(0) = 0.49, X(0) = 80.8, Y(0) = 95.0, Z(0) = 8.7 (units of 10^{-7}M)

TABLE V.5

Computed Eigenvalues of the Jacobian Matrix associated with the Linearized Dynamics of ~~the~~ PO Bistable Model (parameter values are given in the text). (†)

	λ(I)	λ(II)	λ(III)
1	0.0	0.0	0.0
2	-1.3247E-04	+4.2429E-04	-0.00287+0.055i
3	-1.8642	-1.4218	-0.00287-0.055i
4	-2.433+0.752i	-1.8641+0.339i	-1.9177+0.465i
5	-2.433-0.752i	-1.8641-0.339i	-1.9177-0.465i
6	-23.1492	-16.8478	-10.0217
7	-96.950	-114.754	-174.064
8	-948.923	-467.330	-209.880

(†) The function EIGENV was used in the computation. See : Library 45, APL Functions for Numerical Analysis, APL Program Library Project, Computing Services, University of Alberta (C. Leibovitz, ed.),1980.

associated with the middle steady state, SS(II), which is sufficient to make the steady state unstable.

Experimentally, Yamazaki et al.(53) first observed damped oscillations 20 years ago in a system with continuous supply of oxygen. It was also observed(53,54) that the oscillations in oxygen and compound III are synchronized. The present model very well reproduces this synchronized oscillations as shown in figure 5.7. This model also shows the possibility that bistability and damped oscillations can occur simultaneously. Whether or not this is possible in the real system is not yet known.

Dominant Extreme Currents in the 3 Steady States

Figure 5.8 shows a steady state bifurcation diagram of species B (NAD·) with the total enzyme concentration as the bifurcation parameter. With the set of parameters given in this figure, we see that the extent of bistability is very narrow. An interesting observation is the possibility of having 2 positive steady states. Note that as E_t increases, the number of positive steady states changes in the sequence 0,2,3,1.

Let E_t=47.33μM in figure 5.8. The computed steady states for this set of parameters are given in Table V.6. To find the dominant current(s) for each steady state, we use the map

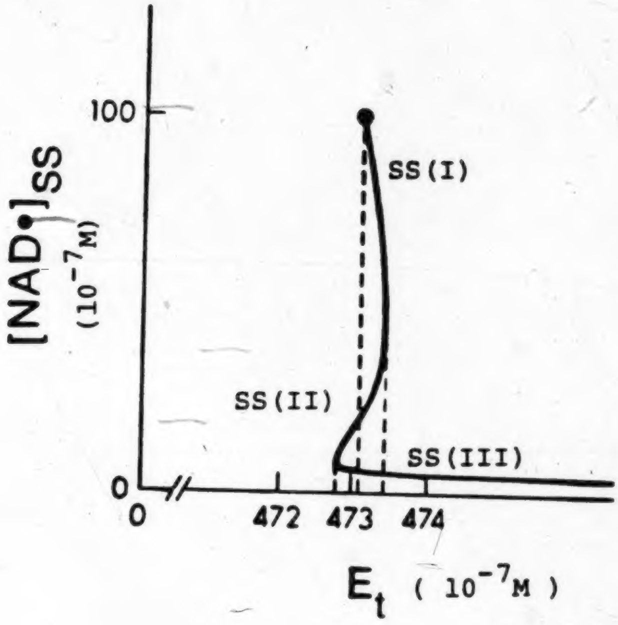

Figure 5.8

Steady state bifurcation diagram for NAD· with the total enzyme concentration E_t as the bifurcation parameter. The network involved is the bistable model for the peroxidase-oxidase reaction shown in figure 5.5. The steady states of all the other species involved are expressible in terms of $[NAD\cdot]_{ss}$ (see text). The steady state curve terminates at a point corresponding to the vanishing of the enzyme species W and Z. The parameters used are : $k_{17}=1.0s^{-1}$, $k_1=k_{10}=10^7M^{-1}s^{-1}$, $k_{11}=10^8M^{-1}s^{-1}$, $k_{12}=10^{-3}s^{-1}$, $k_2=0.6s^{-1}$, $k_3=0.3257s^{-1}$, $k_8=2.4x10^7M^{-1}s^{-1}$, $k_{13}=10^5M^{-1}s^{-1}$, $k_{16}=10^{-5}Ms^{-1}$.

TABLE V.6

Computed Steady State Concentrations for all Species in the PO Bistable Model when the parameters are those used in Figure 5.8 and E_t=47.33μM.

	Concentrations (10^{-7}M)		
Species	SS(I)	SS(II)	SS(III)
(A) H_2O_2	95616.40499	51.54972993	0.018700382
(B) NAD·	78.09017177	14.9575287	2.054731216
(C) $O_2^{\cdot -}$	60980.74927	2237.276648	42.2192037
(F) O_2	0.127893311	0.664119604	4.640950076
(W) Per^{3+}	0.000637764	0.043400356	2.257665289
(X) CoI	166.4535111	165.5598007	158.9317499
(Y) CoII	306.638338	304.991957	292.7818542
(Z) CoIII	0.207513082	2.704841981	19.3287306

$$\Omega : (h,j) \rightarrow (E_t,k)$$

which, for the model, is explicitly given by the following set of expressions:

$$\begin{aligned}
E_t &= h_5^{-1}+h_6^{-1}+h_7^{-1}+h_8^{-1} \\
k_{16} &= j_3+j_5+j_9 \\
k_{17} &= j_3h_4 \\
k_{11} &= (j_5+j_9)h_2h_4 \\
k_{12} &= j_9h_3 \\
k_1 &= j_9h_1h_5 \\
k_2 &= (j_5+j_9)h_6 \\
k_3 &= (j_5+j_9)h_7 \\
k_{10} &= j_5h_3h_5 \\
k_8 &= j_5h_2h_8 \\
k_{13} &= j_9h_2^2 \ .
\end{aligned}$$

From the given values of (E_t,k) and the computed values of h given in Table V.6, one finds the following percentages for the extreme currents :

	SSI	SSII	SSIII
j_3	0.1278933	0.6641196	4.6409501
j_5	38.8913574	97.0986037	95.3168307
j_9	60.9807493	2.2372767	0.0422192

Thus, at the steady state SS(I) (high [NAD·], low [O_2] and low [Per^{3+}]) the current corresponding to the catalytic peroxidase cycle ($\mathbf{E}^1$) is dominant while at the steady state SS(III) (low [NAD·], high [O_2] and high [Per^{3+}]), the current corresponding to the inhibition pathway ($\mathbf{E}^5$) predominates. The inhibition pathway ($\mathbf{E}^5$) attains a maximum current at the middle unstable steady state SS(II).

Simulation of Closed System Kinetics

Attempts to fit some models to experimental data in a closed system have been performed by Yokota and Yamazaki(43) and Fed'kina et al.(46) Let us now show that our model is also capable of accounting for several of the observed characteristic features of the closed system kinetics particularly that of compound III.

To simulate a closed system, we let $k_{16} = k_{17} = 0$. Note that besides the nonzero initial concentrations of oxygen and enzyme ferriperoxidase (W), either O_2^{-} or H_2O_2 must initially be present. Hydrogen peroxide is known to be produced by the auto-oxidation of NADH as represented by the following reaction(43):

$$NADH + O_2 + H^+ \rightarrow NAD^+ + H_2O_2 \ . \qquad (R_{18})$$

R_{18} is slow and can be ignored after the reaction system has started. It is mentioned here to justify the nonzero concentration of H_2O_2 initially. Figure 5.9 shows some concentration-time plots of oxygen and compound III. The

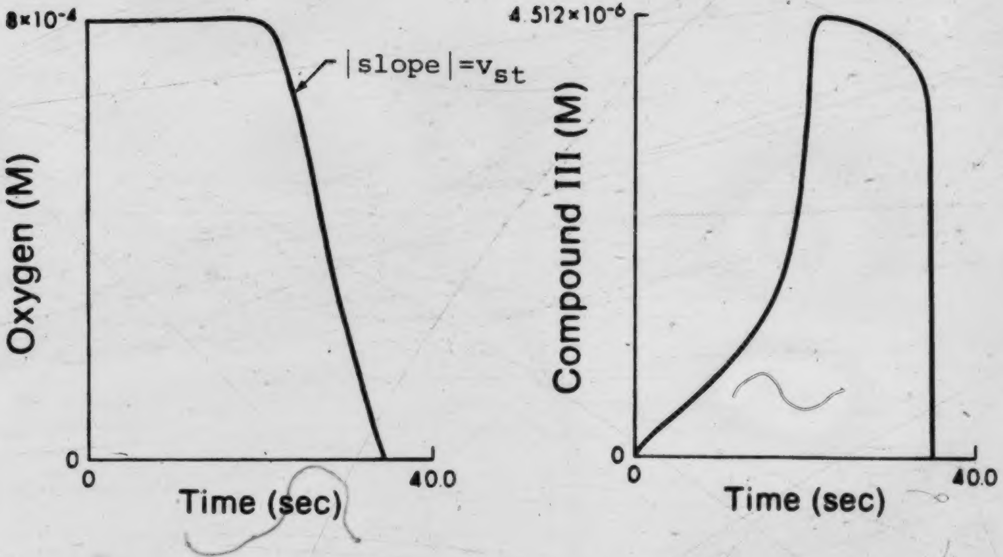

(a) **(b)**

Figure 5.9

A closed system is simulated by letting $k_{16}=k_{17}=0$ with the following initial species concentrations (M) : $[O_2]_0=[H_2O_2]_0=[NAD\cdot]_0=[O_2^-]_0=10^{-8}$, $[NADH]_0=10^{-3}$, $[Per^{3+}]_0=6.75\times10^{-6}$, $[CoII]_0=3\times10^{-8}$ and $[CoI]_0=[CoIII]_0=10^{-8}$. (a)-Time course of oxygen concentration showing an induction period and a steady rate (v_{st}) of oxygen consumption. (b)-Kinetics of compound III showing a rapid increase in its concentration during the oxygen induction period, a near steady state phase, and a rapid termination phase. The parameters used are : $k_{11}=2\times10^9M^{-1}s^{-1}$, $k_{12}'=5.9\times10^3M^{-1}s^{-1}$, $k_1=1.8\times10^7M^{-1}s^{-1}$, $k_2'=5.4\times10^3$, $k_3'=8\times10^2M^{-1}s^{-1}$, $k_{10}=1.9\times10^6M^{-1}s^{-1}$, $k_8=1.3\times10^8M^{-1}s^{-1}$, $k_{13}=10^4M^{-1}s^{-1}$. Reactions R_{12}, R_2 and R_3 involve NADH as a reactant and the corresponding rate constants given above are second order rate constants.

parameter values (given in the figure) are exactly those used by Yokota and Yamazaki(43) in their simulation except for the termination reaction R_{13}, missing in their model, whose rate constant was assigned the value of 10^4 $M^{-1}s^{-1}$. Compound III kinetics involves the following phases likewise observed in experiments (43,46): rapid increase, near 'steady-state' and fast termination. There is no pronounced initial burst because of the low initial concentration of H_2O_2, a feature that is consistent with experiment(46). We also observed that the duration of the induction time (see oxygen-concentration vs. time plot) is independent of the initial oxygen concentration. During the 'steady-state' phase of compound III kinetics, a steady rate of oxygen consumption occurs.

To show explicitly that there is an inhibition of the catalyzed reaction by oxygen, we determine from the oxygen concentration-vs-time plots the steady rates, v_{st}, of oxygen consumption for various initial oxygen concentrations (see figure 5.9a). The result is given in figure 5.10, curve *a*. There is one maximum in the curve which is one characteristic of substrate inhibition of an enzyme reaction. However, as was also observed experimentally by Degn, Olsen and Perram(42), the rate does not fall off to zero at increasing oxygen concentrations as does the rate in the classical substrate inhibition model (see figure 5.3).

The experimental results(42) showed that the peak of the curve is relatively higher than that shown by our model

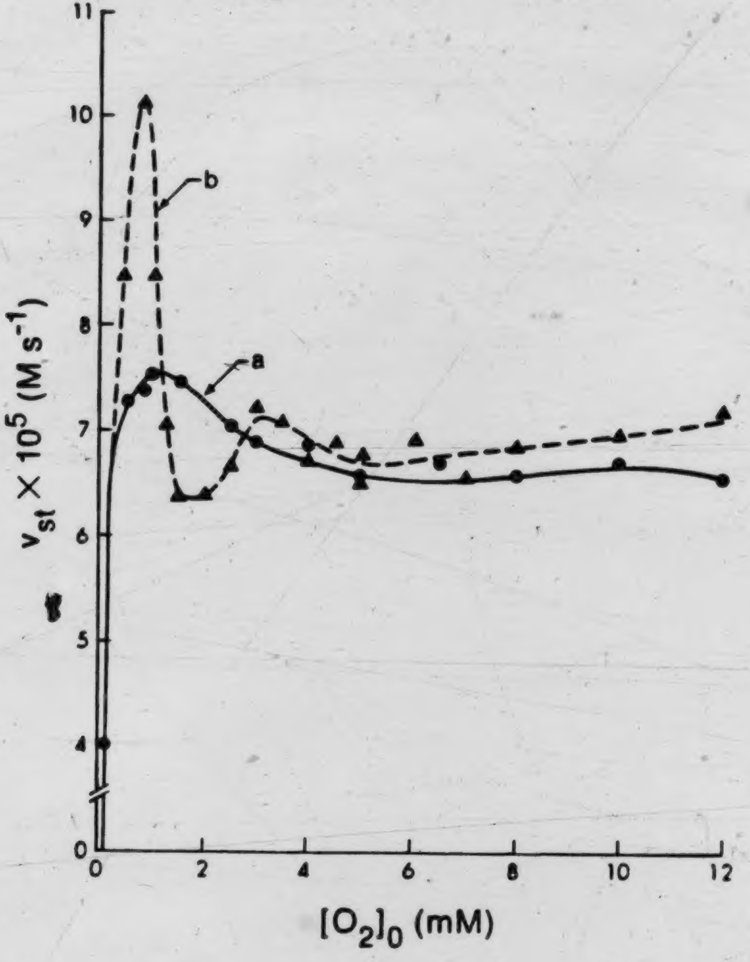

Figure 5.10

Steady rate of oxygen consumption, v_{st} , as a function of initial oxygen concentration for the peroxidase-oxidase reaction in a closed system.
Curve *a* : Simulated experiments exemplified by fig.5.9(a) were repeated for various initial oxygen concentrations and the corresponding v_{st} measured. The bistable model given in fig. 5.5 was used with $k_{16} = k_{17} = 0$ and the same parameters used in fig. 5.9.
Curve *(b)* : Reaction R_7 ($k_7 = 10^3 s^{-1}$) is included in the model and similar simulated experiments were done.

in fig. 5.10, curve *a*. This is probably due to the deletion of other reactions which have a quantitative effect on the simulations. For instance, when we add the slow reaction R_7 to our model we find a higher peak in the curve (see curve *b*). (The rate constant used for this reaction was 100 $M^{-1}s^{-1}$ as given in reference 57). This result can be explained by the higher degree of autocalysis with respect to the NAD· radical introduced by the extreme current E^{14} which will directly increase the rate of oxygen consumption via R_{11}.

Network Steady States vs. Experimental Bistability

Using curve *a* in figure 5.10, we can draw a line corresponding to the transport of oxygen, i.e. $v_{in} = k_{16}-k_{17}[O_2]$, that will intersect this curve at 3 points and therefore get 3 steady states for oxygen (see fig. 5.3). For example, a line characterized by the slope $(=-k_{17})$ of $-8x10^{-4}$ and intercept $(=k_{16})$ of $7.25x10^{-5}$ will do this. Using these values, as well as those already used in figure 5.10, no multiplicity of steady states for the network was found. Recall that we have defined a network steady state to be the state where all internal species are at steady state. It is very possible that there are states where not all but some of the species are at steady state. In fact, depending on the parameters which include the initial conditions, when a particular steady state has eigenvalues with very low magnitudes, that steady state (if stable) is approached very slowly. Laboratory observation time may not be sufficient for the system to reach the actual network steady state. The bistability demonstrated by the PO model and the bistability observed in the experiments will have to be further investigated to determine their correspondence.

F. Conclusions

A systematic way of determining the dominant steady state reaction pathways or extreme currents under bistable conditions had been presented and applied towards the modeling of the bistability observed in the peroxidase-oxidase reaction. The two essential ingredients in our approach are: (a) the structure of the current polytope Π_v showing how the extreme currents are coupled to each other, and (b) the necessary test given by the vanishing of $\alpha_\delta(h,j)$ for the existence of multiple steady states. Our modeling approach also, in effect, gave a convenient method for testing whether or not a given complex mechanism is capable of bistability or multiple steady states in general by looking at the 2-dimensional faces of Π_v.

It was proposed that for bistability or 3 steady states, there must be at least 3 extreme currents comprising a model network. Our model contains the minimum number of extreme currents found from a long list of elementary steps possibly involved in the PO reaction. The analysis of this model given in section E showed that it was able to reproduce several experimentally observed features like damped oscillations which occurred simultaneously with bistability, synchronous oscillation between oxygen and compound III, the characteristic phases of the kinetics in a closed system, and explicitly demonstrated the substrate-inhibition mechanism causing the bistability.

We also saw that three basic elements found both in the classical substrate-inhibition mechanism and in our model are sufficient to cause bistability, namely, (i) reversible flux of the inhibiting substrate, (ii) a catalytic cycle, and (iii) a substrate-inhibition pathway coupled to the catalytic cycle. The virtue of analyzing simpler model mechanisms was also shown.

The results presented here on the peroxidase-oxidase reaction are just a beginning, but a very encouraging one. A powerful technique in analyzing realistic complex networks that can identify the dominant pathways under multistable conditions is at hand. We can now confidently conclude that among the elementary processes that are known or postulated to be involved in the complex mechanism of the PO system, the necessary reaction pathways are indeed available to explain the bistability observed in the open system. It was not the purpose of this work to come up with some quantitative agreement with experiment - this goal is considered premature for the moment because of the lack of precise experimental data on the individual rate constants. Only a joint effort between the theoretician and the experimentalist can eventually achieve this ultimate goal.

Bibliography

(1) M. Feinberg, Lectures on Chemical Reaction Networks, Technical Report of the Mathematics Research Center, University of Wisconsin-Madison, 1980.

(2) M. Feinberg, in Dynamics and Modeling of Reactive Systems, ed. by W. Stewart, W.H. Ray and C. Cowley, Academic Press, New York, 1980, pp.59-130.

(3) G.R. Gavalas, Nonlinear Differential Equations of Chemically Reacting Systems, Springer-Verlag, New York, 1968.

(4) B.L. Clarke, Adv. Chem. Phys. 43, 1(1980).

(5) B.L. Clarke, in Studies in Physical and Theoretical Chemistry, ed. by R.B. King (Elsevier, Amsterdam, 1983), vol. 28, pp. 322-357.

(6) D. Wallwork and A. Perelson, J. Chem. Phys. 65, 284(1976).

(7) N. Ganapathisubramanian and K. Showalter, J. Chem. Phys. 80, 4177(1984).

(8) H.A. Liebhafsky and G.M. Roe, Int. J. Chem. Kinet. 11, 693(1979).

(9) B.L. Clarke, J. Chem. Phys. 75, 4970(1981).

(10) B.J. Edelstein, J. Theor. Biol. 29, 57(1970).

(11) B. von Hohenbalken, Math. Program. 15, 1(1978).

(12) M. Orban and I.R. Epstein, J. Am. Chem. Soc. 104, 5918(1982).

(13) F. Horn and R. Jackson, Arch. Rational Mech. Anal. 47, 81(1972).

(14) F.R. Gantmacher, Applications of the Theory of Matrices, Interscience, New York, 1959.

(15) M.W. Hirsch and S. Smale, Differential Equations, Dynamical Systems and Linear Algebra, Academic Press, New York, 1974.

(16) D. Shear, J. Chem. Phys. 48, 4144(1968).

(17) L. Glass, Proc. Nat. Acad. Sci. USA 72, 2856(1975).

(18) M. Golubitsky and D. Schaeffer, Comm. Pure App. Math. **32**, 21(1979).

(19) A.E.R. Woodcock and T. Poston, A Geometrical Study of the Elementary Catastrophes, Springer-Verlag, New York, 1974.

(20) M. Feinberg, Arch. Rational Mech. Anal. **49**, 187(1973).

(21) F. Horn, Arch. Rational Mech. Anal. **49**, 172(1973).

(22) M. Feinberg and F. Horn, Chem. Eng. Sci. **29**, 775(1974).

(23) F. Horn, Proc. R. Soc. London, Ser. A, **334**, 299(1973).

(24) F. Horn, Proc. R. Soc. London, Ser. A, **334**, 313(1973).

(25) F. Horn, Proc. R. Soc. London, Ser. A, **334**, 331(1973).

(26) R.J. Field, E. Koros and R.M. Noyes, J. Am. Chem. Soc. **94**, 8649(1972).

(27) CRC Handbook of Tables for Mathematics, 3rd ed., 1967, p.131.

(28) M. Golubitsky and W. Langford, 'Classification and Unfoldings of Degenerate Hopf Bifurcations', 1980 (preprint).

(29) R. Lefever and G. Nicolis, J. Theor. Biol. **30**, 267(1971).

(30) R.J. Field and R.M. Noyes, J. Chem. Phys. **60**, 1877(1974).

(31) M. Orban, C. Dateo, P. De Kepper and I. Epstein, J. Am. Chem. Soc. **104**, 5911(1982).

(32) V. Balakotaiah and D. Luss, Chem. Eng. Sci. **37**, 1611(1982).

(33) V. Balakotaiah and D. Luss, Chem. Eng. Commun. **13**, 111(1982).

(34) V. Balakotaiah and D. Luss, Chem. Eng. Sci. **37**, 433(1982).

(35) I. Stewart, Physica D **2**, 245(1981).

(36) A.C. Hearn, Reduce2 User's Manual, 2nd ed., University of Utah, Salt Lake City, 1973.

(37) M. Golubitsky, B. Keyfitz and D. Schaeffer, Comm. Pure

App. Math. **34**, 433(1981).

(38) M. Golubitsky and B. Keyfitz, SIAM J. Math. Anal. 11, 316(1980).

(39) B. Hassard, N. Kazarinoff and Y-H. Wan, Theory and Applications of Hopf Bifurcation, Cambridge U.P., London, 1981.

(40) T. Poston and I. Stewart, Taylor Expansions and Catastrophes, Pitman Pub., London, 1976.

(41) G. Iooss and D.D. Joseph, Elementary Stability and Bifurcation Theory, Springer-Verlag, New York, 1980.

(42) H. Degn, L. Olsen and J.Perram, Ann. N.Y. Acad. Sci. **316**, 623(1979).

(43) K. Yokota and I. Yamazaki, Biochem. **16**, 1913(1977).

(44) V.R. Fed'kina, F.I. Ataullakhanov and T.I. Bronnikova, Biophys. Chem. **19**, 259(1984).

(45) H. Degn and D. Mayer,Biochim. Biophys. Acta **180**, 291(1969).

(46) V.R. Fed'kina, F.I. Ataullakhanov, T.V. Bronnikova and N.K. Balabaev, Stud. Biophys. 72, 195(1978).

(47) L.F. Olsen and H. Degn, Biochim. Biophys. Acta **523**, 321(1978).

(48) L.F. Olsen, Phys. Lett. **94A**, 454(1983).

(49) L.F. Olsen, in Stochastic Phenomena and Chaotic Behaviour in Complex Systems, edited by P. Schuster(Springer-Verlag, Berlin,1984), p.116.

(50) L.J. Aarons and B.F. Gray, Chem. Soc. Rev. **5**, 359(1976).

(51) A. Lotka, J. Phys. Chem. **14**, 271(1910).

(52) I. Yamazaki and L. Piette, Biochim. Biophys. Acta **77**, 47(1963).

(53) I. Yamazaki, K. Yokota and R. Nakajima, Biochem. Biophys. Res. Commun. **21**, 582(1965).

(54) I. Yamazaki and K. Yokota, Biochim. Biophys. Acta **132**, 310(1967).

(55) I. Yamazaki and K. Yokota, Molec. Cell. Biochem. **2**,39(1973).

(56) H. Degn, Biochim. Biophys. Acta 180, 271(1969).

(57) K. Yokota and I. Yamazaki, Biochim. Biophys. Acta 105, 301(1965).

(58) L.F. Olsen, Biochim. Biophys. Acta 527, 212(1978).

(59) E.J. Land and A.J. Swallow, Biochim. Biophys. Acta 234, 34(1971).

(60) V.R. Fed'kina, T.V. Bronnikova and F.I. Ataullakhanov, Stud. Biophys. 82, 159(1981).

(61) H. Degn, Nature 217, 1047(1968).

(62) J.V. Uspensky, Theory of Equations, McGraw-Hill, New York, 1948.

APPENDIX A

Details in the Derivation of Equation (2.23)

Each component of the nxn matrix **D** in equation (2.21) is a vector in R^n. The i-th row of **D** can be expressed as

$$\mathbf{D}_i = (\text{diag } 1/\mathbf{X}^\circ)\nu(\text{diag } \mathbf{v}^\circ)\{(\text{diag } \kappa'_i)\kappa' - \kappa'\mathbf{R}[i]\}$$

where κ'_i is the i-th row of κ and the matrix **R**[i] is a nxn matrix defined as

$$\mathbf{R}[i] = \begin{cases} R_{ii} = 1 \\ R_{nm} = 0 \text{ , } n \neq i \text{ or } m \neq i \text{ .} \end{cases}$$

We then find that

$$\begin{aligned} \Sigma\, \zeta_i \mathbf{D}_i &= (\text{diag } 1/\mathbf{X}^\circ)\nu(\text{diag } \mathbf{v}^\circ)\{\ \Sigma\, \zeta(\text{diag } \kappa'_i)\kappa' \\ &\qquad - \kappa'\Sigma\, \zeta_i \mathbf{R}[i]\} \\ &= (\text{diag } 1/\mathbf{X}^\circ)\nu(\text{diag } \mathbf{v}^\circ)\{(\text{diag } \kappa'\zeta)\kappa' - \kappa'(\text{diag } \zeta)\} \end{aligned}$$

and since

$$\zeta'\mathbf{D}\zeta = (\ \Sigma\, \zeta_i \mathbf{D}_i)\zeta$$

we finally have

$$\zeta = (\text{diag } 1/\mathbf{X}^\circ)\nu(\text{diag } \mathbf{v}^\circ)\{\kappa' - (1/2)\kappa'(\text{diag } \zeta)$$

$$+(1/2)(\mathrm{diag}\ \kappa'\zeta)\kappa'\} \ . \qquad (2.23)$$

APPENDIX B

On the Poincare-Hopf Theorem

The index I of a hyperbolic steady state is defined by

$$I = (-1)^{\sigma}$$

where σ is the number of eigenvalues with negative real parts. The Poincare-Hopf Theorem states that

$$\Sigma I = \chi(M) \tag{B.1}$$

where the summation is over all the steady states of a dynamical system defined on a manifold M, and $\chi(M)$ is the Euler-Poincare characteristic of M. For example, an n-sphere defined by ΣX_i^2 = constant (summation from i = 1 to n+1), has

$$\chi(M) = 1 + (-1)^n . \tag{B.2}$$

Glass[17] argues that the dynamical system corresponding to a network $N \epsilon N_{nee}$ can be mapped onto n-spheres by first associating the boundary of concentration space with a single unstable 'source' (steady state) at the south pole. Equations (B.1) and (B.2) then give

$$\sum_{j=1}^{m} (-1)^{\sigma_j} = 1 + (-1)^n \; . \qquad (B.3)$$

For the j-th steady state, there are n eigenvalues, that is

$$n = \sigma_j + \pi_j$$

where π_j is the number of eigenvalues with positive real parts. Thus,

$$(-1)^{\sigma_j} = (-1)^n(-1)^{\pi_j}$$

and letting the m-th steady state as the unstable south pole (i.e. $\sigma_m=0$), equation (B.3) becomes

$$\sum_{j=1}^{\rho} (-1)^{\pi_j} = 1. \qquad (2.47)$$

We have let ρ be the total number of steady states. Note that the 'artificial' unstable south pole is not included in ρ.

APPENDIX C

Roots of a Cubic Polynomial

The following information is provided by reference 27. An explicit expression for the three roots of the cubic

$$f_3(X') = (X')^3+\rho_1 X'+\rho_0 = 0 \qquad (C.1)$$

in terms of the parameters ρ_0 and ρ_1 can be found using the following trigonometric identity:

$$4\cos^3\theta - 3\cos\theta - \cos(3\theta) \equiv 0. \qquad (C.2)$$

Letting $X' = m\cos\theta$, (C.1) becomes

$$f_3(X') = m^3\cos^3\theta+\rho_1 m\cos\theta+\rho_0 = 0\ . \qquad (C.3)$$

Comparing this, term by term, with (C.2),

$$4/(m^3) = -3/(\rho_1 m) = -\cos(3\theta)/\rho_0$$

from which it follows that

$$m = 2(-\rho_1/3)^{1/2} \quad \text{and} \quad \cos(3\theta) = 3\rho_0/(\rho_1 m)\ . \qquad (C.4)$$

Any solution θ_1 which satisfies (C.4) will also have solutions $[\theta_1 + (2\pi/3)]$ and $[\theta_1 + (4\pi/3)]$. Thus the three roots of (C.1) are

$$\begin{aligned} X'^{(1)} &= 2(-\rho_1/3)^{1/2}\cos(\theta) \\ X'^{(2)} &= 2(-\rho_1/3)^{1/2}\cos[\theta+(2\pi/3)] \\ X'^{(3)} &= 2(-\rho_1/3)^{1/2}\cos[\theta+(4\pi/3)] \end{aligned} \qquad (C.5)$$

where θ is given implicitly as a function of ρ_0 and ρ_1 by (C.4).

APPENDIX D

Equation of the line L_c (eq.3.13)

The characteristic polynomial for d=3 is

$$P(\lambda) = \lambda^3+\alpha_1\lambda^2+\alpha_2\lambda+\alpha_3 = 0 \ . \tag{D.1}$$

Using the transformation given by eq.(3.5), this polynomial becomes

$$P(\lambda') = (\lambda')^3+\rho_1\lambda'+\rho_0 = 0. \tag{D.2}$$

Complex conjugate roots of (D.1) occur only outside the cusp curve Σ^0 (i.e. $K_3 = 4\rho_1{}^3+27\rho_0{}^2 > 0$). Denote this region Λ. For $\rho=(\rho_0,\rho_1) \in \Lambda$, let the real root be λ_1, and the complex pair be λ_2,λ_2* where $\lambda_2 = a+bi$, $b>0$. Then

$$\begin{aligned} P(\lambda) &= (\lambda-\lambda_1)(\lambda-\lambda_2)(\lambda-\lambda_2*) \\ &= \lambda^3-(2a+\lambda_1)\lambda^2+(a^2+b^2+2a\lambda_1)\lambda-(a^2+b^2)\lambda \\ &= 0. \end{aligned} \tag{D.3}$$

Comparing (D.1) and (D.3), we have

$$\begin{aligned} \alpha_1 &= -(2a+\lambda_1) \\ \alpha_2 &= a^2+b^2+2a\lambda_1 \\ \alpha_3 &= -(a^2+b^2)\lambda_1 \ . \end{aligned} \tag{D.4}$$

Eliminating λ_1 and b from (D.4), the implicit expression for a in terms of $\alpha = (\alpha_1, \alpha_2, \alpha_3) \in R^3$ is

$$f(a,\alpha) = a^3+\alpha_1 a^2+(1/4)(\alpha_1^2+\alpha_2)a+(1/8)(\alpha_1\alpha_2-\alpha_3) = 0 \quad (D.5)$$

with $\rho(\alpha) \in \Lambda$, and the desired root a is real.

Now, find the regions in α-space where $a>0$. Letting

$$\begin{aligned} a' &= a+(\alpha_1/3) \\ \delta_1 &= \rho_1/4 \qquad (D.6) \\ \delta_0 &= -\rho_0/8 \end{aligned}$$

we get

$$f(a') = (a')^3+\delta_1 a'+\delta_0 = 0 . \quad (D.7)$$

Because δ_1 and δ_0 are linearly related to ρ_1 and ρ_0, respectively, the regions where f(a) has 3,2,1 or 0 real and positive roots are easily plotted on the ρ_1-ρ_0 plane. Note that the cusp curve associated with f(a')=0 (i.e. $K_3^\delta = 4\delta_1^3+27\delta_0^2 = 0$) is mapped onto the cusp curve associated with $P(\lambda')=0$ (i.e. $K_3^\rho = 4\rho_1^3+27\rho_0^2 = 0$); in fact, we have

$$K_3^\delta = K_3^\rho/64 . \quad (D.8)$$

The line that corresponds to $\delta_0=0$ on the δ_1-δ_0 plane has the equation

$$L_\delta: \qquad \delta_1 = -(3/\alpha_1)\delta_0 - (\alpha_1/3)^2 \qquad \text{(D.8)}$$

and using (D.6), we finally get

$$L_c: \qquad \rho_1 = (3/2\alpha_1)\rho_0 - 4(\alpha_1/3)^2 \qquad \text{(D.9)}$$

APPENDIX E

The Hopf Bifurcation Theorem

According to the Hopf Bifurcation Theorem(39), there are 4 requirements for a given vector field $d\mathbf{X}/dt = \mathbf{F}(\mathbf{X},\mu)$ to possess Hopf bifurcation points. Let $(\mathbf{X},\mu)=(0,0) \in R^n_+ x R$ be a steady state. These requirements are:

(a) $\mathbf{F}(\mathbf{0},\mu)=0$ for μ in an open interval containing 0, and $\mathbf{0} \in R^n_+$ is an isolated steady state of $\mathbf{F}$,

(b) $\mathbf{F}$ is analytic in $\mathbf{X}$ and μ in a neighborhood of $(\mathbf{0},0)$ in $R^n_+ x R$,

(c) $\mathbf{M}(\mu) \equiv d_X \mathbf{F}(0,0)$ has a pair of complex conjugate eigenvalues λ and λ^* such that

$$\lambda(\mu) = a(\mu)+ib(\mu)$$

where

$b(0)>0$, $a(0)=0$ and $da/d\mu(0) \neq 0$.

(d) The remaining $(n-2)$ eigenvalues of $\mathbf{M}(0)$ have strictly negative real parts.

APPENDIX F

Calculation of β_3^C

The slope of the line $L(\rho_2,\beta_3)$ at the cusp points $(\pm\rho_1^C,\rho_0^C)$ is equal to $(-\beta_3^C/4)$ as given by equation (3.23) (see figure 3.13f). The line $L(\rho_2,\beta_3^C)$ satisfies

$$\rho_0 = -\rho_1(\beta_3^C/4)-\rho_2(\beta_3^C/4)^2-(\beta_3^C/4)^4 .$$

From (3.21), for $\rho_2\leq 0$,

$$\rho_0^C = -(\rho_2)^2/12 \text{ and } \pm\rho_1^C = \mp(2/9)\rho_2[-6\rho_2]^{1/2}.$$

Hence,

$$(\beta_3^C/4)^4+\rho_2(\beta_3^C/4)^2\mp(2/9)\rho_2[-6\rho_2]^{1/2}(\beta_3^C/4)-(\rho_2)^2/12 = 0. \tag{F.1}$$

where the (-) sign is used if $\beta_3^C>0$ and the (+) sign if $\beta_3^C<0$.

APPENDIX G

Faces of the Current Polytope Π_v for the Peroxidase-Oxidase Mechanism given in Table V.2

1-FACES: 90

1	2
1	3
1	4
1	5
1	6
1	7
1	9
1	11
1	12
1	15
2	3
2	4
2	7
2	8
2	9
2	10
2	11
2	12
2	15
3	4
3	5
3	6
3	7
3	8
3	9
3	10
3	11
3	12
3	13
3	14
3	15
3	16
3	17
4	5
4	6
4	7
4	8
4	9
4	10
4	11
4	12
4	13
4	14
4	15
5	6
5	7
5	8
5	9
5	13
5	14
5	15
6	7
6	9
6	10
6	15
6	16
6	17
7	8
7	9
7	10
7	11
7	13
7	16
8	9
8	10
8	13
8	14
8	15
9	10
9	12
9	14
9	17
10	15
10	16
10	17
11	12
11	13
11	15
11	16
12	14
12	15
12	17
13	14
13	15
13	16
14	15
14	17
15	16
15	17
16	17

2-FACES: 233

```
 1  2  3
 1  2  4
 1  2  5   8
 1  2  6  10
 1  2  7
 1  2  9
 1  2 11
 1  2 12
 1  2 15
 1  3  4
 1  3  5
 1  3  6
 1  3  7
 1  3  9
 1  3 11
 1  3 12
 1  3 15
 1  4  5
 1  4  6
 1  4  7
 1  4  9
 1  4 11
 1  4 12
 1  4 15
 1  5  6
 1  5  7
 1  5  9
 1  5 11  13
 1  5 12  14
 1  5 15
 1  6  7
 1  6  9
 1  6 11  16
 1  6 12  17
 1  6 15
 1  7  9
 1  7 11
 1  9 12
 1 11 12
 1 11 15
 1 12 15
 2  3  4
 2  3  7
 2  3  8
 2  3  9
 2  3 10
 2  3 11
 2  3 12
 2  3 15
```

```
 2  4  7
 2  4  8
 2  4  9
 2  4 10
 2  4 11
 2  4 12
 2  4 15
 2  7  8
 2  7  9
 2  7 10
 2  7 11
 2  8  9
 2  8 10
 2  8 11  13
 2  8 12  14
 2  8 15
 2  9 10
 2  9 12
 2 10 11  16
 2 10 12  17
 2 10 15
 2 11 12
 2 11 15
 2 12 15
 3  4  5
 3  4  6
 3  4  7
 3  4  8
 3  4  9
 3  4 10
 3  4 11
 3  4 12
 3  4 13
 3  4 14
 3  4 15
 3  5  6
 3  5  7
 3  5  8
 3  5  9
 3  5 13
 3  5 14
 3  5 15
 3  6  7
 3  6  9
 3  6 10
 3  6 15
 3  6 16
 3  6 17
 3  7  8
```

3 7 9
3 7 10
3 7 11
3 7 13
3 7 16
3 8 9
3 8 10
3 8 13
3 8 14
3 8 15
3 9 10
3 9 12
3 9 14
3 9 17
3 10 15
3 10 16
3 10 17
3 11 12
3 11 13
3 11 15
3 11 16
3 12 14
3 12 15
3 12 17
3 13 14
3 13 15
3 13 16
3 14 15
3 14 17
3 15 16
3 15 17
3 16 17
4 5 6
4 5 7
4 5 8
4 5 9
4 5 13
4 5 14
4 5 15
4 6 7
4 6 9
4 6 10
4 6 15
4 7 8
4 7 9
4 7 10
4 7 11
4 7 13
4 7 15 16
4 8 9
4 8 10
4 8 13
4 8 14
4 8 15
4 9 10
4 9 12
4 9 14
4 9 15 17
4 10 15
4 11 12
4 11 13
4 11 15
4 12 14
4 12 15
4 13 14
4 13 15
4 14 15
5 6 7
5 6 8 10
5 6 9
5 6 13 16
5 6 14 17
5 6 15
5 7 8
5 7 9
5 7 13
5 8 9
5 8 13
5 8 14
5 8 15
5 9 14
5 13 14
5 13 15
5 14 15
6 7 9
6 7 10
6 7 16
6 9 10
6 9 17
6 10 15
6 10 16
6 10 17
6 15 16
6 15 17
6 16 17
7 8 9
7 8 10
7 8 13
7 9 10
7 9 11 12
7 9 13 14
7 9 16 17

```
 7  10  16
 7  11  13
 7  11  16
 7  13  16
 8   9  10
 8   9  14
 8  10  13  16
 8  10  14  17
 8  10  15
 8  13  14
 8  13  15
 8  14  15
 9  10  17
 9  12  14
 9  12  17
 9  14  17
10  15  16
10  15  17
10  16  17
11  12  13  14
11  12  15
11  12  16  17
11  13  15
11  13  16
11  15  16
12  14  15
12  14  17
12  15  17
13  14  15
13  14  16  17
13  15  16
14  15  17
15  16  17


3-FACES: 346

1   2   3   4
1   2   3   5   8
1   2   3   6  10
1   2   3   7
1   2   3   9
1   2   3  11
1   2   3  12
1   2   3  15
1   2   4   5   8
1   2   4   6  10
1   2   4   7
1   2   4   9

1   2   4  11
1   2   4  12
1   2   4  15
1   2   5   6   8  10
1   2   5   7   8
1   2   5   9   8
1   2   5  11   8  13
1   2   5  12   8  14
1   2   5  15   8
1   2   6   7  10
1   2   6   9  10
1   2   6  11  10  16
```

```
 1  2  6 12 10 17
 1  2  6 15 10
 1  2  7  9
 1  2  7 11
 1  2  9 12
 1  2 11 12
 1  2 11 15
 1  2 12 15
 1  3  4  5
 1  3  4  6
 1  3  4  7
 1  3  4  9
 1  3  4 11
 1  3  4 12
 1  3  4 15
 1  3  5  6
 1  3  5  7
 1  3  5  9
 1  3  5 11 13
 1  3  5 12 14
 1  3  5 15
 1  3  6  7
 1  3  6  9
 1  3  6 11 16
 1  3  6 12 17
 1  3  6 15
 1  3  7  9
 1  3  7 11
 1  3  9 12
 1  3 11 12
 1  3 11 15
 1  3 12 15
 1  4  5  6
 1  4  5  7
 1  4  5  9
 1  4  5 11 13
 1  4  5 12 14
 1  4  5 15
 1  4  6  7
 1  4  6  9
 1  4  6 15
 1  4  7  9
 1  4  7 11
 1  4  9 12
 1  4 11 12
 1  4 11 15
 1  4 12 15
 1  5  6  7
 1  5  6  9
 1  5  6 11 13 16
 1  5  6 12 14 17
 1  5  6 15
 1  5  7  9
 1  5  7 11 13
 1  5  9 12 14
 1  5 11 12 13 14
 1  5 11 15 13
 1  5 12 15 14
 1  6  7  9
 1  6  7 11 16
 1  6  9 12 17
 1  6 11 12 16 17
 1  6 11 15 16
 1  6 12 15 17
 1  7  9 11 12
 1 11 12 15
 2  3  4  7
 2  3  4  8
 2  3  4  9
 2  3  4 10
 2  3  4 11
 2  3  4 12
 2  3  4 15
 2  3  7  8
 2  3  7  9
 2  3  7 10
 2  3  7 11
 2  3  8  9
 2  3  8 10
 2  3  8 11 13
 2  3  8 12 14
 2  3  8 15
 2  3  9 10
 2  3  9 12
 2  3 10 11 16
 2  3 10 12 17
 2  3 10 15
 2  3 11 12
 2  3 11 15
 2  3 12 15
 2  4  7  8
 2  4  7  9
 2  4  7 10
 2  4  7 11
 2  4  8  9
 2  4  8 10
 2  4  8 11 13
 2  4  8 12 14
 2  4  8 15
 2  4  9 10
 2  4  9 12
 2  4 10 15
 2  4 11 12
 2  4 11 15
```

```
2  4 12 15
2  7  8  9
2  7  8 10
2  7  8 11 13
2  7  9 10
2  7  9 11 12
2  7 10 11 16
2  8  9 10
2  8  9 12 14
2  8 10 11 13 16
2  8 10 12 14 17
2  8 10 15
2  8 11 12 13 14
2  8 11 15 13
2  8 12 15 14
2  9 10 12 17
2 10 11 12 16 17
2 10 11 15 16
2 10 12 15 17
2 11 12 15
3  4  5  6
3  4  5  7
3  4  5  8
3  4  5  9
3  4  5 13
3  4  5 14
3  4  5 15
3  4  6  7
3  4  6  9
3  4  6 10
3  4  6 15
3  4  7  8
3  4  7  9
3  4  7 10
3  4  7 11
3  4  7 13
3  4  7 15 16
3  4  8  9
3  4  8 10
3  4  8 13
3  4  8 14
3  4  8 15
3  4  9 10
3  4  9 12
3  4  9 14
3  4  9 15 17
3  4 10 15
3  4 11 12
3  4 11 13
3  4 11 15
3  4 12 14
3  4 12 15
```

```
3  4 13 14
3  4 13 15
3  4 14 15
3  5  6  7
3  5  6  8 10
3  5  6  9
3  5  6 13 16
3  5  6 14 17
3  5  6 15
3  5  7  8
3  5  7  9
3  5  7 13
3  5  8  9
3  5  8 13
3  5  8 14
3  5  8 15
3  5  9 14
3  5 13 14
3  5 13 15
3  5 14 15
3  6  7  9
3  6  7 10
3  6  7 16
3  6  9 10
3  6  9 17
3  6 10 15
3  6 10 16
3  6 10 17
3  6 15 16
3  6 15 17
3  6 16 17
3  7  8  9
3  7  8 10
3  7  8 13
3  7  9 10
3  7  9 11 12
3  7  9 13 14
3  7  9 16 17
3  7 10 16
3  7 11 13
3  7 11 16
3  7 13 16
3  8  9 10
3  8  9 14
3  8 10 13 16
3  8 10 14 17
3  8 10 15
3  8 13 14
3  8 13 15
3  8 14 15
3  9 10 17
3  9 12 14
```

```
3  9 12 17
3  9 14 17
3 10 15 16
3 10 15 17
3 10 16 17
3 11 12 13 14
3 11 12 15
3 11 12 16 17
3 11 13 15
3 11 13 16
3 11 15 16
3 12 14 15
3 12 14 17
3 12 15 17
3 13 14 15
3 13 14 16 17
3 13 15 16
3 14 15 17
3 15 16 17
4  5  6  7
4  5  6  8 10
4  5  6  9
4  5  6 15
4  5  7  8
4  5  7  9
4  5  7 13
4  5  8  9
4  5  8 13
4  5  8 14
4  5  8 15
4  5  9 14
4  5 13 14
4  5 13 15
4  5 14 15
4  6  7  9
4  6  7 10
4  6  7 15 16
4  6  9 10
4  6  9 15 17
4  6 10 15
4  7  8  9
4  7  8 10
4  7  8 13
4  7  9 10
4  7  9 11 12
4  7  9 13 14
4  7  9 15 16 17
4  7 10 15 16
4  7 11 13
4  7 11 15 16
4  7 13 15 16
4  8  9 10
```

```
4  8  9 14
4  8 10 15
4  8 13 14
4  8 13 15
4  8 14 15
4  9 10 15 17
4  9 12 14
4  9 12 15 17
4  9 14 15 17
4 11 12 13 14
4 11 12 15
4 11 13 15
4 12 14 15
4 13 14 15
5  6  7  8 10
5  6  7  9
5  6  7 13 16
5  6  8  9 10
5  6  8 13 10 16
5  6  8 14 10 17
5  6  8 15 10
5  6  9 14 17
5  6 13 14 16 17
5  6 13 15 16
5  6 14 15 17
5  7  8  9
5  7  8 13
5  7  9 13 14
5  8  9 14
5  8 13 14
5  8 13 15
5  8 14 15
5 13 14 15
6  7  9 10
6  7  9 16 17
6  7 10 16
6  9 10 17
6 10 15 16
6 10 15 17
6 10 16 17
6 15 16 17
7  8  9 10
7  8  9 13 14
7  8 10 13 16
7  9 10 16 17
7  9 11 13 12 14
7  9 11 16 12 17
7  9 13 16 14 17
7 11 13 16
8  9 10 14 17
8 10 13 14 16 17
8 10 13 15 16
```

```
 8 10 14 15 17
 8 13 14 15
 9 12 14 17
10 15 16 17
11 12 13 15 14
11 12 13 16 14 17
11 12 15 16 17
11 13 15 16
12 14 15 17
13 14 15 16 17


4-FACES: 315

 1  2  3  4  5  8
 1  2  3  4  6 10
 1  2  3  4  7
 1  2  3  4  9
 1  2  3  4 11
 1  2  3  4 12
 1  2  3  4 15
 1  2  3  5  6  8 10
 1  2  3  5  7  8
 1  2  3  5  9  8
 1  2  3  5 11  8 13
 1  2  3  5 12  8 14
 1  2  3  5 15  8
 1  2  3  6  7 10
 1  2  3  6  9 10
 1  2  3  6 11 10 16
 1  2  3  6 12 10 17
 1  2  3  6 15 10
 1  2  3  7  9
 1  2  3  7 11
 1  2  3  9 12
 1  2  3 11 12
 1  2  3 11 15
 1  2  3 12 15
 1  2  4  5  6  8 10
 1  2  4  5  7  8
 1  2  4  5  9  8
 1  2  4  5 11  8 13
 1  2  4  5 12  8 14
 1  2  4  5 15  8
 1  2  4  6  7 10
 1  2  4  6  9 10
 1  2  4  6 15 10
 1  2  4  7  9
 1  2  4  7 11
 1  2  4  9 12
```

```
 1  2  4 11 12
 1  2  4 11 15
 1  2  4 12 15
 1  2  5  6  7  8 10
 1  2  5  6  9  8 10
 1  2  5  6 11  8 10 13 16
 1  2  5  6 12  8 10 14 17
 1  2  5  6 15  8 10
 1  2  5  7  9  8
 1  2  5  7 11  8 13
 1  2  5  9 12  8 14
 1  2  5 11 12  8 13 14
 1  2  5 11 15  8 13
 1  2  5 12 15  8 14
 1  2  6  7  9 10
 1  2  6  7 11 10 16
 1  2  6  9 12 10 17
 1  2  6 11 12 10 16 17
 1  2  6 11 15 10 16
 1  2  6 12 15 10 17
 1  2  7  9 11 12
 1  2 11 12 15
 1  3  4  5  6
 1  3  4  5  7
 1  3  4  5  9
 1  3  4  5 11 13
 1  3  4  5 12 14
 1  3  4  5 15
 1  3  4  6  7
 1  3  4  6  9
 1  3  4  6 15
 1  3  4  7  9
 1  3  4  7 11
 1  3  4  9 12
 1  3  4 11 12
 1  3  4 11 15
 1  3  4 12 15
 1  3  5  6  7
 1  3  5  6  9
 1  3  5  6 11 13 16
 1  3  5  6 12 14 17
 1  3  5  6 15
 1  3  5  7  9
 1  3  5  7 11 13
 1  3  5  9 12 14
 1  3  5 11 12 13 14
 1  3  5 11 15 13
 1  3  5 12 15 14
 1  3  6  7  9
 1  3  6  7 11 16
 1  3  6  9 12 17
 1  3  6 11 12 16 17
 1  3  6 11 15 16
 1  3  6 12 15 17
 1  3  7  9 11 12
 1  3 11 12 15
 1  4  5  6  7
 1  4  5  6  9
 1  4  5  6 15
 1  4  5  7  9
 1  4  5  7 11 13
 1  4  5  9 12 14
 1  4  5 11 12 13 14
 1  4  5 11 15 13
 1  4  5 12 15 14
 1  4  6  7  9
 1  4  6  7 11 15 16
 1  4  6  9 12 15 17
 1  4  7  9 11 12
 1  4 11 12 15
 1  5  6  7  9
 1  5  6  7 11 13 16
 1  5  6  9 12 14 17
 1  5  6 11 12 13 14 16 17
 1  5  6 11 15 13 16
 1  5  6 12 15 14 17
 1  5  7  9 11 12 13 14
 1  5 11 12 15 13 14
 1  6  7  9 11 12 16 17
 1  6 11 12 15 16 17
 2  3  4  7  8
 2  3  4  7  9
 2  3  4  7 10
 2  3  4  7 11
 2  3  4  8  9
 2  3  4  8 10
 2  3  4  8 11 13
 2  3  4  8 12 14
```

```
 2  3  4  8 15
 2  3  4  9 10
 2  3  4  9 12
 2  3  4 10 15
 2  3  4 11 12
 2  3  4 11 15
 2  3  4 12 15
 2  3  7  8  9
 2  3  7  8 10
 2  3  7  8 11 13
 2  3  7  9 10
 2  3  7  9 11 12
 2  3  7 10 11 16
 2  3  8  9 10
 2  3  8  9 12 14
 2  3  8 10 11 13 16
 2  3  8 10 12 14 17
 2  3  8 10 15
 2  3  8 11 12 13 14
 2  3  8 11 15 13
 2  3  8 12 15 14
 2  3  9 10 12 17
 2  3 10 11 12 16 17
 2  3 10 11 15 16
 2  3 10 12 15 17
 2  3 11 12 15
 2  4  7  8  9
 2  4  7  8 10
 2  4  7  8 11 13
 2  4  7  9 10
 2  4  7  9 11 12
 2  4  7 10 11 15 16
 2  4  8  9 10
 2  4  8  9 12 14
 2  4  8 10 15
 2  4  8 11 12 13 14
 2  4  8 11 15 13
 2  4  8 12 15 14
 2  4  9 10 12 15 17
 2  4 11 12 15
 2  7  8  9 10
 2  7  8  9 11 12 13 14
 2  7  8 10 11 13 16
 2  7  9 10 11 12 16 17
 2  8  9 10 12 14 17
 2  8 10 11 12 13 14 16 17
 2  8 10 11 15 13 16
 2  8 10 12 15 14 17
 2  8 11 12 15 13 14
 2 10 11 12 15 16 17
 3  4  5  6  7
 3  4  5  6  8 10
```

```
3  4  5  6  9
3  4  5  6 15
3  4  5  7  8
3  4  5  7  9
3  4  5  7 13
3  4  5  8  9
3  4  5  8 13
3  4  5  8 14
3  4  5  8 15
3  4  5  9 14
3  4  5 13 14
3  4  5 13 15
3  4  5 14 15
3  4  6  7  9
3  4  6  7 10
3  4  6  7 15 16
3  4  6  9 10
3  4  6  9 15 17
3  4  6 10 15
3  4  7  8  9
3  4  7  8 10
3  4  7  8 13
3  4  7  9 10
3  4  7  9 11 12
3  4  7  9 13 14
3  4  7  9 15 16 17
3  4  7 10 15 16
3  4  7 11 13
3  4  7 11 15 16
3  4  7 13 15 16
3  4  8  9 10
3  4  8  9 14
3  4  8 10 15
3  4  8 13 14
3  4  8 13 15
3  4  8 14 15
3  4  9 10 15 17
3  4  9 12 14
3  4  9 12 15 17
3  4  9 14 15 17
3  4 11 12 13 14
3  4 11 12 15
3  4 11 13 15
3  4 12 14 15
3  4 13 14 15
3  5  6  7  8 10
3  5  6  7  9
3  5  6  7 13 16
3  5  6  8  9 10
3  5  6  8 13 10 16
3  5  6  8 14 10 17
3  5  6  8 15 10
```

```
3  5  6  9 14 17
3  5  6 13 14 16 17
3  5  6 13 15 16
3  5  6 14 15 17
3  5  7  8  9
3  5  7  8 13
3  5  7  9 13 14
3  5  8  9 14
3  5  8 13 14
3  5  8 13 15
3  5  8 14 15
3  5 13 14 15
3  6  7  9 10
3  6  7  9 16 17
3  6  7 10 16
3  6  9 10 17
3  6 10 15 16
3  6 10 15 17
3  6 10 16 17
3  6 15 16 17
3  7  8  9 10
3  7  8  9 13 14
3  7  8 10 13 16
3  7  9 10 16 17
3  7  9 11 13 12 14
3  7  9 11 16 12 17
3  7  9 13 16 14 17
3  7 11 13 16
3  8  9 10 14 17
3  8 10 13 14 16 17
3  8 10 13 15 16
3  8 10 14 15 17
3  8 13 14 15
3  9 12 14 17
3 10 15 16 17
3 11 12 13 15 14
3 11 12 13 16 14 17
3 11 12 15 16 17
3 11 13 15 16
3 12 14 15 17
3 13 14 15 16 17
4  5  6  7  8 10
4  5  6  7  9
4  5  6  7 13 15 16
4  5  6  8  9 10
4  5  6  8 15 10
4  5  6  9 14 15 17
4  5  7  8  9
4  5  7  8 13
4  5  7  9 13 14
4  5  8  9 14
4  5  8 13 14
```

```
 4  5  8 13 15
 4  5  8 14 15
 4  5 13 14 15
 4  6  7  9 10
 4  6  7  9 15 16 17
 4  6  7 10 15 16
 4  6  9 10 15 17
 4  7  8  9 10
 4  7  8  9 13 14
 4  7  8 10 13 15 16
 4  7  9 10 15 16 17
 4  7  9 11 13 12 14
 4  7  9 11 15 12 16 17
 4  7  9 13 15 14 16 17
 4  7 11 13 15 16
 4  8  9 10 14 15 17
 4  8 13 14 15
 4  9 12 14 15 17
 4 11 12 13 15 14
 5  6  7  8  9 10
 5  6  7  8 13 10 16
 5  6  7  9 13 14 16 17
 5  6  8  9 14 10 17
 5  6  8 13 14 10 16 17
 5  6  8 13 15 10 16
 5  6  8 14 15 10 17
 5  6 13 14 15 16 17
 5  7  8  9 13 14
 5  8 13 14 15
 6  7  9 10 16 17
 6 10 15 16 17
 7  8  9 10 13 14 16 17
 7  9 11 13 16 12 14 17
 8 10 13 14 15 16 17
11 12 13 15 16 14 17


                 5-FACES: 179

                 1  2  3  4  5  6  8 10
                 1  2  3  4  5  7  8
                 1  2  3  4  5  9  8
                 1  2  3  4  5 11  8 13
                 1  2  3  4  5 12  8 14
                 1  2  3  4  5 15  8
                 1  2  3  4  6  7 10
                 1  2  3  4  6  9 10
                 1  2  3  4  6 15 10
                 1  2  3  4  7  9
                 1  2  3  4  7 11
                 1  2  3  4  9 12
```

```
1  2  3  4 11 12
1  2  3  4 11 15
1  2  3  4 12 15
1  2  3  5  6  7  8 10
1  2  3  5  6  9  8 10
1  2  3  5  6 11  8 10 13 16
1  2  3  5  6 12  8 10 14 17
1  2  3  5  6 15  8 10
1  2  3  5  7  9  8
1  2  3  5  7 11  8 13
1  2  3  5  9 12  8 14
1  2  3  5 11 12  8 13 14
1  2  3  5 11 15  8 13
1  2  3  5 12 15  8 14
1  2  3  6  7  9 10
1  2  3  6  7 11 10 16
1  2  3  6  9 12 10 17
1  2  3  6 11 12 10 16 17
1  2  3  6 11 15 10 16
1  2  3  6 12 15 10 17
1  2  3  7  9 11 12
1  2  3 11 12 15
1  2  4  5  6  7  8 10
1  2  4  5  6  9  8 10
1  2  4  5  6 15  8 10
1  2  4  5  7  9  8
1  2  4  5  7 11  8 13
1  2  4  5  9 12  8 14
1  2  4  5 11 12  8 13 14
1  2  4  5 11 15  8 13
1  2  4  5 12 15  8 14
1  2  4  6  7  9 10
1  2  4  6  7 11 10 15 16
1  2  4  6  9 12 10 15 17
1  2  4  7  9 11 12
1  2  4 11 12 15
1  2  5  6  7  9  8 10
1  2  5  6  7 11  8 10 13 16
1  2  5  6  9 12  8 10 14 17
1  2  5  6 11 12  8 10 13 14 16 17
1  2  5  6 11 15  8 10 13 16
1  2  5  6 12 15  8 10 14 17
1  2  5  7  9 11  8 12 13 14
1  2  5 11 12 15  8 13 14
1  2  6  7  9 11 10 12 16 17
1  2  6 11 12 15 10 16 17
1  3  4  5  6  7
1  3  4  5  6  9
1  3  4  5  6 15
1  3  4  5  7  9
```

```
 1  3  4  5  7 11 13
 1  3  4  5  9 12 14
 1  3  4  5 11 12 13 14
 1  3  4  5 11 15 13
 1  3  4  5 12 15 14
 1  3  4  6  7  9
 1  3  4  6  7 11 15 16
 1  3  4  6  9 12 15 17
 1  3  4  7  9 11 12
 1  3  4 11 12 15
 1  3  5  6  7  9
 1  3  5  6  7 11 13 16
 1  3  5  6  9 12 14 17
 1  3  5  6 11 12 13 14 16 17
 1  3  5  6 11 15 13 16
 1  3  5  6 12 15 14 17
 1  3  5  7  9 11 12 13 14
 1  3  5 11 12 15 13 14
 1  3  6  7  9 11 12 16 17
 1  3  6 11 12 15 16 17
 1  4  5  6  7  9
 1  4  5  6  7 11 13 15 16
 1  4  5  6  9 12 14 15 17
 1  4  5  7  9 11 12 13 14
 1  4  5 11 12 15 13 14
 1  4  6  7  9 11 12 15 16 17
 1  5  6  7  9 11 12 13 14 16 17
 1  5  6 11 12 15 13 14 16 17
 2  3  4  7  8  9
 2  3  4  7  8 10
 2  3  4  7  8 11 13
 2  3  4  7  9 10
 2  3  4  7  9 11 12
 2  3  4  7 10 11 15 16
 2  3  4  8  9 10
 2  3  4  8  9 12 14
 2  3  4  8 10 15
 2  3  4  8 11 12 13 14
 2  3  4  8 11 15 13
 2  3  4  8 12 15 14
 2  3  4  9 10 12 15 17
 2  3  4 11 12 15
 2  3  7  8  9 10
 2  3  7  8  9 11 12 13 14
 2  3  7  8 10 11 13 16
 2  3  7  9 10 11 12 16 17
 2  3  8  9 10 12 14 17
 2  3  8 10 11 12 13 14 16 17
 2  3  8 10 11 15 13 16
 2  3  8 10 12 15 14 17
 2  3  8 11 12 15 13 14
```

```
2  3 10 11 12 15 16 17
2  4  7  8  9 10
2  4  7  8  9 11 12 13 14
2  4  7  8 10 11 13 15 16
2  4  7  9 10 11 12 15 16 17
2  4  8  9 10 12 14 15 17
2  4  8 11 12 15 13 14
2  7  8  9 10 11 12 13 14 16 17
2  8 10 11 12 15 13 14 16 17
3  4  5  6  7  8 10
3  4  5  6  7  9
3  4  5  6  7 13 15 16
3  4  5  6  8  9 10
3  4  5  6  8 15 10
3  4  5  6  9 14 15 17
3  4  5  7  8  9
3  4  5  7  8 13
3  4  5  7  9 13 14
3  4  5  8  9 14
3  4  5  8 13 14
3  4  5  8 13 15
3  4  5  8 14 15
3  4  5 13 14 15
3  4  6  7  9 10
3  4  6  7  9 15 16 17
3  4  6  7 10 15 16
3  4  6  9 10 15 17
3  4  7  8  9 10
3  4  7  8  9 13 14
3  4  7  8 10 13 15 16
3  4  7  9 10 15 16 17
3  4  7  9 11 13 12 14
3  4  7  9 11 15 12 16 17
3  4  7  9 13 15 14 16 17
3  4  7 11 13 15 16
3  4  8  9 10 14 15 17
3  4  8 13 14 15
3  4  9 12 14 15 17
3  4 11 12 13 15 14
3  5  6  7  8  9 10
3  5  6  7  8 13 10 16
3  5  6  7  9 13 14 16 17
3  5  6  8  9 14 10 17
3  5  6  8 13 14 10 16 17
3  5  6  8 13 15 10 16
3  5  6  8 14 15 10 17
3  5  6 13 14 15 16 17
3  5  7  8  9 13 14
3  5  8 13 14 15
3  6  7  9 10 16 17
3  6 10 15 16 17
```

```
 3  7  8  9 10 13 14 16 17
 3  7  9 11 13 16 12 14 17
 3  8 10 13 14 15 16 17
 3 11 12 13 15 16 14 17
 4  5  6  7  8  9 10
 4  5  6  7  8 13 10 15 16
 4  5  6  7  9 13 14 15 16 17
 4  5  6  8  9 14 10 15 17
 4  5  7  8  9 13 14
 4  5  8 13 14 15
 4  6  7  9 10 15 16 17
 4  7  8  9 10 13 14 15 16 17
 4  7  9 11 13 15 12 14 16 17
 5  6  7  8  9 13 10 14 16 17
 5  6  8 13 14 15 10 16 17


       6-FACES: 62


 1  2  3  4  5  6  7  8 10
 1  2  3  4  5  6  9  8 10
 1  2  3  4  5  6 15  8 10
 1  2  3  4  5  7  9  8
 1  2  3  4  5  7 11  8 13
 1  2  3  4  5  9 12  8 14
 1  2  3  4  5 11 12  8 13 14
 1  2  3  4  5 11 15  8 13
 1  2  3  4  5 12 15  8 14
 1  2  3  4  6  7  9 10
 1  2  3  4  6  7 11 10 15 16
 1  2  3  4  6  9 12 10 15 17
 1  2  3  4  7  9 11 12
 1  2  3  4 11 12 15
 1  2  3  5  6  7  9  8 10
 1  2  3  5  6  7 11  8 10 13 16
 1  2  3  5  6  9 12  8 10 14 17
 1  2  3  5  6 11 12  8 10 13 14 16 17
 1  2  3  5  6 11 15  8 10 13 16
 1  2  3  5  6 12 15  8 10 14 17
 1  2  3  5  7  9 11  8 12 13 14
 1  2  3  5 11 12 15  8 13 14
 1  2  3  6  7  9 11 10 12 16 17
 1  2  3  6 11 12 15 10 16 17
 1  2  4  5  6  7  9  8 10
 1  2  4  5  6  7 11  8 10 13 15 16
 1  2  4  5  6  9 12  8 10 14 15 17
 1  2  4  5  7  9 11  8 12 13 14
 1  2  4  5 11 12 15  8 13 14
```

```
1  2  4  6  7  9 11 10 12 15 16 17
1  2  5  6  7  9 11  8 10 12 13 14 16 17
1  2  5  6 11 12 15  8 10 13 14 16 17
1  3  4  5  6  7  9
1  3  4  5  6  7 11 13 15 16
1  3  4  5  6  9 12 14 15 17
1  3  4  5  7  9 11 12 13 14
1  3  4  5 11 12 15 13 14
1  3  4  6  7  9 11 12 15 16 17
1  3  5  6  7  9 11 12 13 14 16 17
1  3  5  6 11 12 15 13 14 16 17
1  4  5  6  7  9 11 12 13 14 15 16 17
2  3  4  7  8  9 10
2  3  4  7  8  9 11 12 13 14
2  3  4  7  8 10 11 13 15 16
2  3  4  7  9 10 11 12 15 16 17
2  3  4  8  9 10 12 14 15 17
2  3  4  8 11 12 15 13 14
2  3  7  8  9 10 11 12 13 14 16 17
2  3  8 10 11 12 15 13 14 16 17
2  4  7  8  9 10 11 12 13 14 15 16 17
3  4  5  6  7  8  9 10
3  4  5  6  7  8 13 10 15 16
3  4  5  6  7  9 13 14 15 16 17
3  4  5  6  8  9 14 10 15 17
3  4  5  7  8  9 13 14
3  4  5  8 13 14 15
3  4  6  7  9 10 15 16 17
3  4  7  8  9 10 13 14 15 16 17
3  4  7  9 11 13 15 12 14 16 17
3  5  6  7  8  9 13 10 14 16 17
3  5  6  8 13 14 15 10 16 17
4  5  6  7  8  9 13 10 14 15 16 17
```

7-FACES: 12

```
1  2  3  4  5  6  7  9  8 10
1  2  3  4  5  6  7 11  8 10 13 15 16
1  2  3  4  5  6  9 12  8 10 14 15 17
1  2  3  4  5  7  9 11  8 12 13 14
1  2  3  4  5 11 12 15  8 13 14
1  2  3  4  6  7  9 11 10 12 15 16 17
1  2  3  5  6  7  9 11  8 10 12 13 14 16 17
1  2  3  5  6 11 12 15  8 10 13 14 16 17
1  2  4  5  6  7  9 11  8 10 12 13 14 15 16 17
1  3  4  5  6  7  9 11 12 13 14 15 16 17
2  3  4  7  8  9 10 11 12 13 14 15 16 17
3  4  5  6  7  8  9 13 10 14 15 16 17
```